



SAPIENZA
UNIVERSITÀ DI ROMA

Non-perturbative computation of Kaons oscillation amplitudes in Lattice Quantum Chromodynamics with $N_f = 2 + 1$ sea quarks and Open Boundary Conditions

Facoltà di Scienze Matematiche Fisiche e Naturali
Corso di Laurea Magistrale in Fisica Teorica

Candidate

Emanuele Rosi

ID number 1812180

Thesis Advisor

Prof. Mauro L. Papinutto

Academic Year 2022/2023

Non-perturbative computation of Kaons oscillation amplitudes in Lattice Quantum Chromodynamics with $N_f = 2+1$ sea quarks and Open Boundary Conditions
Master's thesis. Sapienza – University of Rome

© 2023 Emanuele Rosi. All rights reserved

This thesis has been typeset by L^AT_EX and the Sapthesis class.

Author's email: rosiemanuele99@gmail.com

Ai miei genitori.

*A tutte quelle giornate in cui non mi stavo sacrificando per lo studio, stavo facendo
ciò che amo.*

Abstract

Oscillations of neutral Kaons are a well known phenomenon within the framework of the Standard Model (SM) of particle physics. These oscillations arise from quark flavor mixing governed by the Cabibbo-Kobayashi-Maskawa matrix in weak interactions. Furthermore, decay rates of the Kaons are studied to get an indirect measure of CP violation in the Standard Model, quantified through the parameter ϵ_K [7]. Precise theoretical predictions are essential. As I have implicitly mentioned, the Kaons oscillation phenomenon takes place at low energies, where the quarks are confined in mesons and baryons - energies of order of $\Lambda_{\text{QCD}} \sim 250$ MeV [43]. Perturbation theory (PT) represents the most powerful tool of theoretical physicists to understand the world of particle physics. However it imposes the requirement of energies much higher than Λ_{QCD} , requirement not satisfied in the energetic region concerning confinement. The PT approach becomes inefficient and the only other valid approach to QFT is the path integral formalism. Usually, direct calculations in path integral are performed through lattice QFT simulations.

In this work I treat a set of dimension 6 four-quarks operators responsible for the oscillations of neutral Kaons. They constitute an effective Hamiltonian for the oscillating system

$$\mathcal{H}_{\text{eff,BSM}}^{\Delta S=2} = \sum_i \hat{C}_i(\mu) \hat{\Theta}_i(\mu)$$

The first operator $\hat{\Theta}_1$ is the effective operator associated to the SM contribution to the oscillations. The others take place in beyond the standard model (BSM) theories, such as supersymmetry or multi Higgs models [1]. The purpose is to compute parameters associated to the bare Kaon oscillation amplitudes caused by each Θ_i operator:

$$\mathcal{A}_i^{\text{QCD}} = \langle \bar{K}^0 | \Theta_i^{\text{bare}} | K^0 \rangle$$

Such quantities are called *bag parameters* [1] [6]. The renormalization of such operators and parameters is not involved in this work and it is developed in some papers, such as [17]. B -parameters are widely studied in the context of lattice QCD (LQCD) and results of the most recent works can be found in [2].

Lattice simulations suffer from an amount of computational issues such as finite spacetime volume effects or lattice spacing effects. The lattice setup chosen for this work aims to minimize some of these effects. Firstly, there is a computational problem in the generation of gauge configurations; ideally, they should be totally uncorrelated from each other, but their autocorrelation times grow as the lattice spacing is reduced. [39] It is proven that this problem is partially solved by choosing open boundary conditions in temporal direction. [34] Secondly, these boundary conditions protect the fermion determinant from the occurrence of zero eigenvalues of the Wilson-Dirac operator [32]. In this sense open boundary conditions give an efficient alternative to twisted mass QCD (tmQCD) [22] - used in [6] - and allow the simulation program to simulate three flavours of sea quarks, not allowed in tmQCD. The entire simulation is developed to yield $O(a)$ -improved results, i.e. values that differ from the continuum limit ones by terms of order $O(a^2)$ or higher. This is possible thanks to the strategy worked out by Frezzotti and Rossi in [21]. Such strategy involves maximally twisted Osterwalder-Seiler quarks in the valence sector. Further properties of the lattice mixing operators are well explained in [18], such as their mixing pattern under renormalization procedure.

The thesis is structured as follows. The first chapter covers basic concepts of Standard Model QCD, confinement, pseudoscalar mesons, and Kaon oscillations. Moreover I

introduce the bag parameters and the complete set of mixing operators $\{\Theta_i\}$. The second chapter provides an overview of lattice regularizations and improvements; I begin from the basics - Wilson-Dirac action and Wilson Gauge action - and I describe some of their related problems (zero modes, long autocorrelation times, exceptional configurations, $O(a)$ efficiency). Then a description of more advanced regularizations follows. At the end of the chapter I outline the adopted lattice setup as a solution of almost all the presented problems. The chapter 3 is completely dedicated to the construction of three points correlators on the lattice. The operators Θ_i are described in continuum theory, then they are regularized on the lattice by following the strategy in [21]. All the properties are described in detail and most of them are proven. At the end of the chapter I describe the analysis of the asymptotic behaviour of the correlation functions at large Euclidean time, widely used in QFT. In the fourth chapter I present the computational strategies developed to calculate the needed Wick contractions of the two and three points correlators. Particular relevance is given to the calculation of three points correlators through the method of noise spinors, that represents most of the “behind the scenes” thesis work. A conclusive section provides the reader information about the status of the simulation and reports the achievements of this work.

Contents

1	Kaons oscillations beyond the Standard Model and B_i parameters	1
1.1	QCD Symmetries review - the birth of Kaons	1
1.2	Kaon oscillations in the Standard Model and B_K	3
1.3	BSM effects: new operators and B_i parameters	5
1.3.1	Bag parameters	6
2	Lattice regularization and improvements	8
2.1	Lattice regularization of QFT	8
2.2	Gauge action	11
2.3	Fermion actions	12
2.3.1	Wilson-Dirac action	13
2.3.2	$O(a)$ -improvement: Sheikholeslami-Wohlert term	14
2.3.3	Chiral symmetry and fermion zero modes	14
2.3.4	Twisted Mass QCD (tmQCD)	15
2.3.5	Osterwalder-Seiler fermions	18
2.4	Sea vs Valence: need for bosonic ghosts	19
2.5	Adopted lattice setup	20
2.6	Open Boundary Conditions	22
2.6.1	Linking OBC with absence of Wilson-Dirac zero modes	24
3	Operators $\Theta_i^{[+]}$s on the lattice and B_i extraction	26
3.1	Continuum $\Theta_i^{[\pm]}$ s and the new operators $Q_i^{[\pm]}$ s	26
3.2	Flavour replicas on the lattice	28
3.2.1	Proof of equivalence of Wick contractions	29
3.3	From physical basis to twisted basis	30
3.4	Properties of correlators and $O_{i[+]}$ operators	32
3.4.1	Automatic $O(a)$ -improvement	32
3.4.2	Renormalization and mixing of operators $O_{i[\pm]}$	33
3.5	Asymptotic behaviours	35
4	Computational Strategies	39
4.1	Noise spinors method	39
4.2	Simulation program description	43
4.2.1	Computational Basis	43
4.3	Analysis strategy	44
4.4	Status of the work, results and future developments	46
A	Notations and conventions	52

B	Twisted basis vs physical basis	53
B.1	Twisted and physical basis in tmQCD	53
B.2	Twisted and physical basis in OS regularization	55
C	Fierz transformations	57
C.1	Fierz decomposition	57
C.2	Application to Θ_3 and Θ_5	58
D	Some proofs	59
D.1	Proof that $\langle \Omega \bar{K}^0(0) \bar{K}^0 \rangle$ is real	59
D.2	Reality of three point correlators	60
D.3	Proof of $\gamma_5 S_{(i,\pm)}(u,v) \gamma_5 = S_{(i,\mp)}^\dagger(v,u)$	60
D.4	Proof of connection of Gauge fields space	61
D.5	Pseudoscalar propagator with OBC	62

Chapter 1

Kaons oscillations beyond the Standard Model and B_i parameters

In order to present and justify my work, I begin the thesis with an introductive chapter about theory of $K^0 - \bar{K}^0$ system within the Standard Model (SM) of particle physics and beyond. Firstly, I present the Standard Model $K^0 - \bar{K}^0$ oscillations. Then I discuss oscillations beyond the SM by introducing a complete basis of dimension 6 four quarks operators. At the end of the chapter, I stress which quantities can be extracted from these operators matrix elements and how they could be useful to quantify effects of new physics to the $K^0 - \bar{K}^0$ oscillations.

1.1 QCD Symmetries review - the birth of Kaons

As well known, in Quantum Chromodynamics (QCD) the phenomenon of *confinement* arises at low energies, below the scale of $\Lambda_{QCD} \sim 250$ MeV [43]. This happens because of the running coupling in the Gauge group of QCD, i.e. the colour group $SU(3)_C$, that's a non-abelian Lie group. The QCD Lagrangian with massless fermions¹

$$\mathcal{L}_{QCD}^0 = -\frac{1}{4g^2} F_{\mu\nu}^a(x) F_{\mu\nu}^a(x) - \sum_{q=u,d,s} \bar{\psi}_q(x) \gamma_\mu \left(\partial_\mu + iT_\square^a A_\mu^a(x) \right) \psi_q(x) \quad (1.1)$$

has also an accidental symmetry group $SU(3)_V \times SU(3)_A \times U(1)_V \times U(1)_A$. The index q refers to flavour, the matrices T_\square^a are the generators of $SU(3)_C$ in fundamental representation, $A_\mu^a(x)$ s are the gluon fields and $F_{\mu\nu}^a(x)$ is their strength tensor. This accidental group is broken by several instances:

- ▷ $U(1)_A$: This group is broken in two different ways. In the first instance by the axial anomaly due to triangular diagrams (and also non-perturbatively, see [24][23]). In the second instance by the mass term:

$$\mathcal{L}_{QCD}^M = - \sum_{q,q'=u,d,s} \bar{\psi}_q(x) M_{qq'} \psi_{q'}(x)$$

as it causes the mixing of Left and Right Weyl spinors of the same flavour.

¹ I use the Euclidean notation of QFT because it guarantees the convergence of the path integral, useful on the Lattice.

- ▷ $SU(3)_A$: This is broken by the mass term similarly to the $U(1)_A$ case. Moreover it is spontaneously broken because the group is not closed.*
- ▷ $U(1)_V$: This is always preserved and it is responsible for the Baryon quantum number B .
- ▷ $SU(3)_V$: This is the flavour symmetry group of QCD, preserved also in the massive case, but only if the masses are all equal: $m_s = m_u = m_d$.

* The particular breaking mechanism of $SU(3)_A$ is such that the charges Q_A^a don't annihilate the vacuum $Q_A^a \Psi_0 \neq 0$ even in the chiral limit ($m_q = 0 \forall q$). Therefore the Goldstone theorem applies: for each $SU(3)_A$ broken generator there exists a massless bosonic state interpolated by the order parameter operator with index a [26]. The addition of the mass term to the Lagrangian is responsible for the mass of these states, now named *pseudo*-Nambu Goldstone bosons.

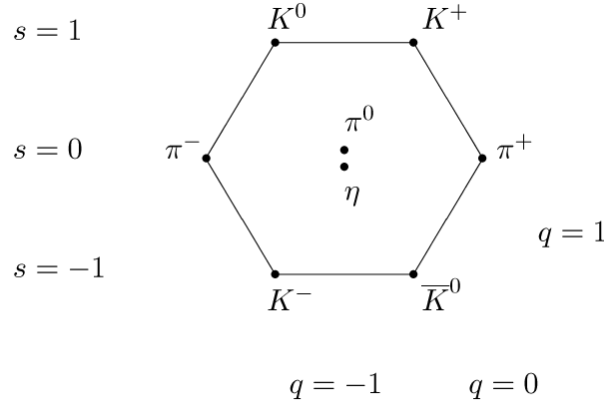


Figure 1.1. QCD pseudoscalar meson octet in the Cartan plane.

They form the pseudoscalar $J^P = 0^-$ meson octet - plus a singlet - of the QCD at low energies $\{\pi^\pm, \pi^0, K^\pm, K^0, \bar{K}^0, \eta, \eta'\}$. *How* quarks are bound together is an unexplained question because it would need a formal non-perturbative development of QFT. For this reason lattice QCD is a very powerful tool, allowing us to compute non-perturbative quantities through path integrals.

To give an example of confinement effects, let's consider a (non singlet flavour) pseudoscalar propagator - or two points functions - $G_{12}(x, y)$:

$$G_{12}(x, y) = \langle 0 | T \left\{ (\bar{\psi}^1 \gamma_5 \psi^2)(x) (\bar{\psi}^2 \gamma_5 \psi^1)(y) \right\} | 0 \rangle$$

for example, by choosing $\psi^1 = u$ and $\psi^2 = d$, the propagator of the π^- is obtained. In principle the two constituent quarks ψ^1, ψ^2 - named *valence* quarks - are subject to a very large number of interactions with the gluons. In first approximation of perturbation theory (PT) one simply neglects these contributions, while at higher orders only few diagrams are involved. However the running coupling phenomenon makes the constant $g(\mu)_{\text{colour}}$ grow at energies below Λ_{QCD} . As a consequence the use of PT is no longer allowed and all the possible contributing diagrams must be considered. The Figure 1.2 gives an idea of the subleading processes to involve.

As can be seen from Figure 1.2, some internal quark loops could arise. These virtual quarks are named *sea* quarks and could differ from the valence quarks. For example,

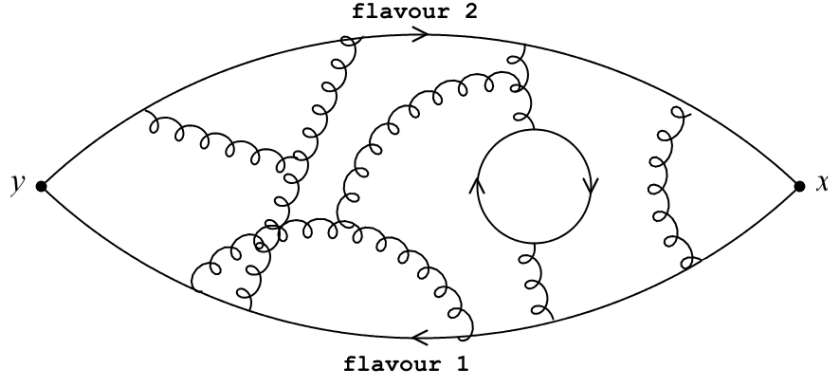


Figure 1.2. Conceptual idea of non perturbative contributions to the correlator $G_{12}(x, y)$.

at some point a pion could contain a couple of charm quarks $c\bar{c}$ without any apparent reason: they are virtual sea quarks. By an appropriate scattering process, they could be even put on shell and extracted. The conceptual difference between valence and sea quarks will be widely used in this work.

1.2 Kaon oscillations in the Standard Model and B_K

The $K^0 - \bar{K}^0$ system ($m_K = 497.611 \pm 0.013$ MeV) is the doublet containing neutral $|s| = 1$ particles of the 0^- octet. Because of decay channels of the Kaons in $2\pi, 3\pi$ and others [45], this is an *open* system - in quantum mechanical sense. For future use, I define two local operators:

$$\begin{aligned} K^0 & \quad \text{neutral Kaon} \\ \bar{K}^0 & \quad \text{neutral anti-Kaon} \end{aligned} \tag{1.2}$$

which interpolate $|K^0\rangle$ and $|\bar{K}^0\rangle$ states. In principle the two neutral Kaons are two different eigenstates of an effective Hamiltonian H_0 ; thus we can choose a basis in which H_0 has the diagonal form:

$$H_0 = \begin{pmatrix} M - \frac{i}{2}\Gamma & 0 \\ 0 & M - \frac{i}{2}\Gamma \end{pmatrix} \quad |K^0\rangle = \begin{vmatrix} 1 \\ 0 \end{vmatrix} \quad |\bar{K}^0\rangle = \begin{vmatrix} 0 \\ 1 \end{vmatrix}$$

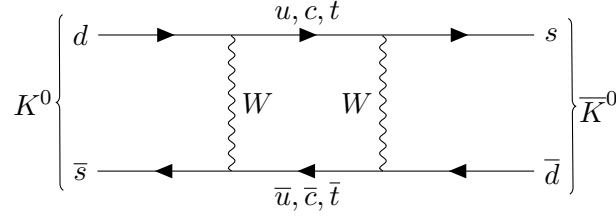
where Γ gives the decay width. This H_0 is associated the effective Schrodinger-like dynamics of the system:

$$i \frac{d}{dt} |\psi(t)\rangle = H_0 |\psi(t)\rangle$$

It is known that weak interactions add the following term to the Lagrangian density:

$$\mathcal{L}_{\text{weak}} = \frac{g_2}{\sqrt{2}} \left[\bar{\psi}_f^L \gamma_\mu W_\mu^+ (V_{\text{CKM}})_{ff'} \psi_{f'}^L + \text{h.c.} \right] \tag{1.3}$$

where L stands for left component of the Dirac spinor, V_{CKM} is responsible for flavour mixing, f, f' are flavour family indices and g_2 is the weak coupling constant. From the previous term this mixing 1-loop diagram follows:



Weak interactions also generate another 1-loop channel and diagrams in higher orders of perturbation theory. Because of the mixing process, the effective Hamiltonian of the $K^0 - \bar{K}^0$ system needs non-diagonal terms parametrized in $H^{\Delta S=2}$. A formal development can be found in [19] and a new diagonal basis is built: the new Kaon states that diagonalize $H_0 + H^{\Delta S=2}$ are K_L and K_S - named K long and K short. Through CP symmetry arguments it comes out that, by considering only SM interactions, the allowed decays are $K_L \rightarrow 3\pi$ and $K_S \rightarrow 2\pi$. Through measures of these decays one can extract some pseudo-observables and parametrize the amount of CP violation in the Standard Model. In particular, phenomenologists use the so called ϵ parameter [19]. In order to quantify the mixing and extract the abovementioned quantities, the mixing amplitudes are needed. Below I will give some arguments needed to define *bag parameters*, strictly related to mixing amplitudes.

At low energies ($E \ll M_W \simeq 80$ GeV) the W propagator can be replaced by $1/M_W^2$ and the effective Fermi interaction can be ruled out. It consists in a pointlike interaction of four fermions, the coupling constant is the Fermi constant $G_F/\sqrt{2}$ and it links together two quarks in the up sector of $SU(2)_L$ with two quarks in the down sector:

$$\mathcal{L}_F = \frac{G_F}{\sqrt{2}} V_{u_1 d_1} V_{u_2 d_2}^* [\bar{u}_1 \gamma_\mu (1 - \gamma_5) d_1] [\bar{d}_2 \gamma_\mu (1 - \gamma_5) u_2] + \text{similar} \quad (1.4)$$

that's a product of currents + flavour mixing.² The original Fermi interaction involves only two families of quarks and the V_{CKM} matrix is replaced by the Cabibbo angle rotation matrix. Through this Lagrangian one can build two *candy* diagrams for Kaons oscillations. By a direct calculation of these diagrams:

- ▷ a loop factor $1/(16\pi^2)$ appears;
- ▷ there is a sum over the up-components intermediate-flavours:

$$\sum_{i,j=u,c,t} V_{id} V_{is}^* V_{jd} V_{js}^*$$

useful to test the unitarity of V_{CKM} matrix;

- ▷ an effective operator $\Theta_1 = [\bar{s} \gamma_\mu (1 + \gamma_5) d] \cdot [\bar{s} \gamma_\mu (1 + \gamma_5) d]$ arises.

The sum of the two diagrams gives:

$$\mathcal{A} + \mathcal{A}' \propto \left(\frac{G_F}{\sqrt{2}} \right)^2 \frac{2}{16\pi^2} \left[\sum_{i,j} V_{id} V_{is}^* V_{jd} V_{js}^* \right] \langle \bar{K}^0 | \Theta_1 | K^0 \rangle$$

² In the notation adopted, the left and right Dirac projectors have these definitions: $P_L = (1 - \gamma_5)/2$, $P_R = (1 + \gamma_5)/2$. Infos about the notation are in Appendix A.

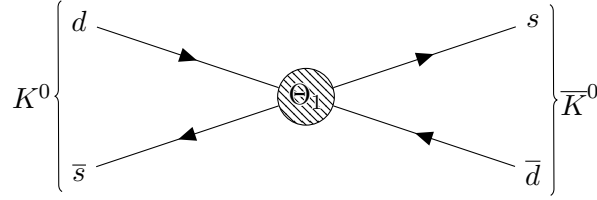
In this evaluation, only 1-loop is considered.

I will now proceed to highlight a problem that is responsible for the lattice calculation done in this thesis work. The oscillation effect is well understood in perturbation theory by the previous argument, but at low energies it is not sufficient to well describe the complete amplitude. Confinement and running coupling generate bound states of quarks and an infinite number of gluon-quark and gluon-gluon interactions take place. These interactions must be involved in a non perturbative calculation of the amplitude. To parametrize them, we introduce a form factor named B_K parameter. For the same reason some form factors (or decay constants) $f_{\pi,K,\dots}$ appear in the PCAC relations.

Then the B_K parameter clearly depends on the renormalization scale μ and parametrizes the deviation from the Vacuum Insertion Approximation (VIA) [14]:

$$\langle \bar{K}^0 | \Theta_1^{\text{ren}}(\mu) | K^0 \rangle_{\text{non pert.}} = B_K(\mu) \langle \bar{K}^0 | \hat{\Theta}_1 | K^0 \rangle_{\text{VIA}} = \frac{8}{3} m_K^2 f_K^2 B_K(\mu) \quad (1.5)$$

Sometimes I will refer to B_K as B_1 and to $\Theta_1^{\text{ren}}(\mu)$ as $\hat{\Theta}_1$. The entire process in the Standard Model is graphically represented - in momentum space - by:



The value of B_K is assessed non perturbatively by the ETM (European Twisted Mass) collaboration and it is reported by the FLAG working group in [2][45]:

$$B_K^{\overline{MS}}(2 \text{ GeV}) = 0.524(13)(12) \quad (1.6)$$

Renormalization constants have been evaluated too.

1.3 BSM effects: new operators and B_i parameters

There exists a set of theories beyond the Standard Model (BSM) that give contributions to the $K^0 - \bar{K}^0$ oscillations - supersymmetry, multi-Higgs models, etc. For this reason it is useful to study other operators $\{\Theta_i, \tilde{\Theta}_j\}$ - similar to Θ_1 - that cause the mixing BSM. They are used to define an effective Hamiltonian for the mixing process:

$$\mathcal{H}_{\text{eff}} = \frac{1}{4} \sum_{i=1}^5 C_i \Theta_i + \frac{1}{4} \sum_{i=1}^3 \tilde{C}_i \tilde{\Theta}_i$$

The operators $\{\Theta_i, \tilde{\Theta}_j\}$ have dimension 6 and are composed by four quark fields, while $\{C_i, \tilde{C}_j\}$ are their Wilson coefficient. They arise at low energies in a way similar to Θ_1 , presented in the previous section. One common choice for the basis of

these operators is the so called *SUSY basis* [1], used in BSM phenomenology:

$$\begin{aligned}
\Theta_1 &= [\bar{s}^a \gamma_\mu (1 - \gamma_5) d^a] \cdot [\bar{s}^b \gamma_\mu (1 - \gamma_5) d^b] \\
\Theta_2 &= [\bar{s}^a (1 - \gamma_5) d^a] \cdot [\bar{s}^b (1 - \gamma_5) d^b] \\
\Theta_3 &= [\bar{s}^a (1 - \gamma_5) d^b] \cdot [\bar{s}^b (1 - \gamma_5) d^a] \\
\Theta_4 &= [\bar{s}^a (1 - \gamma_5) d^a] \cdot [\bar{s}^b (1 + \gamma_5) d^b] \\
\Theta_5 &= [\bar{s}^a (1 - \gamma_5) d^b] \cdot [\bar{s}^b (1 + \gamma_5) d^a] \\
\tilde{\Theta}_1 &= [\bar{s}^a \gamma_\mu (1 + \gamma_5) d^a] \cdot [\bar{s}^b \gamma_\mu (1 + \gamma_5) d^b] \\
\tilde{\Theta}_2 &= [\bar{s}^a (1 + \gamma_5) d^a] \cdot [\bar{s}^b (1 + \gamma_5) d^b] \\
\tilde{\Theta}_3 &= [\bar{s}^a (1 + \gamma_5) d^b] \cdot [\bar{s}^b (1 + \gamma_5) d^a]
\end{aligned} \tag{1.7}$$

where a, b are colour indices³ and within the square brackets $[\cdot]$ a sum over spin is implied. The first operator is the one of the Standard Model cited in the previous section. I will study the bare matrix elements $\langle \bar{K}^0 | \Theta_j | K^0 \rangle$ in a lattice environment in which only strong interactions take place; it is known that strong interactions preserve both \mathbb{C} and \mathbb{P} symmetries, thus only the parity preserving part of these operators, denoted by $\Theta_i^{[+]}$ will be considered [6]. In the case of Θ_j and $\tilde{\Theta}_j$ the parity even parts are the same, then only 5 even operators are needed. A more detailed discussion about these operators and their lattice counterparts is presented in Chapter 3.

1.3.1 Bag parameters

The bag parameters $B_i(\mu)$ s arise through the same confinement argument concerning B_K and a scaling behaviour with μ is naturally expected. $B_i(\mu)$ s are defined by the following equations [1]:

$$\begin{aligned}
\langle \bar{K}^0 | \Theta_1^{[+],\text{ren}}(\mu) | K^0 \rangle &= \frac{8}{3} m_K^2 f_K^2 B_1(\mu) \\
\langle \bar{K}^0 | \Theta_2^{[+],\text{ren}}(\mu) | K^0 \rangle &= -\frac{5}{3} \left(\frac{m_K}{m_s(\mu) + m_d(\mu)} \right)^2 m_K^2 f_K^2 B_2(\mu) \\
\langle \bar{K}^0 | \Theta_3^{[+],\text{ren}}(\mu) | K^0 \rangle &= \frac{1}{3} \left(\frac{m_K}{m_s(\mu) + m_d(\mu)} \right)^2 m_K^2 f_K^2 B_3(\mu) \\
\langle \bar{K}^0 | \Theta_4^{[+],\text{ren}}(\mu) | K^0 \rangle &= 2 \left(\frac{m_K}{m_s(\mu) + m_d(\mu)} \right)^2 m_K^2 f_K^2 B_3(\mu) \\
\langle \bar{K}^0 | \Theta_5^{[+],\text{ren}}(\mu) | K^0 \rangle &= \frac{2}{3} \left(\frac{m_K}{m_s(\mu) + m_d(\mu)} \right)^2 m_K^2 f_K^2 B_3(\mu)
\end{aligned}$$

with $m_d(\mu)$ and $m_s(\mu)$ the renormalized masses of quarks down and strange in the same renormalization scheme applied for $\Theta_i^{[+],\text{ren}}(\mu)$. The previous equations can be rewritten in a more compact way, as in [6]:

$$\begin{aligned}
\langle \bar{K}^0 | \Theta_1^{[+],\text{ren}}(\mu) | K^0 \rangle &= \xi_1 m_K^2 f_K^2 B_1(\mu) \\
\langle \bar{K}^0 | \Theta_j^{[+],\text{ren}}(\mu) | K^0 \rangle &= \xi_j \left(\frac{m_K^2}{m_s(\mu) + m_d(\mu)} \right)^2 f_K^2 B_j(\mu) \quad \text{for } j = 2, \dots, 5
\end{aligned} \tag{1.8}$$

³ Einstein summation convention is used.

with $\xi_i = (8/3, -5/3, 1/3, 2, 2/3)$ numerical factors. The definitions of bare Bag parameters are analogous to the above mentioned but involve only bare quantities. The numerical value of B_i -parameters is extracted in [1] and a large amount of other papers. A relevant work has been done by the ETM collaboration in [6] bringing these results at $\mu_0 = 2$ GeV in the \overline{MS} scheme:

$$\begin{aligned} B_1(\mu_0) &= 0.53(2) & B_2(\mu_0) &= 0.52(2) & B_3(\mu_0) &= 0.89(5) \\ B_4(\mu_0) &= 0.78(3) & B_5(\mu_0) &= 0.57(4) \end{aligned} \quad (1.9)$$

I want to highlight that the $B_1(\mu_0)$ value has a small difference with respect to the one in formula 1.6 - because it comes from a different simulation - but fortunately there is an overlap due to statistical errors. The simulation setup developed in this thesis is very similar to the one used in [6], but some improvements have been done. Such improvements are discussed in the next chapters. Some simulation results at the scale of $\mu = 3$ GeV are reported in the second graph in Figure 1.3.

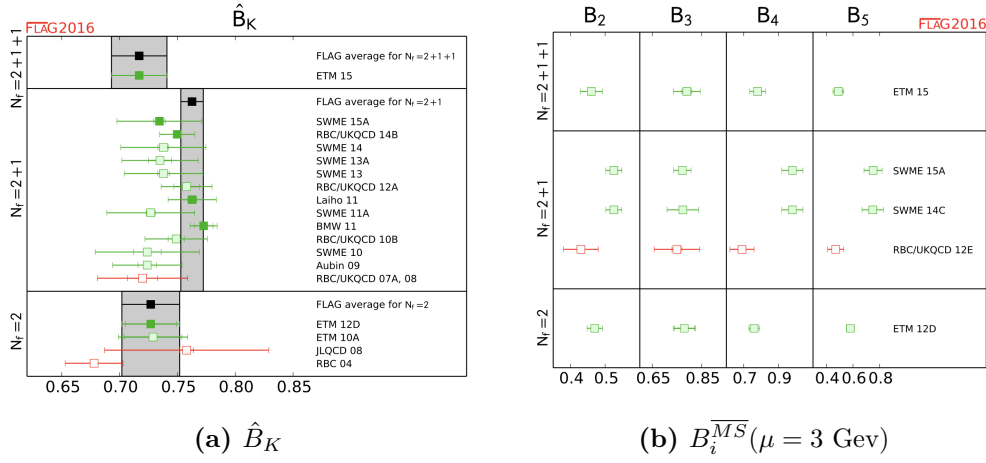


Figure 1.3. Current lattice results until 2016, July 1st, date of publication of the report by FLAG Working Group [2]. Figure (a): lattice results of the renormalization group invariant \hat{B}_K from distinct simulations. Figure (b): lattice results of the renormalized bag parameters with index $i = 2, 3, 4, 5$ in the \overline{MS} scheme at energy scale of 3 GeV.

The first graph refers to \hat{B}_K , a renormalization group invariant for the B_K parameter defined by [2]:

$$\hat{B}_K = \left(\frac{\bar{g}(\mu)^2}{4\pi} \right)^{-\gamma_0/(2\beta_0)} \times \exp \left\{ \int_0^{\bar{g}(\mu)} dg \left(\frac{\gamma(g)}{\beta(g)} + \frac{\gamma_0}{\beta_0 g} \right) \right\} B_K(\mu)$$

The results (1.9) should be compared with the new values estimated through the program of this work. This comparison needs a renormalization of mixing operators (1.7) not involved in this thesis program.

Chapter 2

Lattice regularization and improvements

The purpose of this chapter is to introduce the reader to the fundamentals of lattice regularization and to detail the specific approach adopted in this study. In order to calculate Kaon matrix elements, a non perturbative approach is required and the path integral formulation provides for this [29]. As known, a path integral involves an *infinite* sum of field configurations defined on an *infinite* volume and time extension. Despite this, vacuum expectation values of physical observables yield to *finite* quantities. A well defined simulation needs a regularization that faces the problem of these infinities. For this reason lattice QFT is a very useful regularization. It involves discretizing spacetime, referred to as the lattice, along with a finiteness of the volume. The two most relevant sources of errors are the discretization of the space and the finite volume effects. To deal with these errors, a large number of improvements has been developed through the years and some of them find application in this work.

The first section will provide a general overview of lattice regularization of a quantum field theory. In the second and third sections I will discuss respectively gauge and fermion fields regularizations on the lattice; I will start from the simplest regularizations and I will progressively extend them to the improved ones, which are used. In the fourth section, a specific set of bosonic ghost fields will be described. The fifth section will delineate the lattice regularization employed in the present simulation. Finally, the sixth section provides an overview about the Open Boundary Conditions, which represent one of the two peculiarities of this work compared to those previously carried out.

2.1 Lattice regularization of QFT

A finite and discretized functional integral can be formulated by implementing the following modifications to the continuous functional integral [36][25]:

- ▷ The Minkowski space \mathbb{M}^4 is replaced with an hypercubic lattice of $N_{\text{time}} \times N_{\text{space}}^3$ points. The volume V and time extension T become finite quantities and the separation between two adjacent lattice points takes the name of *lattice spacing* a . Therefore, the lattice space is defined as:

$$\Lambda = \{x = a \cdot (n_1, n_2, n_3, n_4) | n_{1,2,3} = 0, \dots, N_{\text{space}} - 1 \text{ and } n_4 = 0, \dots, N_{\text{time}} - 1\}$$

Clearly the physical extension of the lattice is given by $a \cdot (N_{\text{time}}, N_{\text{space}}^3) = (T, L \times L \times L)$. Continuous spacetime symmetries - e.g. rotations - are now replaced by hypercubic symmetries on the lattice.

- ▷ Consider a set of quantum fields $\tilde{\phi}_i(x), i = 1, \dots, N_{\text{fields}}$ in the continuum theory. In lattice path integral formulation they are treated as smooth local functions defined on Λ :

$$\begin{aligned}\phi_i : \Lambda &\longrightarrow \mathbb{R}, \mathbb{C}, SU(N_C), \dots \\ x &\longmapsto \phi_i(x)\end{aligned}$$

- ▷ The continuum action of the fields $S^{\text{cont}}[\tilde{\phi}_1, \dots, \tilde{\phi}_{N_{\text{fields}}}]$ must be discretized - i.e. replace the derivatives with discrete derivatives and, eventually, add some terms.¹ The fundamental requirement is that the lattice action has the right continuum limit:

$$S^{\text{Lat}}[a; \phi_1, \dots, \phi_{N_{\text{fields}}}] \xrightarrow{a \rightarrow 0} S^{\text{cont}}[\tilde{\phi}_1, \dots, \tilde{\phi}_{N_{\text{fields}}}]$$

- ▷ The integration measure of the path integral takes the following form:

$$\mathcal{D}\tilde{\phi} \longmapsto \prod_{i=1}^{N_{\text{fields}}} \prod_{x \in \Lambda} d\phi_i(x)$$

For notational convenience the measure is again denoted by $\mathcal{D}\phi$.

These changes together constitute the *lattice regularization* of a continuum theory. Sometimes I will use the word “regularization” to refer to the action discretization, that’s the only non trivial part of a lattice regularization procedure.

As usual in continuum path integral, given an observable \mathcal{X} functional of the fields, its expectation value on the vacuum is given by:

$$\langle \mathcal{X}(x_1, \dots, x_K) \rangle = \frac{1}{\mathcal{Z}} \int \mathcal{D}\phi e^{-S_E[\phi_i]} \mathcal{X}[\phi_1, \dots, \phi_{N_{\text{fields}}}] (x_1, \dots, x_K)$$

where \mathcal{Z} is the usual partition function $\mathcal{Z} = \langle 1 \rangle$. The path integral provides theoretical tools to handle a non perturbative theory then all the quantities in lattice simulations must be evaluated through vacuum expectation values of some chosen observables [29]. This fact has consequences, for example the asymptotic extractions described in section 3.5.

In the case of QCD described in the previous chapter, the integration can be split in two parts: the *fermionic integration* $\langle \cdot \rangle_F$ with measure $\mathcal{D}\psi \mathcal{D}\bar{\psi}$ and the *Gauge integration* $\langle \cdot \rangle_G$ with measure $\mathcal{D}U$ ². Since it is impossible to numerically simulate Grassman variables, the fermionic integral requires a theoretical calculation while the simulation allows us to evaluate the Gauge integral:

$$\langle \mathcal{X} \rangle = \left\langle \langle \mathcal{X} \rangle_F^{\text{th.}} \right\rangle_G^{\text{sim.}}$$

¹ The additive terms must vanish in the continuum limit

² About the meaning of the variables U_μ , wait until the next section.

This is a fundamental step for the lattice simulations. If \mathcal{X} is a polynomial on the fermion fields, Wick theorem applies³ and a *fermion determinant* $\det(D[U])$ appears in the functional integral:

$$\begin{aligned}\langle \mathcal{X} \rangle &= \frac{1}{Z} \int \mathcal{D}U \mathcal{D}\psi \mathcal{D}\bar{\psi} e^{-S_G[U] - S_F[\psi, \bar{\psi}, U]} \times \mathcal{X}[\psi, \bar{\psi}] = \\ &= \frac{1}{Z} \int \mathcal{D}U e^{-S_G[U]} \det(D[U]) \times \text{Wick terms}[U] = \\ &= \frac{1}{Z} \int \mathcal{D}U e^{-S_G[U] + \text{Tr} \ln D[U]} \times \text{Wick terms}[U]\end{aligned}\quad (2.1)$$

Sometimes the exponentiated term $S_{\text{eff}}[U] = S_G[U] - \text{Tr} \ln D[U]$ is called *effective Gauge action*. Equation (2.1) and the concept of fermion determinant will be useful in the next sections. A good question is about the role of fermion determinant in the functional integral. It contains the interaction terms between Gauge fields U and fermions, so it introduces the fermion virtual loops in the correlation functions. In other words, the distinction between effective Gauge action and the standard action $S_G[U]$ resides in the presence of quark loops contributions. This can be easily checked in perturbation theory. For this reason, only *sea* quarks need a fermion determinant, while *valence* quarks are inserted only as external fermions. Is it noteworthy the existence of an approximation - not used in this work - called “quenched approximation” in which the fermion determinant is neglected. This approximation corresponds to the neglect of sea quarks loops. To better understand the sea vs valence concept the following image could be useful.

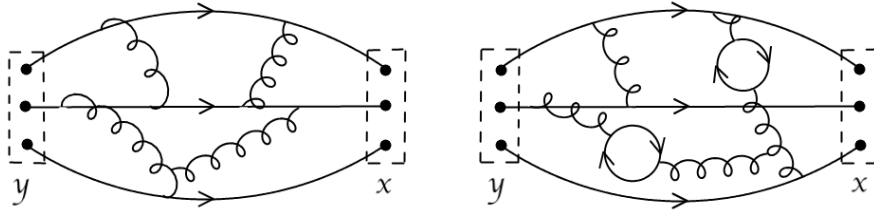


Figure 2.1. On the right: a complete baryon propagator $G_B(x, y) = \langle B(x) B^\dagger(y) \rangle$. On the left: the same propagator in quenched approximation. In non-perturbative QCD, most of the times gluon propagators are not drawn, because they are infinite in number. For this reason next graphs will not include them.

The general strategy to evaluate correlators like $\langle \mathcal{X} \rangle$ follows. First, the correlator must be calculated at different values of lattice spacing $\langle \mathcal{X} \rangle|_a$. Then a *continuum limit* of $\langle \mathcal{X} \rangle \equiv \langle \mathcal{X} \rangle|_0$ can be extracted for $a \rightarrow 0$. Since physics resides in the continuum limit, there is a sort of *residual freedom* in the choice of the regularization. All the valid regularizations share the same physical continuum limit, differing only by $O(a^n)$ terms, with $n \geq 1$. Clearly these terms are nothing but lattice artifacts that don't give contributions to the exact continuum limit and don't have any physical

³ Wick theorem holds only in case of bilinear actions:

$$S_F[\psi, \bar{\psi}, U] = \sum_{x, y} \bar{\psi}(x) D[U](x, y) \psi(y)$$

meaning. However the continuum limit is approached by extrapolation, then actions that contains only $O(a^2)$ lattice terms or higher give more precise values than actions with $O(a)$ terms. These regularized actions are called $O(a)$ -improved actions and some of them are described below. Moreover, an $O(a)$ -improved action can always be obtained from an $O(1)$ -action by adding some counterterms that cancel the $O(a)$ lattice artifacts. In some cases, an $O(a)$ -improved action guarantees an $O(a)$ -improvement only for a particular set of observables; for example a symmetry conservation could cause an $O(a)$ -improvement on some observables that have a definite quantum number under the given symmetry.

2.2 Gauge action

The first proposal to regularize Gauge and fermion action on the lattice was advanced by Wilson in 1974 [44]. Usually Gauge fields are denoted by $A_\mu(x) \equiv A_\mu^a(x)T_\square^a$ and the continuum action is defined in formula (1.1). An alternative way to introduce Gauge fields is to treat them as connections, by defining a Wilson line $W(x, y)$ [41]. This formulation is useful in this case because the steps towards lattice theory are very simple and natural. A Wilson line is defined by:

$$W(x, y) = P \left\{ \exp \left(i \int_y^x A_\mu(\omega) d\omega^\mu \right) \right\}$$

with P denoting the path ordering product. It is proven that a Wilson line transforms in this way under Gauge transformations $\mathcal{U} \in SU(N)$:

$$W(x, y) \mapsto \mathcal{U}(x)W(x, y)\mathcal{U}(y)^\dagger \quad (2.2)$$

By choosing an integration path in direction $\hat{\mu} = (\delta_{\mu 1}, \delta_{\mu 2}, \delta_{\mu 3}, \delta_{\mu 4})$ with length equal to the lattice spacing a , Wilson line is approximated by:

$$W_\mu(x + a\hat{\mu}, x) \approx \exp(iaA_\mu(x)) := U_\mu(x)$$

The line U_μ is called a *link variable* and it will be useful to build a Gauge invariant fermion action in the next section. It is represented as a line connecting a lattice point x with the adjacent point in direction $\hat{\mu}$, i.e. $x + a\hat{\mu}$ (or simply $x + \hat{\mu}$).

To provide a regularized Gauge action, a Gauge invariant quantity must be built. One simple way is to multiply four link variables in a way such that they link the initial point x to itself.

$$U_P^{\mu\nu}(x) \equiv U_\mu(x)U_\nu(x + \hat{\mu})U_{-\mu}(x + \hat{\mu} + \hat{\nu})U_{-\nu}(x + \hat{\nu})$$

This is called *plaquette* of link variables in the $\mu - \nu$ plane and it is shown in Figure 2.2. The trace of a plaquette is Gauge invariant and it is easy to prove by applying formula (2.2) and cyclicity property of the trace. Then the *Wilson Gauge action* is built in the following way:

$$S_G[U] = \frac{\beta}{3} \sum_{\{p\}} \text{Tr} [\mathbb{I} - U(p)] \quad (2.3)$$

where $\{p\}$ is the set of positively oriented plaquettes and $\beta = 6/g_0^2$ depends on the bare coupling g_0 . It can be proven that in the continuum limit this action corresponds to the dynamical part of Gauge action in formula (1.1). To do this,

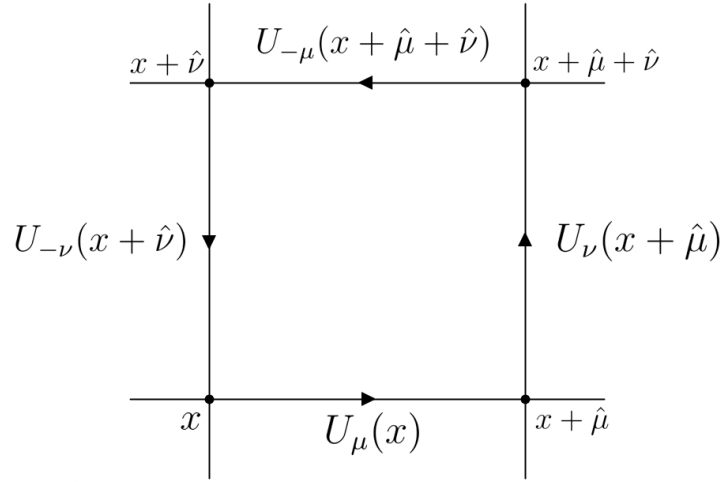


Figure 2.2. A plaquette in the $\mu - \nu$ plane, useful to build (2.3)

just apply BCH formula and the definition of the link variables [25]. By developing explicit calculations, it is clear that this action is not $O(a)$ -improved. Several $O(a)$ -improvements are available and some of them are expressed in the following way:

$$S_G[U] = \frac{1}{g_0^2} \left\{ c_0 \sum_{\{p\}} \text{Tr} [\mathbb{I} - U(p)] + c_1 \sum_{\{r\}} \text{Tr} [\mathbb{I} - U(r)] \right\} \quad (2.4)$$

where $\{r\}$ is a set of rectangles on the lattice, analogous to $\{p\}$. Depending on the choice of the coefficients c_0 and c_1 , it is possible to get different improvements. The chosen one uses $c_0 = 5/3$ and $c_1 = -1/12$ and takes the name of *Luscher-Weisz action* [22].

2.3 Fermion actions

A large number of different regularizations of fermions are available at current times. In this wide section I will describe some of them that differ from each other by improvements and other features. A shortlist of the regularizations described could be useful to clarify the general purpose, that's to give to the reader all the needed tools to understand the adopted regularization of the work (see section 2.5):

- ▷ In 2.3.1 I will introduce the basic actions of lattice QCD: the *Naive action* and the *Wilson-Dirac action*. They serve as a background to build other cutting edge actions.
- ▷ In 2.3.2 I will describe the Sheikholeslami-Wohlert term. It is a term to be added to Wilson-Dirac fermion action to get the $O(a)$ -improvement of the theory. It will also be useful for other reasons explained at the end of the chapter.

- ▷ The subsection 2.3.3 will describe the problem of zero modes related to the Wilson Dirac action. Moreover it introduces the issue of explicit chiral symmetry breaking on the lattice.
- ▷ The *twisted mass QCD* (tmQCD) and *Maximally twisted mass QCD* (Mt-mQCD), described in 2.3.4, are introduced to solve the problem of zero-modes. MtmQCD is a special case of tmQCD. Moreover MtmQCD has the property to be an $O(a)$ -improved action.
- ▷ Despite the powerful properties of tmQCD, it is not used in this work⁴ but it is replaced by the *Osterwalder-Seiler action*, very similar to it. In some particular cases OS action *coincides* with tmQCD. This regularization is described in 2.3.5.
- ▷ In section 2.4 I introduce some bosonic ghost fields needed to well simulate valence quarks.

2.3.1 Wilson-Dirac action

The continuum fermion euclidean lagrangian density $\mathcal{L}_0^E = \bar{\psi}_q(x) (\gamma_\mu D_\mu + m) \psi_q(x)$ can be discretized by following the steps in section 2.1. In order to achieve Gauge invariance, a covariant derivative on the lattice is introduced. The auxiliary Gauge fields take the form of link variables, i.e. Wilson lines. The resulting action is called *naive action* of fermions on the lattice [36][25]:

$$\begin{aligned} S[\psi, \bar{\psi}, U] &= a^4 \sum_{q,x} \bar{\psi}_q(x) \left(\gamma_\mu \frac{U_\mu(x) \psi_q(x + \hat{\mu}) - U_{-\mu}(x) \psi_q(x - \hat{\mu})}{2a} + m_q \psi_q(x) \right) = \\ &= a^4 \sum_{q,x} \bar{\psi}_q(x) \left(\frac{1}{2} \gamma_\mu (\nabla_\mu + \nabla_\mu^*) + m_q \right) \psi_q(x) \end{aligned}$$

where q is the flavour index and a sum over μ is implied. In the last line I've implicitly declared the discretized version of forward and backward covariant derivatives:

$$\begin{aligned} \nabla_\mu \psi(x) &= \frac{1}{a} [U_\mu(x) \psi(x + \hat{\mu}) - \psi(x)] \\ \nabla_\mu^* \psi(x) &= \frac{1}{a} [\psi(x) - U_\mu(x - \hat{\mu}) \psi(x - \hat{\mu})] \end{aligned}$$

It can be easily checked that the Gauge invariance of the action is achieved.

$$\text{Gauge transformations: } \begin{cases} \psi(x) \mapsto \mathcal{U}(x) \psi(x) \\ \bar{\psi}(x) \mapsto \bar{\psi}(x) \mathcal{U}(x)^\dagger \\ U_\mu(x) \mapsto \mathcal{U}(x) U_\mu(x) \mathcal{U}(x + \hat{\mu})^\dagger \end{cases}$$

for example $\bar{\psi}(x) \gamma_\mu U_\mu(x) \psi(x + \hat{\mu}) \mapsto \bar{\psi}(x) \mathcal{U}(x)^\dagger \mathcal{U}(x) \gamma_\mu U_\mu(x) \mathcal{U}(x + \hat{\mu})^\dagger \mathcal{U}(x + \hat{\mu}) \psi(x)$ is invariant; the same holds for the other terms.

In the free case ($U_\mu(x) = \mathbb{I}_3 \forall \mu, x$) this action gives the right continuum fermion propagator for $a \rightarrow 0$, but the problem of *fermion doubling* arises [36]: by taking the discrete Fourier transform of the discretized free Dirac operator, it can be proved that its inverse has poles in $p_\mu = (0, 0, 0, 0)$ and 15 many other non physical momenta - e.g.

⁴ In section 2.6 it will be clear how the tmQCD is not necessary: its properties are achieved in other ways.

$p_\mu = (\pi/a, 0, 0, 0), (0, \pi/a, 0, 0), (\pi/a, \pi/a, 0, 0), \dots$. These non physical momenta are named *doublers* and are suppressed through the insertion of an additive piece to the action:

$$\begin{aligned} S[\psi, \bar{\psi}, U] &= a^4 \sum_{q,x,y} \bar{\psi}_q(x) \left(D_{xy}^W(r_q) + m_q \delta_{xy} \right) \psi_q(y) \\ D_{x,y}^W(r_q) &= -\frac{1}{2a} \sum_{\mu=\pm 1}^{\pm 4} [(\mathbb{I}_4 r_q - \gamma_\mu) U_\mu(x) \delta_{x,y-\hat{\mu}}] + \frac{4r_q}{a} \delta_{xy} = \\ &= \frac{1}{2} \left(\gamma_\mu (\nabla_\mu + \nabla_\mu^*) - a r_q \nabla_\mu^* \nabla_\mu \right)_{xy} \end{aligned} \quad (2.5)$$

where $\gamma_{-\mu} \equiv -\gamma_\mu$ and the Wilson parameters r_q must satisfy $|r_q| \in (0, 1]$ for each q . Whenever the sum over μ is omitted, it is to be understood as a sum over $\mu = 1, \dots, 4$. The usual choice for the parameter r_q is 1, while the value $r_q = 0$ gives the naive action. Action (2.5) is called *Wilson-Dirac action* of fermions on the lattice and it is the most used fermion discretization on the lattice. Because of the additive piece, the doublers gets an infinite mass for $a \rightarrow 0$, thus they tend to inexcitable modes of the theory. In this simple way the doublers problem is solved. The definition of this action is not equal to the one in [36][25] but equivalent. At the current point, there are no $O(a)$ -improvements.

2.3.2 $O(a)$ -improvement: Sheikholeslami-Wohlert term

The theory is $O(a)$ -improved through the insertion of the Sheikholeslami-Wohlert (SW) term in the action [42]. It consists of the following replacement of the Dirac-Wilson operator:

$$D_{xy}^W \mapsto D_{xy}^W + c_{SW} \frac{ia}{4} \sigma_{\mu\nu} \hat{F}_{\mu\nu}(x) \delta_{xy} \quad (2.6)$$

where $\hat{F}_{\mu\nu}$ is the discretized version of the strength tensor $F_{\mu\nu}$. The constant c_{SW} depends on the bare Gauge coupling g_0 and it has to be chosen to get the $O(a)$ -improvement. To achieve the improvement, current densities need counterterms as well, except for the pseudoscalar densities $P^a = \bar{\psi} \gamma_5 \mathcal{T}^a \psi$ - where \mathcal{T}^a are generators of $SU(N_f)$. Currents and densities are modified in the following way:

$$\begin{aligned} A_\mu^{a,\text{ren}} &= Z_A (1 + b_A a m_q) \left[A_\mu^a + a c_A \tilde{\partial}_\mu P^a \right] \\ V_\mu^{a,\text{ren}} &= Z_V (1 + b_V a m_q) \left[V_\mu^a + a c_V \tilde{\partial}_\nu T_{\mu\nu}^a \right] \\ P^{a,\text{ren}} &= Z_P (1 + b_P a m_q) P^a \end{aligned}$$

where the partial derivatives are defined as the direction-symmetrized ones $\tilde{\partial}_\mu = \frac{1}{2}(\partial_\mu^{\text{forw.}} + \partial_\mu^{\text{backw.}}) = \frac{1}{2}(\partial_\mu + \partial_\mu^*)$. The above expressions involve also renormalization constants. The coefficients $\{b_A, b_V, b_P, c_A, c_V\}$ could be determined both non-perturbatively and by perturbation theory expansion [42]. Because of the present purpose, non-perturbative values are chosen. Some results of c_{SW} for different values of g_0 with 3 flavours sea quarks are reported in [11].

2.3.3 Chiral symmetry and fermion zero modes

The Wilson-Dirac action (2.5) preserves the hypercubic lattice symmetry, parity and charge conjugation. However it does not preserve chiral symmetry $SU(N)_A \times U(1)_A$

discussed in Chapter 1. The Wilson term $r_q \bar{\psi}_q(x) \psi_q(x + \hat{\mu})$ explicitly breaks both $SU(N)_A$ and $U(1)_A$, thus these groups are broken also in the massless case, unlike the continuum theory, in which the breakdown occurs for other reasons (not explicitly). In principle this breaking represents a problem because some features of the QCD are strictly related to the spontaneous breaking mechanism of the axial currents, as already discussed in Chapter 1. In fact, this symmetry breaking could cause an unwanted mixing of operators in the renormalization procedure (for example see Chapter 3). One may think about a new regularization that both preserves chiral symmetry and solves the doublers problem, but this is impossible because of a theorem by Nielsen and Ninomiya [36]. One common way to treat chiral symmetry on the lattice is to add some counterterms to observables that restore the symmetry up to $O(a^n)$ effects, namely to treat an approximate chiral symmetry with the right continuum limit. There exists also a fermion regularization that possesses a continuum chiral symmetry without introducing doublers, the *Wilson-Ginsparg* fermions, but they are not used in this work.

Moreover, the Wilson Dirac operator could experience zero modes, i.e. null eigenvalues. If we consider the Wilson-Dirac operator introduced above with mass different from zero, eigenvalues can always be written as:

$$\Lambda_j[U] = m + \lambda_j[U] \quad (2.7)$$

where $\lambda_j[U]$ is the eigenvalue of massless Wilson-Dirac operator. There could exist some gauge configurations called *exceptional configurations* such that $\lambda_i[U] \approx -m$ for some i . Very small eigenvalues $\Lambda[U]$ modify the fermion determinant $\det(D[U])$ in equation (2.1). From a practical point of view, these small eigenvalues and the consequent decrease of the fermion determinant could be problematic [22]. They could cause long autocorrelation times in simulation algorithm HMC (Hybrid Monte Carlo) due to the difficulties in inverting the determinant. Then HMC would require a larger number of resources to suppress autocorrelation effects. In this case the word *autocorrelation* refers to the correlation between different Gauge configurations generated by the HMC algorithm. In principle, they must be uncorrelated from each other to guarantee the randomness of the Monte Carlo method.

In the next sections I will introduce some setup features that help decrease autocorrelation times. The first is the introduction of a *twisted mass term* in the fermion action that plays the role of an infrared cutoff. The other and new feature is the implementation of Open Boundary Conditions, widely described and developed in section 2.6. At the end of this Chapter I will explain how Open Boundary Conditions replace (partially) the role of tmQCD.

2.3.4 Twisted Mass QCD (tmQCD)

In order to solve the problem of zero modes of Wilson-Dirac operator and the consequent broadening of autocorrelation times, a twisted mass term has been added to the action. It works as an infrared cutoff for the spectrum of the Dirac-Wilson operator $D^W \equiv D$, i.e. absolute value of eigenvalues in formula (2.7) will be greater than a given value:

$$|\Lambda_j[U]| = |\lambda_j[U] + m| \geq \Lambda_{\text{IR}} > 0$$

Moreover, twisted mass QCD (tmQCD) can be used as $O(a)$ -improvement in some particular cases. A short explanation follows.

First of all, I need to introduce the *twist transformations* [22]. They apply to

degenerate isospin doublets of fermions in flavour space. For example *up* and *down* quarks are denoted by:

$$\psi = \begin{pmatrix} u \\ d \end{pmatrix}$$

We suppose that the continuum action has a global symmetry group (or subgroup) $SU(2)_F$ in flavour space, with generators $\sigma_i/2$ where $\{\sigma_i\}$ are Pauli matrices. A twist transformation consists in:

$$\begin{cases} \psi \mapsto \psi' = \mathbf{T}(\alpha) \psi \\ \bar{\psi} \mapsto \bar{\psi}' = \bar{\psi} \mathbf{T}(\alpha) \end{cases} \quad \mathbf{T}(\alpha) = \exp \left(i\alpha \gamma_5 \sigma^3 / 2 \right) \quad (2.8)$$

that applies both to continuum and lattice theories. Then it is defined a lattice action of the form:

$$S_{\text{tm}}[\psi, \bar{\psi}, U] = a^4 \sum_{x,y} \bar{\psi}(x) \left(D_{xy} + m\delta_{xy} + i\mu_q \gamma_5 \sigma^3 \delta_{xy} \right) \psi(y) \quad (2.9)$$

with D the massless Wilson-Dirac operator and μ_q the *twisted mass* term. It is important to underline that in this form, the action (2.9) is not a good regularization yet because its continuum limit does not coincide with usual QCD. In fact, in principle the twisted mass term μ_q has no direct physical meaning.⁵ Its presence is just a mathematical trick to modify the fermion determinant in such a way that fermion modes exhibit a positive lower bound:

$$\begin{aligned} \det(D\mathbb{I}_2 + m\mathbb{I}_2 + i\mu_q \gamma_5 \sigma^3) &= \det(D + m + i\mu_q \gamma_5) \cdot \det(D + m - i\mu_q \gamma_5) = \\ &= \det(D + m + i\mu_q \gamma_5) \cdot \det(\gamma_5 [D + m - i\mu_q \gamma_5] \gamma_5) = \\ &= \det(D + m + i\mu_q \gamma_5) \cdot \det(D^\dagger + m - i\mu_q \gamma_5) = \\ &= \det \left((D + m + i\mu_q \gamma_5) \cdot (D^\dagger + m - i\mu_q \gamma_5) \right) = \\ &= \det \left((D + m)(D + m)^\dagger + \mu_q^2 \right) \end{aligned}$$

The relation $\gamma_5 D \gamma_5 = D^\dagger$ was used.⁶ Since the matrix $(D + m)(D + m)^\dagger$ is hermitian and positive definite, it has real eigenvalues ≥ 0 , thus the μ_q^2 term introduce a positive infrared cutoff in the spectrum. One remarkable argument is the need of two degenerate flavours with different twisted mass signs. Then the implementation of a single flavour - e.g. the *strange* quark - is not possible.⁷

By applying a transformation (2.8) the differential operator D is changed (see Appendix B), while the mass terms preserve their form up to a redefinition of terms:

$$\begin{aligned} m' &= m \cos(\alpha) + \mu_q \sin(\alpha) \\ \mu_q' &= -m \sin(\alpha) + \mu_q \cos(\alpha) \end{aligned} \quad (2.10)$$

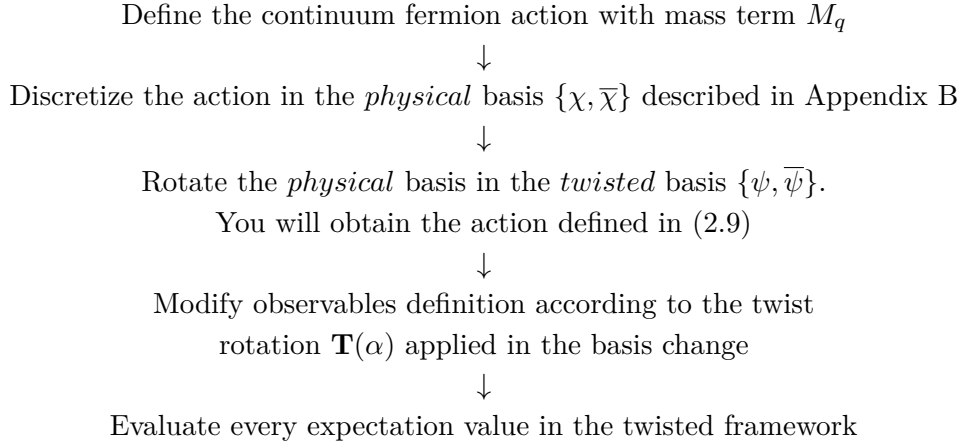
It is straightforward to guess that particular choices for α exist. For example, $\alpha = \arctan(\mu_q/m)$ makes the twisted mass μ_q' vanish, while $\alpha = \pm\pi/2$ gives the so called *Maximal Twist* described below. The latter choice is particularly relevant because it implies an automatic $O(a)$ -improvement, as we will see below.

⁵ I will explain later how to relate μ_q to a physical parameter.

⁶ This relation holds in case of Wilson-Dirac operator D^W but there are regularizations in which this relation is not valid.

⁷ In fact, the current sea configurations with u, d, s quarks do not use tmQCD but solve the null determinant problem through the Open Boundary Conditions.

In principle there are no reasons to introduce a finite non physical term μ_q in the action. In fact the tmQCD action (2.9) does not have the right continuum limit to be a “well defined” action, but there exists an excamotage to make it useful. Through a transformation (2.8) it is possible to define another fermion basis, named *physical basis* $\{\chi, \bar{\chi}\}$, rotated with respect to the *twisted basis* $\{\psi, \bar{\psi}\}$ that gives the tmQCD. In Appendix B it is shown how this change of variables affects the action and how this tends - in the continuum limit $a \rightarrow 0$ - to the standard QCD action. Because of the variables change $\{\chi, \bar{\chi}\} \leftrightarrow \{\psi, \bar{\psi}\}$ the new action mass parameters (m, μ_q) are subjected to (2.10). The new *physical* mass term is defined by $M_q = \sqrt{m^2 + \mu_q^2}$ while the new twisted mass term vanishes: the twist transformation (2.8) “brings” a fraction of M_q into the twisted mass according to α and viceversa. Then the term M_q is the “true” mass term of lattice theory, while m and μ_q are just its *polar components*. Then a good definition of twisted mass lattice QCD is achieved by following this path:



The fourth step is an essential point in the evaluation of correlators in tmQCD. Details about it are reported in Appendix B and a wide use of it is into the next Chapter. Let’s consider an example in the case of maximal twist ($\alpha = \pm\pi/2$):

$$A_{\mu}^{1,\text{phys}} \xrightarrow{\mathbf{T}(\alpha=\pm\pi/2)} \left(\cos(\alpha) A_{\mu}^{1,\text{tw}} + \sin(\alpha) V_{\mu}^{2,\text{tw}} \right) \Big|_{\alpha=\pm\pi/2} = \pm V_{\mu}^{2,\text{tm}}$$

where the superscript “phys” means that the physical basis $\{\chi, \bar{\chi}\}$ it is used. Similarly for the superscript “tm” and the basis $\{\psi, \bar{\psi}\}$. The integer superscripts 1, 2 refers to the generators of $SU(2)_F$.

Maximal Twist (MtmQCD) and $O(a)$ –improvement

Twisted mass QCD was first introduced to solve the problem of exceptional configurations and the zero modes of Wilson-Dirac operator D . Nevertheless its feature to be $O(a)$ –improved at maximal twist is equally - or more - relevant.

This is not the place for a detailed and long proof, so I limit myself to report some results based on the paper by R. Frezzotti and G. C. Rossi [20]. The setup consists in a MtmQCD with a Sheikholeslami-Wohlert term. The proof is based on the fact that the continuum QCD with two massless flavours has the following discrete symmetry:

$$\psi \mapsto i\gamma_5 \sigma^1 \psi \quad \bar{\psi} \mapsto i\bar{\psi} \gamma_5 \sigma^1$$

Then every operator \mathcal{X} can be splitted in an even and an odd part of the above transformation. The achievements are the following:

- Expectation values of even operators $\langle \mathcal{X}^{(+)} \rangle$ are $O(a)$ -improved, i.e. free of $O(a)$ terms. As a consequence some of the $O(a)$ -improved quantities are hadronic masses and decay constants.
- Expectation values of odd operators $\langle \mathcal{X}^{(-)} \rangle$ are null in the continuum limit. In particular there are no $O(1)$ terms and there are at least $O(a)$ terms.
- Matrix elements $\langle \Psi^1 | \mathcal{X} | \Psi^2 \rangle$ in which the parity of \mathcal{X} is equal to the product of the parities of the external states are $O(a)$ -improved.

I conclude this short section with a report of MtmQCD action in both physical and twisted basis plus the SW term needed in [20]:

$$S_{\text{tm}}^{\text{phys}}[\chi, \bar{\chi}, U] = a^4 \sum_{x,y} \bar{\chi}(x) \left(D_{xy}^{\text{tm}} + M_q \mathbb{I}_2 \delta_{xy} + \frac{ia}{4} c_{SW} \sigma_{\mu\nu} \hat{F}_{\mu\nu}(x) \delta_{xy} \right) \chi(y)$$

$$S_{\text{tm}}^{\text{tw}}[\psi, \bar{\psi}, U] = a^4 \sum_{x,y} \bar{\psi}(x) \left(D_{xy} + m_{\text{cr}} \delta_{xy} + i\mu_q \gamma_5 \sigma^3 \delta_{xy} \right) \psi(y)$$

where, in the twisted basis, the physical mass is set to the critical value in order to get a null renormalized mass. In this case the Wilson parameter is $r = 1$ for each flavour.

2.3.5 Osterwalder-Seiler fermions

A discretization very similar to tmQCD can be developed and the corresponding fermions take the name of *Osterwalder-Seiler* (OS) fermions. The conceptual framework follows. The abovementioned work about tmQCD and twist rotations is replicated with just one difference: there is no flavour space and each flavour is treated alone. Thus I define another set of transformations similar to eq. (2.8), without the generator $\sigma^3/2$ and acting of a single flavour $\{\psi, \bar{\psi}\}$:

$$\begin{cases} \psi \mapsto \psi' = \mathbf{J}(\alpha, r) \psi \\ \bar{\psi} \mapsto \bar{\psi}' = \bar{\psi} \mathbf{J}(\alpha, r) \end{cases} \quad \mathbf{J}(\alpha, r) = \exp \left(ir \frac{\alpha}{2} \gamma_5 \right) \quad (2.11)$$

One remarkable argument is the presence of the Wilson parameter r in the rotation \mathbf{J} . This has some implications, for example the following property:

$$\mathbf{J}(\alpha, r = \pm 1) = \mathbf{J}(\pm \alpha, r = 1)$$

As a consequence, the rotation of $\pi/2$ of a flavour with $r = -1$ and the rotation of $-\pi/2$ of an $r = 1$ flavour are equivalent. It will be useful to treat the $O(a)$ -improvement proposed in [21], described in next chapters.

Also in the OS case it is possible to define a physical basis $\{f, \bar{f}\}$ and a twisted basis $\{q, \bar{q}\}$. They are related to each other through an OS twist $\mathbf{J}(\alpha, r)$ and described in Appendix B. The actions in the two basis - at maximal twist $\alpha = \pi/2$ - are:

$$S_{\text{OS}}^{\text{phys}}[f, \bar{f}, U] = a^4 \sum_{x,y} \bar{f}(x) \left(D_{xy}^{\text{OS}} + M_q \delta_{xy} \right) f(y)$$

$$\text{with } D^{\text{OS}} = \frac{1}{2} \gamma_\mu (\nabla_\mu + \nabla_\mu^*) + i \frac{a}{2} \gamma_5 \nabla_\mu^* \nabla_\mu - i \gamma_5 m_{\text{cr}}$$

$$\text{and } M_q = \sqrt{m_{\text{cr}}^2 + \mu_q^2}$$

$$S_{\text{OS}}^{\text{tw}}[q, \bar{q}, U] = a^4 \sum_{x,y} \bar{q}(x) \left(D_{xy} + m_{\text{cr}} \delta_{xy} + ir_q \mu_q \gamma_5 \delta_{xy} \right) q(y)$$

Now I want to give an interpretation of these actions with respect to the tmQCD case. Consider an isospin degenerate doublet $\chi = (f_1, f_2)$. In the case of tmQCD the flavours f_1 and f_2 are subject to rotation (2.8), then the first flavour rotate of an angle α while the latter of $-\alpha$ because of the presence of σ_3 . In the case of OS twist (2.11) each flavour rotates independently. Obviously by taking the two flavours f_1 and f_2 with equal masses and rotations respectively $\pm\alpha$, the tmQCD is recovered. Another way to recover tmQCD is to choose the same rotation angle $\alpha = \pi/2$ and $r_1 = -r_2$.

As in tmQCD, the change of basis $\{f, \bar{f}\} \leftrightarrow \{q, \bar{q}\}$ leaves the expectation value of an observable \mathcal{X} unchanged.

$$\langle \mathcal{X}[f, \bar{f}] \rangle_{(M_q, 0)} = \langle \mathcal{X}[\mathbf{J}(\alpha, r)q, \bar{q}\mathbf{J}(\alpha, r)] \rangle_{(m_q, \mu_q)} = \langle \mathcal{X}_{OS}^{\text{tw}}[q, \bar{q}] \rangle_{(m_q, \mu_q)}$$

To be coherent in the basis change, one must (OS) twist also the observable $\mathcal{X} \mapsto \mathcal{X}_{OS}^{\text{tw}}$. The basis change and the operators change ($P, S, A_\mu, V_\mu, T_{\mu\nu}, \bar{T}_{\mu\nu}$) are described in Appendix B. Notice the subscripts $(M_q, 0)$ and (m_q, μ_q) : they explicitly define action parameters. Such parameters transform according to equations (2.10), formulae used in the tmQCD case.

Clearly the proof in section 2.3.4 about the positivity of fermion determinant, in general, is no longer valid. Open Boundary Conditions will solve this problem. Moreover I will explain in Section 3.4 how $O(a)$ -improvement is recovered with OS fermions, thanks to the strategy worked out by R. Frezzotti and G. C. Rossi [21]. In such a way tmQCD is no longer necessary.

2.4 Sea vs Valence: need for bosonic ghosts

As already mentioned, QCD quarks are split in two sets: valence and sea quarks. In particular, sea quarks are responsible of the virtual loops taking part in the interactions. This is clarified by Figure 2.1. These interactions are entirely embedded in the fermion determinant in equation (2.1). In perturbation theory it is possible to prove the last statement⁸ order by order. Now, let's imagine that valence and sea quarks are represented by different fermions, eventually two copies of each flavour: u_v, d_v, s_v for valence and u_s, d_s, s_s in the sea.⁹ It should be clear that only sea quarks must give contributions through their determinant. So a natural question arises: how can I avoid to treat valence quarks determinant?

The procedure to answer the question was first introduced by Morel [37] and it is very similar to the one introduced by de Wit, Faddeev and Popov to quantize non abelian Gauge fields [43]. Integrating over valence fields $\{\psi, \bar{\psi}\}$, one automatically gets a $\det(D^{\text{val}}[U])$. Moreover I know that a Gaussian-like integral over bosonic complex variables has the following result:

$$\int \prod_{k=1}^N d\xi_k d\xi_k^\dagger e^{-\sum_{ij} \xi_i^\dagger M_{ij} \xi_j} = \frac{(2\pi)^N}{\det(M)}$$

The strategy involves the introduction of a set of *fermion ghosts* $\{\phi, \bar{\phi}\}$ in order to cancel the un-wanted fermion determinant. These fermion ghosts are nothing but

⁸ Done in the course of Quantum Field Theory 2022-2023 by Mauro L. Papinutto.

⁹ Moreover, suppose that sea and valence are regularized in different ways. Sea quarks involve a bilinear operator D_{xy}^{sea} , while valence quark D_{xy}^{val} .

Dirac spinors, colour equipped and satisfying a bosonic commutation relation:

$$\begin{aligned} [\phi_\alpha(\vec{x}, t), \bar{\phi}_\beta(\vec{y}, t)] &= \delta_{\alpha\beta} \delta^{(3)}(\vec{x} - \vec{y}) \\ [\bar{\phi}_\alpha(\vec{x}, t), \bar{\phi}_\beta(\vec{y}, t)] &= [\phi_\alpha(\vec{x}, t), \phi_\beta(\vec{y}, t)] = 0 \end{aligned}$$

Let \mathcal{X} be any observable which depends only on valence quarks and Gauge fields. Then the integral over both a valence quark¹⁰ $\{\psi_v, \bar{\psi}_v\}$ and its respective bosonic ghost $\{\phi_v, \bar{\phi}_v\}$ reads:

$$\begin{aligned} W[U] &= \\ &= \int \mathcal{D}\psi_v \mathcal{D}\bar{\psi}_v \mathcal{D}\phi_v \mathcal{D}\bar{\phi}_v e^{-\sum_{x,y} (\bar{\psi}_v(x) D_{xy}^{\text{val}} \psi_v(y) + \bar{\phi}_v(x) D_{xy}^{\text{val}} \phi_v(y))} \mathcal{X}[\psi_v, \bar{\psi}_v, U] = \\ &= \int \mathcal{D}\phi_v \mathcal{D}\bar{\phi}_v e^{-\sum_{xy} \bar{\phi}(x) D_{xy}^{\text{val}} \phi(y)} \det(D^{\text{val}}[U]) \times \text{Wick terms}[U] = \\ &= \frac{\det(D^{\text{val}}[U])}{\det(D^{\text{val}}[U])} \times \text{Wick terms}[U] = \text{Wick terms}[U] \end{aligned}$$

The meaning of the above calculation is very simple. The integral gives only the Wick contractions which depend on fixed Gauge field U . The vacuum expectation value $\langle \mathcal{X} \rangle$ is obtained by integrating \mathcal{X} over *all* the fields, i.e., by integrating $W[U]$ over the Gauge fields and the sea quarks $\{\psi_s, \bar{\psi}_s\}$:

$$\begin{aligned} \langle \mathcal{X} \rangle &= \frac{1}{\mathcal{Z}} \int \mathcal{D}U \mathcal{D}\psi_s \mathcal{D}\bar{\psi}_s e^{-S_G[U] - S_{\text{sea}}[\psi_s, \bar{\psi}_s, U]} W[U] = \\ &= \frac{1}{\mathcal{Z}} \int \mathcal{D}U e^{-S_G[U]} \det(D_{\text{sea}}[U]) W[U] = \\ &= \frac{1}{\mathcal{Z}} \int \mathcal{D}U e^{-S_{\text{eff}}[U]} \times \text{Wick terms}[U] \end{aligned}$$

This completes the proof that the ghost strategy introduced in [37] does work. In fact in the above formula Wick terms are integrated over all the possible internal quantum processes generated by the effective action $S_{\text{eff}}[U]$. This is exactly what the functional integral should do in quantum field theory.

2.5 Adopted lattice setup

In lattice QCD usually fields of the sea sector (Gauge and sea quarks) are generated through very long and complex simulations. These sets of fields - called *ensembles* - are used to evaluate expectation values of observables as explained at the beginning of this chapter (Formula (2.1)). In the present work I use a set of configurations by CLS [10] (Coordinated Lattice Simulations)¹¹, generated through the **open-QCD**¹² simulation programs for lattice QCD. The ensembles are generated with $N_f = 2 + 1$ quarks in the sea sector, clearly referred to the flavour doublet *up-down* and the *strange*. Periodic boundary conditions in space directions are used, while the time direction is subject to Open Boundary Conditions (OBC). To avoid misunderstandings, the notation used in the rest of the work is the one described below. I briefly report the adopted actions in the sea sector and the action used for the valence

¹⁰ the extension to many flavours is trivial.

¹¹ Coordinated Lattice Simulations: <https://wiki-zeuthen.desy.de/CLS/>

¹² Open-QCD packages: <https://luscher.web.cern.ch/luscher/openQCD/index.html>

quarks [27].

Gauge action: Lüscher-Weisz $O(a)$ -improved Gauge action as in formula (2.4):

$$S_G[U] = \frac{1}{g_0^2} \left(\frac{5}{3} \sum_{\{p\}} \text{Tr} [\mathbb{I} - U(p)] - \frac{1}{12} \sum_{\{r\}} \text{Tr} [\mathbb{I} - U(r)] \right)$$

Sea quarks action: Wilson-Dirac fermions equipped with the Sheikholeslami-Wohlert term (2.6) to ensure the $O(a)$ -improvement. From now on the sea quarks are denoted by $\{f_q, \bar{f}_q\} = \{f_u, \bar{f}_u, f_d, \bar{f}_d, f_s, \bar{f}_s\}$.

$$S^{\text{sea}}[f, \bar{f}, U] = a^4 \sum_{q=u,d,s} \sum_x \bar{f}_q(x) \left[D^{WD} + \frac{ia}{4} c_{SW} \sigma_{\mu\nu} \hat{F}_{\mu\nu} + m_q^{\text{bare}} \right] f_q(x) \quad (2.12)$$

The quark mass parameters are set in very peculiar way. In order to achieve $O(a)$ -improvement, the bare coupling g_0 is modified by additive terms proportional to $\text{Tr}(M_q^{\text{bare}}) = 2m_{ud}^{\text{bare}} + m_s^{\text{bare}}$ [8]:

$$\tilde{g}_0^2 = g_0^2 \left(1 + \frac{1}{3} a \cdot b_g \cdot \text{Tr}(M_q^{\text{bare}}) \right)$$

with b_g constant to be determined. The generated ensembles differ from each other by the value of the bare quark masses, but the trace $\text{Tr}(M_q^{\text{bare}})$ is kept constant in order to preserve the $O(a)$ -improvement of g_0 . I want to stress that the constant trace of bare masses does not imply that the trace of renormalized masses is constant.

Valence quarks action: Osterwalder-Seiler fermions with the Sheikholeslami-Wohlert term. In this case the fermions are denoted by $\{\psi_q, \bar{\psi}_q\}$ and the action is expressed in the (OS) twisted basis.

$$S^{\text{val}}[\psi, \bar{\psi}, U] = a^4 \sum_{q,x} \bar{\psi}_q(x) \left[D^{WD} + \frac{ia}{4} c_{SW} \sigma_{\mu\nu} \hat{F}_{\mu\nu} + \mathbf{m}_{qq}^{\text{cr}} + i\gamma_5 \boldsymbol{\mu}^{\text{bare}} \right] \psi_q(x) \quad (2.13)$$

where $\mathbf{m}^{\text{cr}} = \text{diag}(m_{\text{cr}}, \dots, m_{\text{cr}})$ contains the bare mass parameters of the action, which are set to the critical value. In such a way the maximal twist $\alpha = \pi/2$ is achieved and the physical bare masses are entirely embedded in the twisted mass terms in $\boldsymbol{\mu}^{\text{bare}}$. Thus the matrix $\boldsymbol{\mu}^{\text{bare}}$ is diagonal and it contains the physical bare masses of the theory. To be precise, it contains the values $r_q \cdot \mu_q$ but, from this point on, the Wilson parameters r_q are absorbed in the μ_q .

The value of the flavour index q is a not trivial argument. By following the work of Frezzotti and Rossi [21], each valence quark must have a partner of the same flavour. In this sense, the the index q runs over this set $\{u, u', d, d', s, s'\}$. Particular attention must be given to the difference between two replicas of the same flavour - for example d, d' . I know from [21] that, chosen certain observables involving only two physical QCD flavours, twisted masses of lattice flavours q_1, q'_1, q_2, q'_2 must satisfy these relations:

$$\begin{aligned} |\mu_1| &= |\mu'_1| & |\mu_2| &= |\mu'_2| \\ \mu_1, \mu'_1, \mu_2 &> 0 & \mu'_2 &< 0 \end{aligned}$$

Since in this work I only use pions and neutral Kaons, the possible flavour couples are (u, d) and (d, s) . A simple way to satisfy previous relations is the following:

$$\boldsymbol{\mu}^{\text{bare}} = \text{diag}(\mu_l, \mu_l, \mu_l, -\mu_l, \mu_s, \mu_s)$$

To better explain, $\mu_u = \mu_{u'} = \mu_d = -\mu_{d'} := \mu_l$ (l stands for “light”), while $\mu_s = \mu_{s'}$ (s stands for “strange”). Moreover, because of the relative minus sign between the parameters of u, u' and d' , I can state that the regularization is not only an OS one, but also a MtmQCD regularization in which the flavour doublet can be either (u, d) or (u', d) .

Valence ghosts action: As explained in the previous section, bosonic Dirac-spinor ghosts need to be involved to cancel the valence fermions determinant. I refer to ghosts through the symbols $\{\phi_q, \bar{\phi}_q\}$. The ghosts action is analogous to the valence quarks action:

$$S^{\text{gh}}[\phi, \bar{\phi}, U] = a^4 \sum_{q,x} \bar{\phi}_q(x) \left[D^{WD} + \frac{ia}{4} c_{SW} \sigma_{\mu\nu} \hat{F}_{\mu\nu} + \mathbf{m}_{qq}^{\text{cr}} + i\gamma_5 \boldsymbol{\mu}^{\text{bare}} \right] \phi_q(x) \quad (2.14)$$

Notes

(1) In order to describe the same physical quarks, the renormalized masses of sea and valence must be matched. There are two $O(a)$ –improved procedures to do that, both described in [12]. The first provides a direct matching of renormalized quark masses extracted from the PCAC¹³ relations:

$$\mu_q^{\text{ren}}|_{\text{valence}} = m_q^{\text{ren}}|_{\text{sea}} + o(a)$$

This method requires some counterterms for an $O(a)$ –improved determination of $m_i^{\text{ren}}|_{\text{sea}}$. A very precise treatment of the problem can be found in [13]. The second method is simpler and consists in the match of pseudoscalar mesons masses evaluated from both sea and valence quarks.

$$\begin{cases} m_\pi|_{\text{valence}} = m_\pi|_{\text{sea}} \\ m_K|_{\text{valence}} = m_K|_{\text{sea}} \end{cases} \implies \mu_q^{\text{ren}}|_{\text{valence}} = m_q^{\text{ren}}|_{\text{sea}} + o(a)$$

It is proven that the second method ensures a natural $O(a)$ –improvement, without the requirement of additive counterterms a la Symanzik. In this case m_π represents the mass of charged pions π^\pm and m_K is the mass of the Kaons.

(2) Another relevant feature is the presence of SW term in both sea and valence fermion actions. It enforces the sea and valence sectors to share the same renormalization constants, that’s a great simplification.

(3) The use of Open Boundary Conditions in time direction is an artefact that allows low autocorrelation times of the simulation. It is the principal feature of this work and it is described below.

2.6 Open Boundary Conditions

To conclude this chapter I give an overview of the Open Boundary Conditions, one of the two principal features of this work. They were introduced by S. Luscher and S. Schaefer [34] to solve the problem of long autocorrelation times of some observables of the sea configurations. This paragraph doesn’t contain formal or overly technical developments but simply provides an overview of what Open Boundary Conditions

¹³ PCAC must be revisited in the twisted basis. For more infos see Appendix B.

are and where they emerge in the context of Lattice QCD. A quick reformulation of Lattice QFT will be necessary.

As previously mentioned, Gauge configurations are generated through algorithms that transition from a configuration to another with a certain probability. Examples of these algorithms include HMC (Hybrid Monte Carlo) or SMD (Stochastic Molecular Dynamics, a.k.a. Generalized HMC). An ideal goal of a lattice simulation is the generation of totally uncorrelated Gauge configurations, which is evidently impossible at 100%. This is because uncorrelated configurations better simulate the path integral. To quantify the correlation between different configurations, certain observables are introduced and their autocorrelation functions are studied. The most commonly used observable is the *topological charge*:

$$Q_{\text{top}} = -\frac{1}{32\pi^2} \int_M d^4x \epsilon_{\mu\nu\rho\sigma} \text{Tr} [F_{\mu\nu}(x) F_{\rho\sigma}(x)]$$

In the above formula Q_{top} is defined in the continuum limit. A similar definition can be easily worked out in lattice environment. Sometimes other observables are chosen, for example the square of the topological charge. In fact, the VEV of topological charge in pure Yang Mills $SU(3)$ theory is expected to vanish for parity reasons¹⁴, then Q_{top}^2 seems to be a better choice. For each observable, a specific time τ is defined, known as the *autocorrelation time* of the observable.¹⁵ The τ quantifies the autocorrelation of the given observable at two different times. It has been observed that the autocorrelation time of the topological charge, τ_Q , grows as a^{-5} as the continuum limit is approached [31]. This leads to extremely large autocorrelation times.

This catastrophic behaviour was confirmed both by direct computations and from a theoretical framework. The birth of Open Boundary Conditions resides in the computational observation of such long autocorrelation times, both for Q_{top} [40] and Q_{top}^2 [39]. In the theoretical framework, there exists a theorem [31] which states that “the space of all lattice gauge fields satisfying a certain smoothness condition decomposes into topological charge sectors very much like the space of continuous fields in the classical continuum theory”. In other words, in the continuum limit the Gauge fields space tends to be disconnected. This implies that the simulation algorithms cannot evolve a Gauge configuration in a given subspace to a configuration defined in another - disconnected - subspace. Then the entire fields space cannot be explored. The very long autocorrelation times are just a consequence of that.

The innovative work of Luscher and Schaefer addressed this topological issue. Until this point, the boundary conditions imposed on Gauge and fermionic fields were Periodic Boundary Conditions (PBC) in both the temporal and spatial directions. This choice was made in order to achieve temporal and spatial translation invariance. The modification introduced by Luscher involved Open Boundary Conditions in time direction with the natural consequence of the breaking of time translation symmetry. A sketchy representation of the topological differences is shown in Figure 2.3. The conditions to impose on fields are [34]:

$$\begin{aligned} F_{0i}(\vec{x}, x_4 = 0) &= F_{0i}(\vec{x}, x_4 = T) = 0 & \forall i = 1, 2, 3 \\ P_+ \psi(\vec{x}, 0) &= P_- \psi(\vec{x}, T) = 0 & P_{\pm} = \frac{1}{2} (\mathbb{I} \pm \gamma_5) \\ \bar{\psi}(\vec{x}, 0) P_- &= \bar{\psi}(\vec{x}, T) P_+ = 0 \end{aligned}$$

¹⁴ Reminder: strong interactions preserve parity; Q_{top} is parity even.

¹⁵ The word ‘time’ in this case refers to simulation time, i.e. the time of evolution of a specific Markov chain.

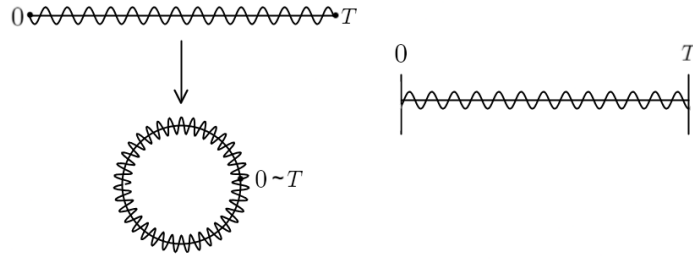


Figure 2.3. Sketchy representation of the Periodic Boundary Conditions vs Open Boundary Conditions in time direction

The peculiar conditions on fermion fields are chosen in order to achieve parity and time reflection. In Appendix D.4 I report a proof of the connection of the space of Gauge fields defined with the new boundary conditions. This connection of the space solves - not at all - the problem of large scaling of autocorrelation times. With this choice, the scaling behaviour of some observables comes out to scale $\propto a^{-2}$, instead of $\propto a^{-5}$. There is a variety of papers confirming that Open Boundary Conditions decrease autocorrelation times. For example, look at the following table from [31]:

	$\tau_{\text{int}}[Q]$	$\tau_{\text{int}}[Q^2]$	$\tau_{\text{int}}[E]$		$\tau_{\text{int}}[Q]$	$\tau_{\text{int}}[Q^2]$	$\tau_{\text{int}}[E]$
periodic	68(6)	33(2)	44(3)	periodic	615(90)	286(34)	86(6)
open	61(6)	27(2)	38(3)	open	384(56)	155(20)	77(6)

Figure 2.4. Comparison of autocorrelation times measured on lattices with periodic and open boundary conditions in time direction. The table on the left refers to a lattice with $a = 0.1$ fm. The one on the right to a lattice with $a = 0.07$ fm. The difference between OBC and PBC increases as the lattice spacing tends to zero. [31]

Another aspect to keep in mind follows. The formulation of lattice quantum physics with OBC in this case remains the same in the bulk¹⁶. However, the vacuum state $|\Omega\rangle$ at the time boundaries differs from the vacuum state $|0\rangle$ in the bulk, which represents the physical vacuum. It is proven [34] that both vacuum states possess the physical vacuum quantum numbers. Thus a formulation of Lattice QFT similar to the case of periodic boundary conditions is allowed. Given a local operator of the fields $\mathcal{X}(x_1, \dots, x_n)$, its vacuum expectation value is defined in the following way:

$$\langle \mathcal{X}(x_1, \dots, x_n) \rangle = \langle \Omega | T \{ \mathcal{X}(x_1, \dots, x_n) \} | \Omega \rangle$$

The formalism of transfer matrix $\mathbb{T} = e^{-a\hat{H}}$ is still valid. A good reference that explains how to treat vacuum expectation values of observables is [9]. The same topic - along with some generalizations to three point correlators - is presented at the end of the Chapter 3.

2.6.1 Linking OBC with absence of Wilson-Dirac zero modes

In this subsection I want to justify the use of Open Boundary Conditions to simulate sea configurations and explain how they protect the sea fields against Wilson-Dirac

¹⁶ “bluk”: the sub-lattice from which the boundaries with $x_4 = 0, x_4 = T$ are removed

zero modes. In fact, from this perspective, OBC could represent a smart alternative to tmQCD.

One of the primary purposes of lattice QFT simulations is the evaluation of low-energy QCD quantities. To accurately describe the sea sector in low-energy QCD, the minimal quark content required is the doublet (u, d) . In this case tmQCD represents a very good regularization choice for the sea sector for the reasons described in 2.3.3, in particular because it provides a non null fermion determinant.

A further step could be the introduction of the *strange* quark in sea sector. However, its description through tmQCD regularization is only feasible when coupled to the *charm* quark. From an ideal perspective, it can be a good solution, but the insertion of a fourth quark flavour represents a computational challenge. Moreover, the mass m_c is sufficiently large to make the c quark uneffective at energies below Λ_{QCD} . In theoretical particle physics it is said to be “integrated out”. The best compromise between computational advantage and physical content seems to be the set of (u, d, s) quarks in the sea.

Therefore, the key question arises: *How can we simulate $N_f = 2 + 1$ sea flavours while avoiding the Dirac-Wilson zero modes?* It is precisely at this point that Open Boundary Conditions emerge as a powerful alternative to twisted mass QCD. In fact the use of OBC in the quark fields

$$\begin{aligned} P_+ \psi(\vec{x}, 0) = P_- \psi(\vec{x}, T) = 0 \\ \bar{\psi}(\vec{x}, 0) P_- = \bar{\psi}(\vec{x}, T) P_+ = 0 \end{aligned} \quad P_{\pm} = \frac{1}{2} (\mathbb{I} \pm \gamma_5) \quad (2.15)$$

protects the theory from zero modes of the Wilson-Dirac operator. The proof is reported in a paper by S. Lüscher [32], one of the creators of the Open Boundary Conditions.

At this stage, it should be clear why sea quark action (2.12) does not make use of twisted mass terms:

- (i) The $O(a)$ -improvement is guaranteed by the SW term.
- (ii) The Open Boundary Conditions provide a protection against zero modes.

Hence the same attributes of tmQCD are achieved, albeit through different ways.

Chapter 3

Operators $\Theta_i^{[+]}$ s on the lattice and B_i extraction

The previous chapter outlined the general framework of lattice QCD, paying particular attention to the regularization employed in the present work. In this chapter such peculiar regularization is used to build the mixing operators $\{\Theta_i\}$ on the lattice. Some properties of the discretized lattice operators are described. Such properties consist in:

1. An automatic $O(a)$ -improvement of two and three points meson correlators with no need of multiple simulations (Wilson average) or other specific strategies. Such correlators are required to extract matrix elements $\langle \bar{K}^0 | \Theta_i^{[+]} | K^0 \rangle$ or bag parameters.
2. The absence of wrong chirality mixing of operators $\{\Theta_i^{[\pm]}\}$ in renormalization procedure. In principle they should mix because Wilson term in action (2.13) explicitly breaks chiral symmetry. Despite the symmetry breaking, this mixing comes out to be absent for symmetry reasons.
3. A specific basis choice for the operators that gives a blocks-like renormalization matrix Z_{ij} , which simplify the renormalization procedure.

In order to achieve these properties, some reformulations of the operators and strategies are required. The initial and majority of the chapter is dedicated to describing the four-fermion, dimension-six, mixing operators on the lattice. The second part of the chapter is reserved to a detailed description of the strategy to extract bag parameters and matrix elements $\langle \bar{K}^0 | \Theta_i^{[+]} | K^0 \rangle$ from two and three points correlators.

3.1 Continuum $\Theta_i^{[\pm]}$ s and the new operators $Q_i^{[\pm]}$ s

The SUSY operator basis for $K^0 - \bar{K}^0$ oscillations was introduced in (1.7). Despite its historical significance, the basis $\{\Theta_i\}$ will be replaced by another basis $\{Q_i\}$ because of its particular renormalization properties. However, before introducing this new basis, I need to present some modifications to the “old” SUSY basis.

I aim to reformulate operators Θ_3 and Θ_5 by rearranging the spin and colour indices contractions within the same couple of quarks. This can be done by applying the

Fierz relations [29] along with calculation of $\Theta_{3,5}$, as outlined in Appendix C. The new set of operators comes out to be:

$$\begin{aligned}\Theta_1 &= [\bar{s}^a \gamma_\mu (1 + \gamma_5) d^a] [\bar{s}^b \gamma_\mu (1 + \gamma_5) d^b] \\ \Theta_2 &= [\bar{s}^a (1 + \gamma_5) d^a] [\bar{s}^b (1 + \gamma_5) d^b] \\ \Theta_3 &= -[\bar{s}^a P_R d^a] [\bar{s}^b d^b] - [\bar{s}^a P_R d^a] [\bar{s}^b \gamma_5 d^b] + [\bar{s}^a P_R \sigma_{\mu\nu} d^a] [\bar{s}^b \sigma_{\mu\nu} d^b] \\ \Theta_4 &= [\bar{s}^a (1 + \gamma_5) d^a] [\bar{s}^b (1 - \gamma_5) d^b] \\ \Theta_5 &= -[\bar{s}^a P_R \gamma_\mu d^a] [\bar{s}^b \gamma_\mu d^b] - [\bar{s}^a P_R \gamma_\mu \gamma_5 d^a] [\bar{s}^b \gamma_\mu \gamma_5 d^b]\end{aligned}$$

where $\{\tilde{\Theta}_i\}$ are omitted. From this point on the notation described in Appendix A is used. The shortway to write the above operators is:

$$\begin{aligned}\Theta_1 &= VV + AA + VA + AV \\ \Theta_2 &= SS + PP + SP + PS \\ \Theta_3 &= \frac{1}{2} (-SS - PS - SP - PP + TT + \tilde{T}T) \\ \Theta_4 &= SS + PS - SP - PP \\ \Theta_5 &= \frac{1}{2} (-VV + AV - VA + AA)\end{aligned}$$

Then the parity even parts $\{\Theta_i^{[+]}\}$ and parity odd parts $\{\Theta_i^{[-]}\}$ are:

$$\begin{aligned}\Theta_1^{[+]} &= VV + AA & \Theta_1^{[-]} &= VA + AV \\ \Theta_2^{[+]} &= SS + PP & \Theta_2^{[-]} &= SP + PS \\ \Theta_3^{[+]} &= \frac{1}{2} (-SS - PP + TT) & \Theta_3^{[-]} &= \frac{1}{2} (-SP - PS + \tilde{T}T) \\ \Theta_4^{[+]} &= SS - PP & \Theta_4^{[-]} &= PS - SP \\ \Theta_5^{[+]} &= \frac{1}{2} (AA - VV) & \Theta_5^{[-]} &= \frac{1}{2} (AV - VA)\end{aligned} \tag{3.1}$$

For reasons that will be clear later in this chapter, I introduce a new basis $\{Q_i^{[\pm]}\}$ of parity even and parity odd operators [18]:

$$\begin{aligned}Q_1^{[+]} &= VV + AA & Q_1^{[-]} &= VA + AV \\ Q_2^{[+]} &= VV - AA & Q_2^{[-]} &= VA - AV \\ Q_3^{[+]} &= SS - PP & Q_3^{[-]} &= PS - SP \\ Q_4^{[+]} &= SS + PP & Q_4^{[-]} &= PS + SP \\ Q_5^{[+]} &= TT & Q_5^{[-]} &= \tilde{T}T\end{aligned} \tag{3.2}$$

Once evaluated the matrix elements $\langle \bar{K}^0 | Q_i^{[\pm]} | K^0 \rangle$, the elements $\langle \bar{K}^0 | \Theta_i^{[\pm]} | K^0 \rangle$ can be recovered by applying:

$$\begin{aligned} \Theta_i^{[\pm]} &= \Lambda_{ij} Q_j^{[\pm]} \text{ and} \\ \langle \bar{K}^0 | \Theta_i^{[\pm]} | K^0 \rangle &= \Lambda_{ij} \langle \bar{K}^0 | Q_j^{[\pm]} | K^0 \rangle \end{aligned} \quad \Lambda_{ij} = \begin{pmatrix} 1 & 0 & 0 & 0 & 0 \\ 0 & 0 & 0 & 1 & 0 \\ 0 & 0 & 0 & -\frac{1}{2} & +\frac{1}{2} \\ 0 & 0 & 1 & 0 & 0 \\ 0 & -\frac{1}{2} & 0 & 0 & 0 \end{pmatrix}$$

The $\{Q_i^{[\pm]}\}$ operators possess a relevant advantage with respect to the $\{\Theta_i^{[\pm]}\}$: once regularized as outlined in this chapter, they have renormalization mixing properties that simplify the evaluation of renormalized operators and renormalization constants. This will be better explained in 3.4.2.

I will show in section 3.5 how the bag parameters can be extracted from two and three points correlators. Firstly, I introduce such correlators¹ in continuum QFT:

$$C_i^{\text{QCD}}(x_4, y_4, z_4) = \int d^3y d^3z \langle \bar{K}^0(x) Q_i(y) \bar{K}^0(z) \rangle \quad (3.3)$$

$$G_{K^0 \bar{K}^0}^{\text{QCD}}(x_4, y_4) = \int d^3y \langle \bar{K}^0(x) K^0(y) \rangle$$

$$X_{\bar{K}^0}^{\text{QCD}}(x_4, y_4) = \int d^3y \langle A_0^{(\bar{d}s)}(x) \bar{K}^0(y) \rangle$$

The source operators \bar{K}^0 and K^0 are defined in Chapter 1 as the pseudoscalar densities of d and s doublet of quarks, while the superscript QCD stresses that these are the correlation functions in continuum quantum chromodynamics. The current $A_\mu^{(\bar{d}s)} = \bar{d} \gamma_\mu \gamma_5 s$ is the axial current associated to Kaons. The amplitudes

$$\mathcal{A}_i^{\text{QCD}} = \langle \bar{K}^0 | Q_i^{[+]} | K^0 \rangle$$

needed for the bag parameters are isolated from higher mass states contributions by considering asymptotic behaviour of correlators for $0 \ll z_4 \ll y_4 \ll x_4 \ll T$. So the condition $x_4 > y_4 > z_4$ is supposed to be always satisfied. The full discussion about the extraction is left to section 3.5.

3.2 Flavour replicas on the lattice

The regularized action (2.13) contains replicas of the d and s flavours, then the entire set of valence quarks is u, d, d', s, s' . The choice of multiple quarks of the same flavour comes from [21] and is formulated to achieve specific properties of the three-point correlators; such properties are outlined in section 3.4. I refer to the model with flavour replicas as the FR model (::Flavour Replicas).

I focus on *how* the FR model must be built in order to simulate the same flavour content of the standard QCD (simply named QCD). Specifically, I aim to construct three points correlators in the FR model such that they yield the same Wick contractions of functions (3.3). The proof is given below.

¹ To be precise, these are not the usual n -points correlators but their projections over null momenta.

3.2.1 Proof of equivalence of Wick contractions

Let's consider a general three points correlator in standard QCD:

$$G^{\text{QCD}}(x, y, z) = \left\langle \left(\bar{d}(x) \Gamma_{\xi} s(x) \right) \left(\bar{s}(y) \Gamma_{\rho} d(y) \bar{s}(y) \Gamma_{\sigma} d(y) \right) \left(\bar{d}(z) \Gamma_{\omega} s(z) \right) \right\rangle$$

with $\Gamma_{\xi, \rho, \sigma, \omega}$ some matrices in spin space. The correlation functions (3.3) are nothing but the sum over spatial components of the above quantity. The Wick contractions of such correlator follow:²:

$$\begin{aligned} G_{d1}^{\text{QCD}}(x, y, z) &: \overbrace{\bar{d}(x) \Gamma_{\xi} s(x)}^{\text{---}} \cdot \overbrace{\bar{s}(y) \Gamma_{\rho} d(y)}^{\text{---}} \cdot \overbrace{\bar{s}(y) \Gamma_{\sigma} d(y)}^{\text{---}} \cdot \overbrace{\bar{d}(z) \Gamma_{\omega} s(z)}^{\text{---}} \\ G_{d2}^{\text{QCD}}(x, y, z) &: \overbrace{\bar{d}(x) \Gamma_{\xi} s(x)}^{\text{---}} \cdot \overbrace{\bar{s}(y) \Gamma_{\rho} d(y)}^{\text{---}} \cdot \overbrace{\bar{s}(y) \Gamma_{\sigma} d(y)}^{\text{---}} \cdot \overbrace{\bar{d}(z) \Gamma_{\omega} s(z)}^{\text{---}} \\ G_{c1}^{\text{QCD}}(x, y, z) &: \overbrace{\bar{d}(x) \Gamma_{\xi} s(x)}^{\text{---}} \cdot \overbrace{\bar{s}(y) \Gamma_{\rho} d(y)}^{\text{---}} \cdot \overbrace{\bar{s}(y) \Gamma_{\sigma} d(y)}^{\text{---}} \cdot \overbrace{\bar{d}(z) \Gamma_{\omega} s(z)}^{\text{---}} \\ G_{c2}^{\text{QCD}}(x, y, z) &: \overbrace{\bar{d}(x) \Gamma_{\xi} s(x)}^{\text{---}} \cdot \overbrace{\bar{s}(y) \Gamma_{\rho} d(y)}^{\text{---}} \cdot \overbrace{\bar{s}(y) \Gamma_{\sigma} d(y)}^{\text{---}} \cdot \overbrace{\bar{d}(z) \Gamma_{\omega} s(z)}^{\text{---}} \end{aligned}$$

They generates single or double traces functions:

$$\begin{aligned} G_{d1}^{\text{QCD}}(x, y, z) &= \left\langle \text{Tr} \left[\Gamma_{\xi} S_s(x, y) \Gamma_{\rho} S_d(y, x) \right] \text{Tr} \left[\Gamma_{\omega} S_s(z, y) \Gamma_{\sigma} S_d(y, z) \right] \right\rangle \\ G_{d2}^{\text{QCD}}(x, y, z) &= \left\langle \text{Tr} \left[\Gamma_{\xi} S_s(x, y) \Gamma_{\sigma} S_d(y, x) \right] \text{Tr} \left[\Gamma_{\omega} S_s(z, y) \Gamma_{\rho} S_d(y, z) \right] \right\rangle \\ G_{c1}^{\text{QCD}}(x, y, z) &= - \left\langle \text{Tr} \left[\Gamma_{\xi} S_s(x, y) \Gamma_{\rho} S_d(y, z) \Gamma_{\omega} S_s(z, y) \Gamma_{\sigma} S_d(y, x) \right] \right\rangle \\ G_{c2}^{\text{QCD}}(x, y, z) &= - \left\langle \text{Tr} \left[\Gamma_{\xi} S_s(x, y) \Gamma_{\sigma} S_d(y, z) \Gamma_{\omega} S_s(z, y) \Gamma_{\rho} S_d(y, x) \right] \right\rangle \end{aligned} \quad (3.4)$$

then the total contribution to $G^{\text{QCD}}(x, y, z)$ is given by:

$$G^{\text{QCD}}(x, y, z) = G_{d1}^{\text{QCD}}(x, y, z) + G_{d2}^{\text{QCD}}(x, y, z) + G_{c1}^{\text{QCD}}(x, y, z) + G_{c2}^{\text{QCD}}(x, y, z)$$

I want to replicate this contributions using the new flavours d, d', s, s' built on the lattice. The strength of this method lies in the fact that primed and unprimed flavours cannot contract with each other. Therefore I can build an appropriate operator for each contraction. I define an antikaon source in x with primed flavours $\bar{d}'(x) \Gamma_{\xi} s'(x)$ and another in z with unprimed flavours $\bar{d}(z) \Gamma_{\omega} s(z)$. The intermediate operator is replaced by:

$$\begin{aligned} \Phi_{\rho, \sigma}(y) &= \bar{s}(y) \Gamma_{\rho} d(y) \bar{s}'(y) \Gamma_{\sigma} d'(y) + \bar{s}(y) \Gamma_{\sigma} d(y) \bar{s}'(y) \Gamma_{\rho} d'(y) + \\ &+ \bar{s}(y) \Gamma_{\rho} d'(y) \bar{s}'(y) \Gamma_{\sigma} d(y) + \bar{s}(y) \Gamma_{\sigma} d'(y) \bar{s}'(y) \Gamma_{\rho} d(y) \end{aligned}$$

In this case the correlator:

$$G^{\text{FR}}(x, y, z) = \left\langle \bar{d}'(x) \Gamma_{\xi} s'(x) \Phi_{\rho, \sigma}(y) \bar{d}(z) \Gamma_{\omega} s(z) \right\rangle$$

gives only one contraction for each term of $\Phi_{\rho, \sigma}(y)$, thus four contractions identical to equations (3.4) up to primed flavours. Such contractions are labeled by $G_{d1}^{\text{FR}}, G_{d2}^{\text{FR}}, G_{c1}^{\text{FR}}, G_{c2}^{\text{FR}}$ and are shown in Figure 3.1.

² I use the pedsubscripts c, d to refer to connected or disconnected diagrams

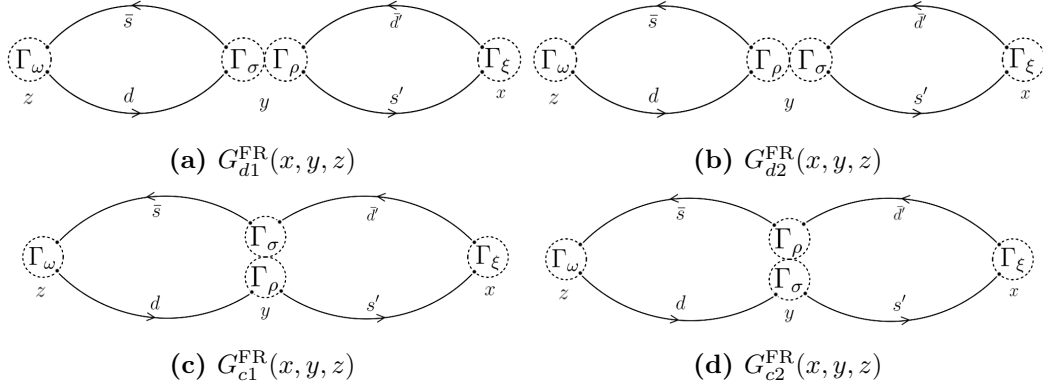


Figure 3.1. Wick contractions that contribute to the correlator $G^{\text{FR}}(x, y, z)$ in the framework of QCD with flavours replicas.

3.3 From physical basis to twisted basis

Thanks to the previous proof, the parity even operators $Q_i^{[+]}$ (equation (3.2)) can be built on the lattice in the FR framework by introducing four different flavours. The flavours used are the lattice regularized Osterwalder-Seiler quarks, as described in previous Chapter. The following notation for valence flavours is adopted:

$$\begin{array}{llll}
 \text{physical OS basis:} & \chi^1 = s_{\text{ph}} & \chi^3 = s'_{\text{ph}} & \\
 & \chi^2 = d_{\text{ph}} & \chi^4 = d'_{\text{ph}} & \\
 \text{twisted OS basis:} & \psi^1 = s_{\text{tw}} & \psi^3 = s'_{\text{tw}} & \text{with } \chi^i = \mathbf{J}(\pi/2, r_i)\psi^i \\
 & \psi^2 = d_{\text{tw}} & \psi^4 = d'_{\text{tw}} &
 \end{array}$$

The operators $Q_i^{[+]}$ in continuum QCD are replaced by the new operators $O_{i,[+]}^{\text{phys}}$ in the lattice QCD fermion physical basis:

$$\begin{aligned}
 O_{1[+]}^{\text{phys}} &= 2 \left\{ [\bar{\chi}^1 \gamma_\mu \chi^2] [\bar{\chi}^3 \gamma_\mu \chi^4] + [\bar{\chi}^1 \gamma_\mu \gamma_5 \chi^2] [\bar{\chi}^3 \gamma_\mu \gamma_5 \chi^4] + (2 \leftrightarrow 4) \right\} \\
 O_{2[+]}^{\text{phys}} &= 2 \left\{ [\bar{\chi}^1 \gamma_\mu \chi^2] [\bar{\chi}^3 \gamma_\mu \chi^4] - [\bar{\chi}^1 \gamma_\mu \gamma_5 \chi^2] [\bar{\chi}^3 \gamma_\mu \gamma_5 \chi^4] + (2 \leftrightarrow 4) \right\} \\
 O_{3[+]}^{\text{phys}} &= 2 \left\{ [\bar{\chi}^1 \chi^2] [\bar{\chi}^3 \chi^4] - [\bar{\chi}^1 \gamma_5 \chi^2] [\bar{\chi}^3 \gamma_5 \chi^4] + (2 \leftrightarrow 4) \right\} \\
 O_{4[+]}^{\text{phys}} &= 2 \left\{ [\bar{\chi}^1 \chi^2] [\bar{\chi}^3 \chi^4] + [\bar{\chi}^1 \gamma_5 \chi^2] [\bar{\chi}^3 \gamma_5 \chi^4] + (2 \leftrightarrow 4) \right\} \\
 O_{5[+]}^{\text{phys}} &= 2 \left\{ [\bar{\chi}^1 \sigma_{\mu\nu} \chi^2] [\bar{\chi}^3 \sigma_{\mu\nu} \chi^4] + (2 \leftrightarrow 4) \right\}
 \end{aligned}$$

According to what is explained in section 2.3.5, I need to transform the operators from the physical to twisted basis. To do that I apply the OS rotations $\mathbf{J}(\pi/2, r_i)$ and I remember that:

$$r_1 = r_2 = r_3 = -r_4 = \pm 1$$

It could be useful to use cases **# 1** (formula (B.2)) and **# 2** (formula (B.3)) derived in Appendix B. The resulting operators are the following:

$$\begin{aligned}
O_{1[+]}^{\text{tw}} &= \mp 2i \left\{ [\bar{\psi}^1 \gamma_\mu \psi^2] [\bar{\psi}^3 \gamma_\mu \gamma_5 \psi^4] + [\bar{\psi}^1 \gamma_\mu \gamma_5 \psi^2] [\bar{\psi}^3 \gamma_\mu \psi^4] + (2 \leftrightarrow 4) \right\} \\
O_{2[+]}^{\text{tw}} &= \mp 2i \left\{ [\bar{\psi}^1 \gamma_\mu \psi^2] [\bar{\psi}^3 \gamma_\mu \gamma_5 \psi^4] - [\bar{\psi}^1 \gamma_\mu \gamma_5 \psi^2] [\bar{\psi}^3 \gamma_\mu \psi^4] - (2 \leftrightarrow 4) \right\} \\
O_{3[+]}^{\text{tw}} &= \pm 2i \left\{ [\bar{\psi}^1 \gamma_5 \psi^2] [\bar{\psi}^3 \psi^4] - [\bar{\psi}^1 \psi^2] [\bar{\psi}^3 \gamma_5 \psi^4] - (2 \leftrightarrow 4) \right\} \\
O_{4[+]}^{\text{tw}} &= \pm 2i \left\{ [\bar{\psi}^1 \gamma_5 \psi^2] [\bar{\psi}^3 \psi^4] + [\bar{\psi}^1 \psi^2] [\bar{\psi}^3 \gamma_5 \psi^4] + (2 \leftrightarrow 4) \right\} \\
O_{5[+]}^{\text{tw}} &= \pm 2i \left\{ [\bar{\psi}^1 \tilde{\sigma}_{\mu\nu} \psi^2] [\bar{\psi}^3 \sigma_{\mu\nu} \psi^4] + [\bar{\psi}^1 \sigma_{\mu\nu} \psi^4] [\bar{\psi}^3 \tilde{\sigma}_{\mu\nu} \psi^2] \right\}
\end{aligned} \tag{3.5}$$

where the signs \pm, \mp depend on the choice of $r_1 = \pm 1$. The other quantities that need to be twisted are the Kaon sources:

$$\begin{aligned}
\bar{K}^0 &= P_{21}^{\text{phys}} = \bar{\chi}^2 \gamma_5 \chi^1 = \pm i \bar{\psi}^2 \psi^1 = \pm i S_{21}^{\text{tw}} \\
\bar{K}'^0 &= P_{43}^{\text{phys}} = \bar{\chi}^4 \gamma_5 \chi^3 = \bar{\psi}^4 \gamma_5 \psi^3 = P_{43}^{\text{tw}}
\end{aligned} \tag{3.6}$$

It is notable that the OS twist maps the parity even operators into parity odd ones. However also the source K^0 changes parity, then the overall sign of the correlator under \mathbb{P} is preserved and equal to $+1$, as strong interactions should do. Now the work in Maximally twisted OS valence QCD is well defined and, by construction, the correlation functions:

$$C_i^{\text{FR}}(x_4, y_4, z_4) = \pm i a^6 \sum_{\vec{x}, \vec{y}, \vec{z}} \left\langle \left(\bar{\psi}^4 \gamma_5 \psi^3 \right) (x) O_{i[+]}^{\text{tw}}(y) \left(\bar{\psi}^2 \psi^1 \right) (z) \right\rangle \tag{3.7}$$

give the same Wick contractions of the correlators in equation (3.3), showed in Figure 3.1. To be rigorous, in this definition there is one more sum with respect to equation (3.3). This additive sum over \vec{x} is a (sort of) statistical average and it is used to give more precise results in the simulation. Similarly, the integrated two points correlation functions are:

$$\begin{aligned}
G_{34}^{\text{FR}}(x_4, y_4) &= a^3 \sum_{\vec{x}, \vec{y}} \left\langle \left(\bar{\psi}^4 \gamma_5 \psi^3 \right) (x) \left(\bar{\psi}^3 \gamma_5 \psi^4 \right) (y) \right\rangle \\
G_{12}^{\text{FR}}(x_4, y_4) &= -a^3 \sum_{\vec{x}, \vec{y}} \left\langle \left(\bar{\psi}^2 \psi^1 \right) (x) \left(\bar{\psi}^1 \psi^2 \right) (y) \right\rangle
\end{aligned} \tag{3.8}$$

the use of the first or the second correlator is - in principle - equivalent, since one consists in the “flavour replica” of the other and vice versa. Both describe a neutral anti-Kaon \bar{K}^0 propagator. Nevertheless there are lattice artefacts due to the different regularizations of d, d' that make the pseudoscalar densities \bar{K}^0 and \bar{K}'^0 generate slightly different Kaons.

Similar definitions hold for G_{21}^{FR} and G_{43}^{FR} . They differ from (3.8) by an exchange of flavours ($1 \leftrightarrow 2$) or ($3 \leftrightarrow 4$) and correspond to the propagator of the kaon K^0 instead of an antikaon \bar{K}^0 .

At the end of the chapter I will use two other correlators to extract the parameter

B_K , following the method explained in [16]:

$$\begin{aligned}
X_{34}^{\text{FR}}(x_4, y_4) &= a^3 \sum_{\vec{x}, \vec{y}} \langle A_{0,43}^{\text{phys}}(x) P_{34}^{\text{phys}}(y) \rangle = \pm i a^3 \sum_{\vec{x}, \vec{y}} \langle V_{0,43}^{\text{tw}}(x) P_{34}^{\text{tw}}(y) \rangle \\
&= \pm i a^3 \sum_{\vec{x}, \vec{y}} \langle (\bar{\psi}^4 \gamma_0 \psi^3)(x) (\bar{\psi}^3 \gamma_5 \psi^4)(y) \rangle \\
X_{12}^{\text{FR}}(x_4, y_4) &= a^3 \sum_{\vec{x}, \vec{y}} \langle A_{0,21}^{\text{phys}}(x) P_{12}^{\text{phys}}(y) \rangle = \pm i a^3 \sum_{\vec{x}, \vec{y}} \langle A_{0,21}^{\text{tw}}(x) S_{12}^{\text{phys}}(y) \rangle \\
&= \pm i a^3 \sum_{\vec{x}, \vec{y}} \langle (\bar{\psi}^2 \gamma_0 \gamma_5 \psi^1)(x) (\bar{\psi}^1 \psi^2)(y) \rangle
\end{aligned} \tag{3.9}$$

where I have used again the results in Appendix B.2. These two correlators give, in the continuum limit and in regime of asymptotic behaviour (Section 3.5), the matrix element $\langle 0 | A_0^{(\bar{d}s)}(x) | \bar{K}^0(\vec{p}) \rangle$.

3.4 Properties of correlators and $O_{i[+]}$ operators

3.4.1 Automatic $O(a)$ –improvement

In the first paper by Frezzotti and Rossi [20] a strategy to $O(a)$ –improve observables based on of Wilson Dirac fermions or twisted fermions has been introduced. The operation needed to improve the observables is called *Wilson Average* (WA) and it consists of averaging observables evaluated with different signs of Wilson parameters r_i . In a shorthand notation I refer to the set of Wilson parameters of the theory with $R = \{r_1, \dots, r_N\}$.

Given an observable \mathcal{X} functional of the valence fields and Gauge fields, the WA of its vacuum expectation value is:

$$\langle \mathcal{X} \rangle \Big|_{WA}^a = \frac{1}{2} \left(\langle \mathcal{X} \rangle \Big|_{+R}^a + \langle \mathcal{X} \rangle \Big|_{-R}^a \right) = \zeta_{\mathcal{X}}(R) \langle \mathcal{X} \rangle \Big|_{\text{continuum}} + O(a^2)$$

where $\zeta_{\mathcal{X}}(R)$ is a constant, dependent on Wilson parameters, needed to match lattice VEV with continuum VEV. The proof that the Wilson average gives an $O(a)$ –improvement is reported in [20].

The WA method implies that multiple simulations must be done. However there are particular cases in which this is not necessary because each $\langle \mathcal{X} \rangle \Big|_{\pm R}^a$ is automatically improved and the WA is not necessary. This is exactly the case of correlators of the type (3.7) and (3.8). In fact the valence and sea actions (2.13) and (2.12) admit the spurionic symmetry $\mathbb{P} \times (R \mapsto -R)$. In particular \mathbb{P} is the parity operation ($\mathbb{P}x = x_p$) and $(R \mapsto -R)$ is the change of signs of the Wilson parameters. Under this discrete symmetry a correlator of the type (3.7) is mapped into itself because of the symmetry property and it is also mapped into the one with $(R \mapsto -R)$ because of the identity:

$$\sum_{\vec{x}, \vec{y}, \vec{z}} f(x, y, z) = \sum_{\vec{x}_p, \vec{y}_p, \vec{z}_p} f(x_p, y_p, z_p)$$

for any function f of the lattice coordinates. Then, in simple words, the statement asserts that in this case $\langle \mathcal{X} \rangle \Big|_{+R}^a = \langle \mathcal{X} \rangle \Big|_{-R}^a$ and then the WA is not necessary for the $O(a)$ –improvement. The same proof can be applied to a simple meson propagator

of the type³:

$$G(x, y) = a^3 \sum_{\vec{x}, \vec{y}} \left\langle \bar{\psi}^1(x) \Gamma^\alpha \psi^2(x) \bar{\psi}^2(y) \bar{\Gamma}^\alpha \psi^1(y) \right\rangle$$

and then to two points correlators. It is important to notice that this proof holds not only for $r_1 = r_2 = r_3 = -r_4$ but for all the possible values of each r_i independently chosen.

3.4.2 Renormalization and mixing of operators $O_{i[\pm]}$

There are two arguments left to be tested, as mentioned at the very beginning of the chapter. Both points concern the specific renormalization properties owned by the parity even and parity odd operators $O_{i, [\pm]}^{\text{phys}}$. The following has been taken from the paper [18].

First of all I need notations. In this section, I will denote generic parity even operators (PE) with the index E , and generic parity odd operators (PO) with O . I define the following quantities:

$$\begin{aligned} \Phi_{AB} &= \left(\bar{\psi}^1 \Gamma^A \psi^2 \right) \left(\bar{\psi}^3 \Gamma^B \psi^4 \right) \\ \Phi_{AB}^F &= \left(\bar{\psi}^1 \Gamma^A \psi^4 \right) \left(\bar{\psi}^3 \Gamma^B \psi^2 \right) \\ \Phi_{AB \pm CD} &= \Phi_{AB} \pm \Phi_{CD} \\ \Phi_{AB}^\pm &= \Phi_{AB} \pm \Phi_{AB}^F \end{aligned}$$

In the last definition, note that the signs \pm have nothing to do with parity, but indicate the sign of the flavour exchange.

To address the mixing issue under renormalization, both natural and accidental symmetries of these operators will be used. Before that, it must be noted that these operators composed of four quarks (*i*) do not mix with higher dimensional operators due to a well known renormalization theorem [15] and (*ii*) do not mix with lower dimensional operators because it is not possible to replicate four fermions flavour content through lower dimensions less than 6. As a consequence, I can define a *set of four-quarks dimension-6 operators, closed under renormalization procedure* (3.10). At this point, I define the symmetries used:

- Parity \mathbb{P} : $\psi^i(x) \mapsto \gamma_4 \psi^i(x_p)$
- Charge conjugation \mathbb{C} : $\psi^i(x) \mapsto C \left(\bar{\psi}^i \right)^T(x)$
- First flavour exchange \mathbb{S} : $(\psi^2 \leftrightarrow \psi^4)$
- Second flavour exchange \mathbb{S}' : $(\psi^1 \leftrightarrow \psi^2, \psi^3 \leftrightarrow \psi^4)$
- Third flavour exchange \mathbb{S}'' : $(\psi^1 \leftrightarrow \psi^4, \psi^2 \leftrightarrow \psi^3)$

Clearly, the symmetry \mathbb{S} maps Φ to Φ^F and vice versa. Other useful properties are $\mathbb{S}'' = \mathbb{S} \cdot \mathbb{S}'$, $\mathbb{S}' = \mathbb{S} \cdot \mathbb{S}''$, $\mathbb{S}^2 = 1$. Next, the following parity even (left column) and

3 about the symbol $\bar{\Gamma}^\alpha$ see Appendix A

parity odd (right column) operators are defined:

$$\begin{aligned}
O_{1,E}^{\pm} &= \Phi_{VV+AA}^{\pm} & O_{1,O}^{\pm} &= \Phi_{VA+AV}^{\pm} \\
O_{2,E}^{\pm} &= \Phi_{VV-AA}^{\pm} & O_{2,O}^{\pm} &= \Phi_{VA-AV}^{\pm} \\
O_{3,E}^{\pm} &= \Phi_{SS-PP}^{\pm} & O_{3,O}^{\pm} &= \Phi_{PS-SP}^{\pm} \\
O_{4,E}^{\pm} &= \Phi_{SS+PP}^{\pm} & O_{4,O}^{\pm} &= \Phi_{PS+SP}^{\pm} \\
O_{5,E}^{\pm} &= \Phi_{TT}^{\pm} & O_{5,O}^{\pm} &= \Phi_{T\tilde{T}}^{\pm}
\end{aligned} \tag{3.10}$$

This set consists of 20 operators composed by four fermions and dimensionality 6. It should be clear that the $O_{i[\pm]}$ used in this work are some operators in the above set. Below is a table taken from [18] that shows how these symmetry transformations act on basis operators.

Φ_{AB}	P	CS'	CS''	CPS'	CPS''
Φ_{VV}	+1	+1	+1	+1	+1
Φ_{AA}	+1	+1	+1	+1	+1
Φ_{PP}	+1	+1	+1	+1	+1
Φ_{SS}	+1	+1	+1	+1	+1
Φ_{TT}	+1	+1	+1	+1	+1
Φ_{VA}	-1	-1	$-\Phi_{AV}$	+1	Φ_{AV}
Φ_{AV}	-1	-1	$-\Phi_{VA}$	+1	Φ_{VA}
Φ_{SP}	-1	+1	Φ_{PS}	-1	$-\Phi_{PS}$
Φ_{PS}	-1	+1	Φ_{SP}	-1	$-\Phi_{SP}$
$\Phi_{T\tilde{T}}$	-1	+1	+1	-1	-1

Table 3.1. Transformations acting on operators. The trivial \mathbb{S} transformation and the flavour exchanged operators Φ^F are not shown.

The crux of the proof of the mixing of these operators lies in the fact that the considered transformations are symmetries of the Wilson action and the operators defined above. Therefore, the quantum numbers - or charges - associated with these symmetries are conserved. So only operators with the same quantum numbers can mix with each other. As can be inferred from the table, there is no simplification in the mixing of the PE operators; they all mix with each other. On the other hand, the situation for the PO operators is different. The renormalization matrix is a block diagonal matrix:

$$O_{i,O}^{\pm,\text{ren}} = Z_{ij}^{\pm} O_{i,O}^{\pm} \quad Z_{ij} = \begin{pmatrix} Z_{11} & 0 & 0 & 0 & 0 \\ 0 & Z_{22} & Z_{23} & 0 & 0 \\ 0 & Z_{32} & Z_{33} & 0 & 0 \\ 0 & 0 & 0 & Z_{44} & Z_{45} \\ 0 & 0 & 0 & Z_{54} & Z_{55} \end{pmatrix}$$

This greatly simplifies the renormalization process. About the PE operators, the situation is more complicated, and the reader must refer to the paper [18]. Explicit chiral symmetry breaking introduced by the Wilson term plays a fundamental role and allows the operators to mix their chirality. However, the matrix elements are $O(a)$ -improved, so even the effects of mixing with wrong chirality have an effect of order $O(a^2)$ or higher.

To conclude this section, I want to revisit a brilliant reasoning made in [6]. For vanishing twisted masses μ_i , the action of Wilson and Osterwalder-Seiler fermions

in the twisted basis is indistinguishable. Therefore, using a massless renormalization scheme, the renormalization properties of the parity odd operators $O_{i[+]}^{\text{tw}}$ are reflected in those of the parity even operators before the base twist $O_{i[+]}^{\text{phys}}$. This result has been formally developed in [21].

3.5 Asymptotic behaviours

The last pending issue of this chapter is the method to isolate the bare amplitudes $\langle \bar{K}^0 | Q_i | K^0 \rangle$ in the continuum limit from correlators (3.7) and to extract bag parameters from them. Such method is based on asymptotic behaviours of correlators at large euclidean times and it is a standard extraction method [36], adapted to the case of Open Boundary Conditions [9]. In this section I will consider a generic (integrated) three points correlator of this form:

$$C(x_4, y_4, z_4) = a^6 \sum_{\vec{x}, \vec{y}, \vec{z}} \langle M_A(x) \Xi(y) M_B(z) \rangle \quad (3.11)$$

where M_A and M_B are meson sources and Ξ is the intermediate mixing operator. Again I suppose $x_4 > y_4 > z_4$. Notice that the sum over spatial components is a projection over zero momenta of the correlator. To prove it, let's consider a lattice function $f(\vec{x}, \vec{y}, \vec{z})$ and its discrete Fourier transform $\tilde{f}(\vec{p}_x, \vec{p}_y, \vec{p}_z)$. Due to periodic boundary conditions in space directions, the above correlator is space translation invariant. Thus I suppose $f(\vec{x}, \vec{y}, \vec{z}) = f(0, \vec{y} - \vec{x}, \vec{z} - \vec{x})$. At this point the sum over spatial components is nothing but the discrete Fourier transform calculated in null momenta:

$$\begin{aligned} \sum_{\vec{x}, \vec{y}, \vec{z}} f(\vec{x}, \vec{y}, \vec{z}) &= \mathcal{F}[f](\vec{p}_x, \vec{p}_y, \vec{p}_z) \Big|_{\vec{p}_i=0} = \sum_{\vec{x}, \vec{y}, \vec{z}} f(0, \vec{y} - \vec{x}, \vec{z} - \vec{x}) = \\ &= \sum_{\vec{x}, \vec{y}', \vec{z}'} f(\vec{0}, \vec{y}', \vec{z}') \exp(i(\vec{p}_x + \vec{p}_y + \vec{p}_z)\vec{x} + i\vec{p}_y \cdot \vec{y}' + i\vec{p}_z \cdot \vec{z}') \Big|_{\vec{p}_i=0} = \\ &= \sum_{\vec{x}} \bar{f}(x' = 0, \vec{p}_y = 0, \vec{p}_z = 0) \end{aligned}$$

where \bar{f} is an intermediate function in which only two of three variables are Fourier transformed. It is worth noting that a sort of statistical sum over \vec{x} appears. This will be helpful to reduce noise in data analysis procedure. The projection over zero momenta is a clever trick because all the involved physical states will have an energy equal to the mass of such state $E = m$ and then a non perturbative extraction of the masses can be done⁴.

Now I want to show how the amplitudes can be asymptotically isolated [36] from

⁴ In this work there are no mass extractions, but previous papers do it in a very precise way. For example see [28][33] for 0^- mesons masses with CLS ensembles.

correlator (3.11). Before of that, a theoretical background is introduced:

Vacuum state: $\Omega \quad H|\Omega\rangle = 0$

Other states: $\Psi_{n,p} \quad H|\Psi_{n,p}\rangle = \left(\sum_i E_i(p_i)\right) |\Psi_{n,p}\rangle$

Other states projected on zero momenta: $\Psi_n \quad H|\Psi_n\rangle = \left(\sum_i m_i\right) |\Psi_n\rangle$

where i runs over the set of particles in the given state.

I use the transfer matrix formalism to re-express M_A, M_B and Ξ :

$$\begin{aligned} \langle M_A(x)\Xi(y)M_B(z) \rangle &= \langle \Omega | \mathbb{T}^{T-x_4} M_A(0, \vec{x}) \mathbb{T}^{x_4-y_4} \Xi(0, \vec{y}) \mathbb{T}^{y_4-z_4} M_B(0, \vec{z}) \mathbb{T}^{z_4} | \Omega \rangle = \\ &= \langle \Omega | e^{-H(T-x_4)} M_A(0, \vec{x}) e^{-H(x_4-y_4)} \Xi(0, \vec{y}) e^{-H(y_4-z_4)} M_B(0, \vec{z}) e^{-Hz_4} | \Omega \rangle = \\ &= \langle \Omega | M_A(0, \vec{x}) e^{-H(x_4-y_4)} \Xi(0, \vec{y}) e^{-H(y_4-z_4)} M_B(0, \vec{z}) | \Omega \rangle \end{aligned}$$

I insert a complete set of states between each pair of operators and I use the property of any local operator \mathcal{O} :

$$\mathcal{O}(\vec{x}) = \exp(i\vec{P} \cdot \vec{x}) \mathcal{O}(\vec{0}) \exp(-i\vec{P} \cdot \vec{x})$$

The projection over zero momenta allows to simplify the expression. The resulting correlator is:

$$\begin{aligned} C(x_4, y_4, z_4) &= \\ &= a^6 \sum_{\vec{y}} \sum_{n,k} \langle \Omega | M_A(0) [\Psi_n \Psi_n^\dagger] \Xi(0) [\Psi_k \Psi_k^\dagger] M_B(0) | \Omega \rangle e^{-m_n(x_4-y_4)-m_k(y_4-z_4)} \end{aligned}$$

Suppose to consider the case $x_4 \gg y_4 \gg z_4$. Then, because of the exponentials, only the smallest masses m_n and m_k give a relevant contribution, while all the other states are suppressed. Supposing that the meson operators M_A and M_B interpolate some single meson states Ψ_A and Ψ_B :

$$\begin{aligned} C(x_4, y_4, z_4) &\approx \\ &\approx a^6 \sum_{\vec{y}} \langle \Omega | M_A(0) | \Psi_A \rangle \langle \Psi_A | \Xi(0) | \bar{\Psi}_B \rangle \langle \bar{\Psi}_B | M_B(0) | \Omega \rangle e^{-m_A(x_4-y_4)-m_B(y_4-z_4)} \end{aligned} \quad (3.12)$$

I can follow the same procedure applied to the two points correlation function with meson operators, i.e. the non perturbative meson propagator:

$$G_{C\bar{C}}(x_4, y_4) = a^3 \sum_{\vec{x}, \vec{y}} \langle M_C(x) \bar{M}_C(y) \rangle \quad (3.13)$$

For $x_4 \gg y_4$ it can be proved that the asymptotic behaviours of such correlator is:

$$G_{C\bar{C}}(x_4, y_4) \approx a^3 \sum_{\vec{y}} \langle \Omega | M_C(0) | \Psi_C \rangle \langle \Psi_C | \bar{M}_C(0) | \Omega \rangle e^{-m_C(x_4-y_4)} \quad (3.14)$$

Let's focus on the particular case of this work. To evaluate matrix elements I will use $M_A = \bar{K}'^0$, $M_B = \bar{K}^0$ and $\Xi = O_{i[+]}$. Such choices give the three points correlators

C_i^{FR} in formula (3.7). By choosing M_C as $\bar{K}^{0'}$ or \bar{K}^0 the two points functions $G_{34}^{\text{FR}}, G_{12}^{\text{FR}}$ in formula (3.8) are obtained. By choosing M_C as the 0-th component of the kaon axial current and replacing \bar{M}_C with K^0 or $K^{0'}$, I get the correlators $X_{34}^{\text{FR}}, X_{12}^{\text{FR}}$ in formula (3.9). Because of their different regularizations (3.6), I suppose that Kaons generated by $\bar{K}^{0'}$ and \bar{K}^0 to have different masses $m_{K'} \neq m_K$ for a lattice spacing different from zero. Thus their asymptotic behaviours are:

$$\begin{aligned} C_i^{\text{FR}}(x_4, y_4, z_4) &\approx \\ &\approx a^6 \sum_{\vec{y}} \langle \bar{K}^{0'} | O_{i[+]} | K^0 \rangle \langle \Omega | \bar{K}^{0'} | \bar{K}^{0'} \rangle \langle K^0 | \bar{K}^0 | \Omega \rangle e^{-m_{K'}(x_4-y_4)-m_K(y_4-z_4)} \\ G_{34}^{\text{FR}}(x_4, y_4) &\approx a^3 \sum_{\vec{y}} \left| \langle \Omega | \bar{K}^{0'} | \bar{K}^{0'} \rangle \right|^2 e^{-m_{K'}(x_4-y_4)} \\ G_{12}^{\text{FR}}(x_4, y_4) &\approx a^3 \sum_{\vec{y}} \left| \langle \Omega | K^0 | K^0 \rangle \right|^2 e^{-m_K(x_4-y_4)} \\ X_{34}^{\text{FR}}(x_4, y_4) &\approx a^3 \sum_{\vec{y}} \langle \Omega | A_{0,43}^{\text{phys}} | \bar{K}^{0'} \rangle \langle \bar{K}^{0'} | K^{0'} | \Omega \rangle e^{-m_{K'}(x_4-y_4)} \\ X_{12}^{\text{FR}}(x_4, y_4) &\approx a^3 \sum_{\vec{y}} \langle \Omega | A_{0,21}^{\text{phys}} | K^0 \rangle \langle \bar{K}^0 | K^0 | \Omega \rangle e^{-m_K(x_4-y_4)} \end{aligned}$$

Fortunately the two matrix elements $\langle \Omega | \bar{K}^0 | \bar{K}^0 \rangle$ and $\langle K^0 | \bar{K}^0 | \Omega \rangle$ are equal and real because of the PCAC relation. The same using $\bar{K}^{0'}$. I leave the very simple proof of that in Appendix D.1. In particular I use the following chain:

$$\langle \Omega | \bar{K}^0 | \bar{K}^0 \rangle = \langle K^0 | \bar{K}^0 | \Omega \rangle \neq \langle \Omega | \bar{K}^{0'} | \bar{K}^{0'} \rangle = \langle K^{0'} | \bar{K}^{0'} | \Omega \rangle$$

The extraction of bare bag parameters is based on a simplification of mesons amplitudes and decay constants. Bare bag parameters definitions are analogous to with definitions analogous to the renormalized ones, in (1.8). It is straightforward to prove that the following quantities, in asymptotic regime, give the bag parameters with indices 2, ..., 5 at lattice spacing a :

$$\begin{aligned} \mathcal{B}_i(a; y_4) &\approx \frac{1}{\xi_i} \sum_{j=2}^5 \Lambda_{ij} \mathcal{F}_j(a; y_4) \\ \mathcal{F}_j(a) &= \frac{C_i^{\text{FR}}(x_4, y_4, z_4)}{G_{34}^{\text{FR}}(x_4, y_4) \cdot G_{12}^{\text{FR}}(y_4, z_4)} \approx \frac{\sum_{\vec{y}} \langle \bar{K}^{0'} | O_{i[+]} | K^0 \rangle \langle \Omega | \bar{K}^{0'} | \bar{K}^{0'} \rangle \langle K^0 | \bar{K}^0 | \Omega \rangle}{\left[\sum_{\vec{y}} \left| \langle \Omega | \bar{K}^{0'} | \bar{K}^{0'} \rangle \right|^2 \right] \left[\sum_{\vec{y}} \left| \langle \Omega | K^0 | K^0 \rangle \right|^2 \right]} \end{aligned} \quad (3.15)$$

Using formula (D.1) I can express:

$$\langle \Omega | K^{0'} | K^{0'} \rangle = \frac{F_{K'} m_{K'}}{m_3 + m_4} \quad \langle \Omega | K^0 | K^0 \rangle = \frac{F_K m_K}{m_1 + m_2}$$

These quantities simplify some terms in the definition of bag parameters (1.8). It should be noted that, although the quantities $\mathcal{F}_j(a, y_4)$ don't explicitly depend on y_4 , the results show a residual dependence from it because of computational reasons. Thus it is possible to recover the parameters $\{B_2^{\text{bare}}, B_3^{\text{bare}}, B_4^{\text{bare}}, B_5^{\text{bare}}\}$ through the continuum limit extrapolation.

About the first parameter B_K , the strategy adopted is similar. In its definition (1.8)

the terms in front of B_K differ from the others. For this reason, the needed ratio to extract B_K is different and it involves the use of axial current [16]. The property to use is strictly related to the PCAC relation for the neutral Kaons:

$$\langle \Omega | A_\mu^{(ds)}(x) | K^0(\vec{p}) \rangle = F_K p_\mu e^{ipx}$$

In the present case $\vec{p} = \vec{0}$ due to the projection over zero momenta. Thus, taking $\mu = 0$, I obtain $F_K m_K$. This holds for both $\bar{K}^{0'}$ and \bar{K}^0 sources. At this point I can use the correlators $X_{12}^{\text{FR}}(x, y)$ and $X_{34}^{\text{FR}}(x, y)$ in (3.9) to define \mathcal{F}_1 and the first bag parameter on the lattice \mathcal{B}_1 :

$$\mathcal{B}_1(a; y_4) \approx \frac{1}{\xi_1} \mathcal{F}_1(a; y_4) \quad (3.16)$$

$$\begin{aligned} \mathcal{F}_1(a; y_4) &= \frac{C_i^{\text{FR}}(x_4, y_4, z_4)}{X_{34}^{\text{FR}}(x_4, y_4) \cdot X_{12}^{\text{FR}}(y_4, z_4)} \approx \\ &\approx \frac{\sum_{\vec{y}} \langle \bar{K}^{0'} | O_{1[+]} | K^0 \rangle \langle \Omega | \bar{K}^{0'} | \bar{K}^{0'} \rangle \langle K^0 | \bar{K}^0 | \Omega \rangle}{\left[\sum_{\vec{y}} \langle \Omega | A_{0,43} | \bar{K}^{0'} \rangle \langle \bar{K}^{0'} | K^{0'} | \Omega \rangle \right] \left[\sum_{\vec{y}} \langle \Omega | A_{0,21} | \bar{K}^0 \rangle \langle \bar{K}^0 | K^0 | \Omega \rangle \right]} \approx \\ &\approx \frac{\sum_{\vec{y}} \langle \bar{K}^{0'} | O_{1[+]} | K^0 \rangle}{\left[\sum_{\vec{y}} \langle \Omega | A_{0,43} | \bar{K}^{0'} \rangle \right] \left[\sum_{\vec{y}} \langle \Omega | A_{0,21} | \bar{K}^0 \rangle \right]} \sim \xi_1 B_K \end{aligned}$$

To conclude this section I mention again the continuum limit extrapolation that gives the physical bare bag parameters:

$$\text{On the lattice: } \mathcal{B}_i(a; y_4) \approx \frac{1}{\xi_i} \sum_{j=1}^5 \Lambda_{ij} \mathcal{F}_j(a; y_4) \quad \forall i \quad (3.17)$$

$$\text{Continuum limit: } \mathcal{B}_i(a; y_4) \xrightarrow{a \rightarrow 0} B_i^{\text{bare}} + O(a^2)$$

In Section 4.3 I will explain the analysis strategy to extract them from lattice data. There exist also an other set of relevant ratios that may be calculated:

$$\mathcal{R}_i(a, y_4) = \sum_{j=2}^5 \Lambda_{ij} \frac{C_j^{\text{FR}}(x_4, y_4, z_4)}{C_1^{\text{FR}}(x_4, y_4, z_4)} \approx \sum_{j=2}^5 \frac{\sum_{\vec{y}} \langle \bar{K}^{0'} | \Lambda_{ij} O_{j[+]} | K^0 \rangle}{\sum_{\vec{y}} \langle \bar{K}^{0'} | O_{1[+]} | K^0 \rangle}$$

that, in continuum limit, are proportional to the ratios of amplitudes of the bag parameters for $i = 2, \dots, 5$ on the first B_K .

$$\text{Continuum limit: } \mathcal{R}_i(a; y_4) \xrightarrow{a \rightarrow 0} R_i^{\text{bare}} + O(a^2)$$

Chapter 4

Computational Strategies

The present chapter describes the computational side of this work. First of all, I will introduce the noise spinors method implemented to evaluate two points Green functions. It allows to achieve a great computational advantage on resources efficiency in the simulation procedure. Then the noise spinors method is extended to the case of three points correlators. In both cases a proof of the equivalence with the Wick contractions is given. Section 4.2 describes the input parameters and output data of the simulation program. A subsection will introduce the “computational basis” for the lattice operators, built for computational convenience and to make the program flexible. In fact it can be adapted to evaluate *every* three point correlator with a given fermion structure. In the third section I will outline the data analysis strategy that must be implemented to extract bare B_i parameters in the continuum limit. I conclude with a section describing what has been done and how the work should proceed to achieve results for B_i^{bare} .

4.1 Noise spinors method

In order to isolate bag parameters with the method of asymptotic behaviours of formula (3.17), I need two and three points correlators integrated over spatial coordinates. In this section I choose a prototype for these two and three point correlation functions and I work out applicative methods to evaluate them.

First of all, the computation of these quantities requires the knowledge of dressed quark propagators $S_{(i,\pm)}[U](x, y)$ for each given Gauge configuration¹. These propagators are defined on the lattice by the equation:

$$\sum_z \left(D^W \pm i\mu_i \gamma_5 \right) (x, z) S_{(i,\pm)}(z, y) = \delta_{x,y}^{(4)}$$

The inversion of the Dirac operator² in a simulation program requires, in principle, the inversion of a matrix in $\text{Mat}(N \times N, \mathbb{R})$, where

$$N = N_T \times N_{L_x} \times N_{L_y} \times N_{L_z} \times N_{\text{colours}} \times 4 \times 2$$

The multiplicative factor 4 is the number of components in a Dirac spinor while the factor 2 is given because the matrix elements are complex numbers. The inversion of

1 i is the flavour index. The sign \pm refers to twisted mass sign in twisted basis (i.e. the sign of the Wilson parameter r_i in physical basis)

2 To be rigorous, I must call it “Osterwalder-Seiler operator” because of the presence of twisted mass term. I will call it simply Dirac operator because it should be clear that the OS-QCD is the chosen regularization.

this matrix gives the propagator of a single flavour for a given Gauge configuration. It is not difficult to guess that the number of computational resources needed to directly compute the inversion is very large. For this reason smarter solutions have been developed.

One solution consists in a kind of “stochastic inversion”, worked out by Tomasz Korzec for two points meson correlators (2013) [30]. It makes use of some random Dirac spinors equipped with colour quantum numbers, called *stochastic sources* for reasons that will become obvious soon. For each inversion I generate N_{noise} sources η that will be used to evaluate *noise averages* of some quantities. I refer to a noise average with the angle-brackets $\langle \cdot \rangle^{\text{noise}}$. Components of noise spinors can be taken from one of the following randomic distributions: $\mathbb{Z}_2, U(1), \text{Norm}(0, 1)$. The required properties of the noise spinors are:

$$\begin{aligned} \langle \eta_{a\alpha}(u) \rangle^{\text{noise}} &= 0 \\ \langle \eta_{a\alpha}^*(u) \eta_{b\beta}(v) \rangle^{\text{noise}} &= \delta_{a,b} \delta_{\alpha,\beta} \delta_{\vec{u},\vec{v}} \delta_{u_4,x_4} \delta_{v_4,x_4} \end{aligned} \quad (4.1)$$

for euclidian time x_4 fixed. Such spinor is said to rely in the timeslice x_4 , or equivalently centered in x_4 .

In the two following paragraphs I will explain the strategies to evaluate $G_{12}^{\text{FR}}(x_4, y_4)$, $G_{34}^{\text{FR}}(x_4, y_4)$, $X_{12}^{\text{FR}}(x_4, y_4)$, $X_{34}^{\text{FR}}(x_4, y_4)$ and $C_i^{\text{FR}}(x_4, y_4, z_4)$ respectively defined in formulae (3.8), (3.9) and (3.7). These two and three points correlators are needed to extract B_i s. Two different - but very similar - computational strategies are used.

Two point meson correlators

Let's first analyze the case of two point correlators. I can recognize $G_{12,34}^{\text{FR}}$ and $X_{12,34}^{\text{FR}}$ in a more general form:

$$\begin{aligned} G(x_4, y_4) &= \sum_{\vec{x}, \vec{y}} \left\langle \bar{\psi}^1(x) \Gamma^\alpha \psi^2(x) \bar{\psi}^2(y) \Gamma^\beta \psi^1(y) \right\rangle^{\text{sea}} \\ &= - \sum_{\vec{x}, \vec{y}} \left\langle \text{Tr} \left[\Gamma^\alpha S_{(2,+)}(x, y) \Gamma^\beta S_{(1,+)}(y, x) \right] \right\rangle^{\text{sea}} \end{aligned} \quad (4.2)$$

for generic flavours ψ^1, ψ^2 . This correlator generates the meson propagator diagram shown in Figure 1.2. Again, I suppose $x_4 > y_4$. The strategy to evaluate meson correlator of this type has been developed in a guide-paper by Tomasz Korzec [30]. It consist into generating a single set of stochastic spinors $\eta(u)$ centered in timeslice x_4 . For each $\eta(u)$, two daughter stochastic quantities are defined:

$$\begin{aligned} \zeta^{(i,\pm)}(u) &= \sum_v S_{(i,\pm)}(u, v) \eta(v) \\ \xi^{(i,\pm)}(u) &= \sum_v S_{(i,\pm)}(u, v) \gamma_5 \Gamma^{\alpha\dagger} \eta(v) \end{aligned}$$

Because of the second property in (4.1), I can rewrite the correlator as:

$$G(x_4, y_4) = - \sum_{\vec{y}} \sum_{\vec{u}, \vec{v}} \left\langle \left\langle \eta^\dagger(u) \Gamma^\alpha S_2(u, y) \Gamma^\beta S^1(y, v) \eta(v) \right\rangle^{\text{noise}} \right\rangle^{\text{sea}}$$

There are some lines of calculations that I do not report. The only relevant property I used is $\gamma_5 S_{(i,\pm)}(u, v) \gamma_5 = S_{(i,\mp)}^\dagger(v, u)$, proved in Appendix D.3. The overall result

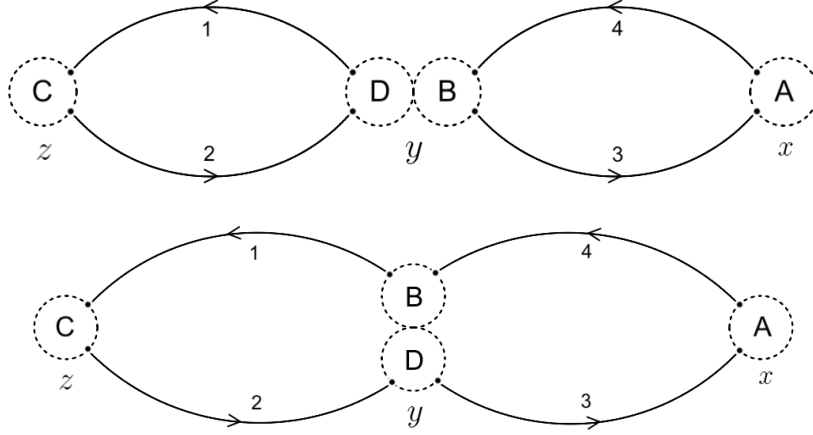


Figure 4.1. On the top: graph of disconnected Wick contraction. On the bottom: graph of connected Wick contraction. The variables are such that $x_4 > y_4 > z_4$.

is:

$$G(x_4, y_4) = - \sum_{\vec{y}} \left\langle \left\langle \left(\xi^{(2,-)}(y) \right)^\dagger \gamma_5 \Gamma^\beta \zeta^{(1,+)}(y) \right\rangle^{\text{noise}} \right\rangle^{\text{sea}}$$

Then, for each correlator, I need to evaluate only two quantities for each y and for each noise spinor: $\xi^{(2,-)}(y)$ and $\zeta^{(1,+)}(y)$. This noise average gives directly the trace for a given sea configuration. The average over sea Gauge configurations gives the usual VEV in path integral formulation.

Three point meson correlators

The case of three points correlators is a complexified version of the previous paragraph, but there are no conceptual innovations. The method is the same and the followed steps are similar to the two points correlator case. I want to calculate correlation functions of the following two types:

$$\begin{aligned} G_d(x_0, y_0, z_0) &= \sum_{\vec{x}, \vec{y}, \vec{z}} \left\langle \bar{\psi}_4(x) \Gamma_A \psi_3(x) \bar{\psi}_1(y) \Gamma_D \psi_2(y) \bar{\psi}_3(y) \Gamma_B \psi_4(y) \bar{\psi}_2(z) \Gamma_C \psi_1(z) \right\rangle^{\text{sea}} \\ G_c(x_0, y_0, z_0) &= \sum_{\vec{x}, \vec{y}, \vec{z}} \left\langle \bar{\psi}_4(x) \Gamma_A \psi_3(x) \bar{\psi}_1(y) \Gamma_B \psi_4(y) \bar{\psi}_3(y) \Gamma_D \psi_2(y) \bar{\psi}_2(z) \Gamma_C \psi_1(z) \right\rangle^{\text{sea}} \end{aligned} \quad (4.3)$$

The subscripts c and d refer to *connected* and *disconnected* correlators. The flavour exchange between the two correlators is not $(2 \leftrightarrow 4)$ but $(1 \leftrightarrow 3)$. The reason behind that will be clear soon. Picture 4.1 shows the correlators in a simple representative way for $x_4 > y_4 > z_4$.

After Wick contractions, the correlators read:

$$\begin{aligned} G_d &= \sum_{\vec{x}, \vec{y}, \vec{z}} \left\langle \text{Tr} \left[\Gamma_A S_{(3,+)}(x, y) \Gamma_B S_{(4,+)}(y, x) \right] \cdot \text{Tr} \left[\Gamma_C S_{(1,+)}(z, y) \Gamma_D S_{(2,+)}(y, z) \right] \right\rangle^{\text{sea}} \\ G_c &= - \sum_{\vec{x}, \vec{y}, \vec{z}} \left\langle \text{Tr} \left[\Gamma_A S_{(3,+)}(x, y) \Gamma_D S_{(2,+)}(y, z) \Gamma_C S_{(1,+)}(z, y) \Gamma_B S_{(4,+)}(y, x) \right] \right\rangle^{\text{sea}} \end{aligned} \quad (4.4)$$

I generate N_{noise} stochastic spinors in the timeslice x_0 and N_{noise} stochastic spinors in the timeslice z_0 . I refer to the formers with η^1 and the latters with η^2 . These stochastic spinors have again a Dirac index (α, β, \dots) and a colour index (a, b, \dots) . The properties (4.1) must be generalized to:

$$\begin{aligned}\langle \eta_{a\alpha}^1(u) \rangle^{\text{noise}} &= \langle \eta_{b\beta}^2(u) \rangle^{\text{noise}} = 0 \\ \langle \eta_{a\alpha}^{1*}(u) \eta_{b\beta}^2(v) \rangle^{\text{noise}} &= \langle \eta_{a\alpha}^{2*}(u) \eta_{b\beta}^1(v) \rangle^{\text{noise}} = 0 \\ \langle \eta_{a\alpha}^{1*}(u) \eta_{b\beta}^1(v) \rangle^{\text{noise}} &= \delta_{a,b} \delta_{\alpha,\beta} \delta_{\vec{u},\vec{v}} \delta_{u_0,x_0} \delta_{v_0,x_0} \\ \langle \eta_{a\alpha}^{2*}(u) \eta_{b\beta}^2(v) \rangle^{\text{noise}} &= \delta_{a,b} \delta_{\alpha,\beta} \delta_{\vec{u},\vec{v}} \delta_{u_0,z_0} \delta_{v_0,z_0}\end{aligned}\tag{4.5}$$

I define the following derived stochastic spinors:

$$\begin{aligned}\zeta_j^{(i,\pm)}(u) &= \sum_v S_{(i,\pm)}(u,v) \eta^j(v) \\ \xi_{j,X}^{(i,\pm)}(u) &= \sum_v S_{(i,\pm)}(u,v) \gamma_5 \Gamma_X^\dagger \eta^j(v)\end{aligned}\tag{4.6}$$

It could be easily checked that the contractions in (4.4) are obtained by the following formulae:

$$\begin{aligned}G_d &= \sum_{\vec{y}} \left\langle \left\langle \left(\gamma_5 \xi_{1,A}^{(3,-)}(y) \right)^\dagger \Gamma_B \zeta_1^{(4,+)}(y) \cdot \left(\gamma_5 \xi_{C,2}^{(1,-)}(y) \right)^\dagger \Gamma_D \zeta_2^{(2,+)}(y) \right\rangle^{\text{noise}} \right\rangle^{\text{sea}} \\ G_c &= - \sum_{\vec{y}} \left\langle \left\langle \left(\gamma_5 \xi_{1,A}^{(3,-)}(y) \right)^\dagger \Gamma_D \zeta_2^{(2,+)}(y) \cdot \left(\gamma_5 \xi_{C,2}^{(1,-)}(y) \right)^\dagger \Gamma_B \zeta_1^{(4,+)}(y) \right\rangle^{\text{noise}} \right\rangle^{\text{sea}}\end{aligned}\tag{4.7}$$

Then, to evaluate the previous couple of Wick contraction I need only four quantities for each couple of stochastic spinors:

$$\xi_{1,A}^{(3,-)}(y) \quad \zeta_1^{(4,+)}(y) \quad \xi_{C,2}^{(1,-)}(y) \quad \zeta_2^{(2,+)}(y)$$

To summarize, the path to evaluate the correlators is:

- ▷ For each Gauge-sea configuration evaluate $2N_{\text{noise}}$ spinors - N_{noise} for η^1 and N_{noise} for η^2 .
- ▷ For each noise spinor evaluate the quantities $\zeta_j^{(i,\pm)}$ and $\xi_{j,X}^{(i,\pm)}$ needed.
- ▷ Evaluate the correlators and evaluate the noise average.
- ▷ Iterate the procedure and calculate the sea average.
- ▷ At the end, the simulation program gives back the correlator $G_d + G_c$.

Let's look at the **computational advantage**. Each time I compute the quantities $\xi_{j,X}^{(i,\pm)}$ of $\zeta_j^{(i,\pm)}$ I'm *not* evaluating the inverse of a matrix in $\text{Mat}(N \times N, \mathbb{R})$, but its inverse on a vector of length N . Then the needed computational resources are decreased and the simulation algorithms result improved. Furthermore, I need "only" $4 \cdot N_{\text{noise}} \cdot N_{\text{noise}} \cdot N_{\text{configurations}}$ inversion of this kind for each three points correlator. Then, for a reasonable choice of N_{noise} , the advantage is successfully achieved³.

³ in practice, almost always.

4.2 Simulation program description

The program is structured to generate three points correlation functions and it is based on a previous version that calculates meson propagators. It makes use of modules from `OpenQCD-1.2`⁴, allowing calculations with open boundary conditions. The program takes in input an ensemble of sea configurations and produces the correlators of the form (3.7) with x_4, z_4 fixed and y_4 running in the time region $[z_4, x_4]$. Instead of read some external configurations, it is also possible to set the link variables to identity $U_\mu(x) = \mathbb{I}_3$ (absence of interactions, because $A_{\mu,j}^i = 0$) or to randomly generate them. These two options were very useful to test the correct behaviour of the simulation. The program requires the following input parameters:

- The coefficient of the Sheikholeslami-Wohlert term c_{SW} and c_F , another coefficient for the boundary counterterms of the fermionic action. The latter is set to $c_F = 1$.
- Informations about the noise spinor method: the number of noise vectors N_{noise} per set and the generating distribution chosen from one of the following $U(1)$, **Gauss**, \mathbb{Z}_2 .
- Quark flavours informations: the critical mass M_{cr}^i and the bare twisted mass parameter μ_i for each quark.
- Dirac matrices: $\Gamma_\omega, \Gamma_\xi$ for the source bilinears and $\Gamma_\sigma, \Gamma_\rho$ for the intermediate operator. The program allows to insert different operators within the same sources and calculate their Wick contractions. It is also possible to choose which quark to insert in each propagator.

At the end the program stores output data in a file written in `LITTLE_ENDIAN` or `BIG_ENDIAN` depending on the machine used. The output data are already summed over all the spatial components.

4.2.1 Computational Basis

One might wonder the reason behind the choice of exchange operators $\Gamma_B \leftrightarrow \Gamma_D$ between the terms G_d and G_c of the previous method (look at equations (4.3)). It could seem an unreasonable choice because it has the form of a flavour exchange ($1 \leftrightarrow 3$) instead of ($2 \leftrightarrow 4$), that one might expect. Behind this choice lies a subtlety developed for computational convenience.

I can rewrite the set of operators $\{O_{i,[+]}^{\text{tw}}\}$ in equations (3.5) in the following compact forms:

$$\begin{aligned}
 O_{1[+]}^{\text{tw}} &= \mp 2i \left(V^{12} A^{34} + A^{12} V^{34} + V^{14} A^{32} + A^{14} V^{32} \right) \\
 O_{2[+]}^{\text{tw}} &= \mp 2i \left(V^{12} A^{34} - A^{12} V^{34} - V^{14} A^{32} + A^{14} V^{32} \right) \\
 O_{3[+]}^{\text{tw}} &= \pm 2i \left(P^{12} S^{34} - S^{12} P^{34} - P^{14} S^{32} + S^{14} P^{32} \right) \\
 O_{4[+]}^{\text{tw}} &= \pm 2i \left(P^{12} S^{34} + S^{12} P^{34} + P^{14} S^{32} + S^{14} P^{32} \right) \\
 O_{5[+]}^{\text{tw}} &= \pm 2i \left(\tilde{T}^{12} T^{34} + T^{14} \tilde{T}^{32} \right)
 \end{aligned} \tag{4.8}$$

⁴ <https://luscher.web.cern.ch/luscher/openQCD/index.html>

Clarifications about the notation can be found in Appendix A. I want to group together the minimal elements to compute the C_i^{FR} s in a simulation. This strategy brought me to redefine again - and for the last time - the operators. They read:

$$\begin{aligned}
\Psi_1 &= V^{12}A^{34} + A^{14}V^{32} & O_{1[+]}^{\text{tw}} &= \mp 2i(\Psi_1 + \Psi_2) \\
\Psi_2 &= A^{12}V^{34} + V^{14}A^{32} & O_{2[+]}^{\text{tw}} &= \mp 2i(\Psi_1 - \Psi_2) \\
\Psi_3 &= P^{12}S^{34} + S^{14}P^{32} & O_{3[+]}^{\text{tw}} &= \pm 2i(\Psi_3 - \Psi_4) \\
\Psi_4 &= S^{12}P^{34} + P^{14}S^{32} & O_{4[+]}^{\text{tw}} &= \pm 2i(\Psi_3 + \Psi_4) \\
\Psi_5 &= \tilde{T}^{12}T^{34} + T^{14}\tilde{T}^{32} & O_{5[+]}^{\text{tw}} &= \pm 2i \cdot \Psi_5
\end{aligned}$$

As usual, through them I recover the operators $O_{i[+]}^{\text{tw}}$. Each of the new operators has the form:

$$\Psi_i = \bar{\psi}_1 \Gamma_D \psi_2 \cdot \bar{\psi}_3 \Gamma_B \psi_4 + \bar{\psi}_1 \Gamma_B \psi_4 \cdot \bar{\psi}_3 \Gamma_D \psi_2$$

that is a flavour exchange $1 \leftrightarrow 3$ and *not* $2 \leftrightarrow 4$. Thus I directly evaluate this kind of correlator $\forall i$:

$$\left\langle \bar{K}^{i0}(x) \Psi_i(y) \bar{K}^0(z) \right\rangle \sim \left\langle \left(\bar{\psi}_4 \Gamma_A \psi_3 \right)(x) \Psi_i(y) \left(\bar{\psi}_2 \Gamma_C \psi_1 \right)(z) \right\rangle$$

and it can be verified that it gives exactly the contractions $G_c + G_d$ of Figure 4.1. With the symbol \sim I refer to the fact that the two correlators have the same structure, i.e. they are *similar* from a computational point of view. Then the output data of simulation program has no physical meaning until I perform the basis change in data analysis time.⁵

4.3 Analysis strategy

This section provides an overview of the analysis strategy needed to recover the lattice bag parameters $\mathcal{B}_i(a)$ through the method based on asymptotic behaviours outlined in section 3.5. Once recovered the $\mathcal{B}_i(a)$ s at different values of lattice spacing a , the continuum limit $a \rightarrow 0$ will give the best estimate of the physical parameters B_i . The analysis is divided in some steps, that I report below. This analysis strategy holds for all the data generated from gauge configurations with open boundary conditions, involving CLS ensembles.

First step: determination of minimal “asymptotic distance” δ_4

In order to perform the calculation in (3.17):

$$\begin{aligned}
\mathcal{B}_1(a; y_4) &= \frac{1}{\xi_1} \cdot \frac{C_1^{\text{FR}}(x_4, y_4, z_4)}{X_{34}^{\text{FR}}(x_4, y_4) \cdot X_{12}^{\text{FR}}(y_4, z_4)} \\
\mathcal{B}_i(a; y_4) &= \frac{1}{\xi_i} \sum_j \Lambda_{ij} \frac{C_i^{\text{FR}}(x_4, y_4, z_4)}{G_{34}^{\text{FR}}(x_4, y_4) \cdot G_{12}^{\text{FR}}(y_4, z_4)}
\end{aligned}$$

I need the values of such two points and three points correlators in the temporal regions in which the asymptotic behaviour of Section 3.5 is allowed. In other words, I need to quantify the minimum value of $\delta_4 = |x_4 - y_4|$ such that the exponentials

⁵ To be precise, the physical meaning is achieved only in the continuum limit $a \rightarrow 0$.

$e^{-\delta_4 m_i}$ - for $m_i > m_K$ - are *sufficiently* suppressed with respect to the first level contribution $e^{-\delta_4 m_K}$. To estimate it, I make use of two points correlators $G_{12}^{\text{FR}}(y_4, z_4)$ and $G_{34}^{\text{FR}}(x_4, y_4)$, namely the mesons propagators. Let's start with the first. From the proof D.5 I know that, in the asymptotic regime $y_4 \gg z_4$ ⁶:

$$G_{12}^{\text{FR}}(y_4, z_4) \approx \frac{\sinh(m_K(T - y_4)) \cdot \sinh(m_K z_4)}{2m_K \sinh(m_K T)} \propto \sinh(m_K(T - y_4)) \quad (4.9)$$

In the last equality I fixed $z_4 = a$, choice valid in the entire simulation. I fix $z_4 = a$ and run the simulation for all the $y_4 \in (z_4 + a, T - a)$. The case $y_4 = T$ will not produce physical results because of open boundary conditions on fermion fields. The strategy consists in performing a fit of the hyperbolic sine in different regions of the space. I start to fit in the maximal region $[a, T - a]$ and decrease it step by step $[2a, T - 2a], [3a, T - 3a], \dots$ until the goodness of the fit reaches a satisfactory previously chosen value. Up to now, no such goodness parameters has been chosen. The first satisfactory region gives the value of δ_4 : $[\delta_4, T - \delta_4]$. At this point I will have determined both m_K as a parameter and the “minimal asymptotic distance” δ_4 . In this region I also have the values of $G_{12}^{\text{FR}}(y_4, z_4 = a) = \hat{G}_{12}^{\text{FR}}(y_4, a)$ subject to a well defined asymptotic expansion. I denote them with the *hat* identifier to stress that these data are the ones to be used to recover the wanted quantities. Then the same procedure must be done for the other two points correlator, $G_{34}^{\text{FR}}(x_4, y_4)$. In this case x_4 must be intended as fixed to $T - a$, while $y_4 < x_4$ varies. In this case the complete formula of the correlator is again (4.9), but the fit must be on the second variable:

$$G_{34}^{\text{FR}}(x_4, y_4) \propto \sinh(m_{K'} y_4)$$

By repeating the previous analysis, one should get a value of $m_{K'}$ and a data set of correlators $G_{34}^{\text{FR}}(x_4 = T - a, y_4) = \hat{G}_{34}^{\text{FR}}(T - a, y_4)$ useful for the next setps. Moreover there comes another value of minimal asymptotic distance δ'_4 . I simply chose to use the larger of the two, that I call again δ_4 .

With x_4 and z_4 fixed I will take, by varying y_4 , the data to be used in (3.17), namely $\hat{X}_{12}^{\text{FR}}(y_4, a)$ with $y_4 - a > \delta_4$ and $\hat{X}_{34}^{\text{FR}}(T - 1, y_4)$ with $T - a - y_4 > \delta_4$.

Second step: recovering lattice bag parameters \mathcal{B}_i

At this point I will be ready to analyze three points correlators $C_i^{\text{FR}}(x_4, y_4, z_4)$. I take a set of correlators with $z_4 = a$, $x_4 = T - a$ while y_4 varies in $(z_4 + \delta_4, x_4 - \delta_4)$ because I know from the analysis of $G_{12,34}^{\text{FR}}$ that the higher mass states are already suppressed. Thus the only relevant contribution comes from lattice Kaons. In such region I rename them $\hat{C}_i^{\text{FR}}(x_4, y_4, z_4)$.

The results of previous steps are used to recover values of the $\mathcal{B}_i(a)$ for a given set of Gauge configuration, i.e. for a given value of lattice spacing a :

$$\mathcal{B}_i(a; y_4) = \frac{1}{\xi_i} \sum_{j=1}^5 \Lambda_{ij} \mathcal{F}_j(a; y_4)$$

I have different values of \mathcal{B}_i corresponding to different choices of y_4 . It is possible that some *residues* of higher mass states contribution are still present. A fit on a

⁶ In the paper [33] by Luscher it is not given the complete result, but only the last y_4 dependence. A proof of the complete result is a personal achievement reported in the Appendix D.

plateaux region of the graph $\mathcal{A}_i(a)(y_4)$ vs y_4 will help to remove them. I expect to see that plateaux region for values of the euclidean time y_4 much larger than z_4 and sufficiently smaller than x_4 . At this point, I will have extracted the best estimate for the lattice bag parameters $\mathcal{B}_i(a)$.

Third step: continuum limit extrapolation of B_i^{bare}

A set of configurations it is always generated by setting some parameters, for example the inverse of coupling constant g . By analyzing some observables of the gauge fields it is possible to recover the value of the lattice spacing a associated to an ensemble of configurations.

Repeating the previous analysis for different sets of gauge ensembles brings to a set of parameters for different values of the lattice spacing $\mathcal{B}_i(a_1), \mathcal{B}_i(a_2), \dots$. The essential step to get the *physical* values of the bag parameters B_i is the continuum limit extrapolation. It consists in: (i) a fit of lattice values versus their associated lattice spacing that gives the function $\mathcal{B}_i^{\text{fit}}(a)$ and (ii) an $O(a)$ -improved extrapolation of the physical values through $B_i = \mathcal{B}_i^{\text{fit}}(0) + O(a^2)$.

4.4 Status of the work, results and future developments

In this section I outline the status of this work and possible future developments. The program behaviour has been tested both in the vacuum $U_\mu(x) = \mathbb{I}_3 \forall \mu, x$ and through unphysical random configurations. The relevant tests reported consist into two checks of gauge invariance of two and three points correlators. Gauge invariance is an essential property of QFTs; for this reason it is one of the most checked in lattice QCD simulations. Then the program has been tested on two ensembles of quenched⁷ gauge fields with OBC.

The first test furnishes a direct proof that the Dirac inverter preserves gauge invariance property. Unwanted errors could be found from a lack in this test. A set of pointlike spinors has been generated. I define *pointlike* spinor an η defined by:

$$\eta_\alpha^a(x) = \delta^{a,\bar{a}} \delta_{\alpha,\bar{\alpha}} \delta_{x,\bar{x}}$$

with $\bar{a}, \bar{\alpha}, \bar{x}$ fixed colour, Dirac and lattice indices. This has been done for all the $3 \times 4 = 12$ combinations of fixed Dirac and colour indices, meanwhile \bar{x} was kept unchanged. By inverting the Osterwalder-Seiler operator on them, the propagators was expected to have this structure:

$$\left(S^{(f)}(y, \bar{x})[U] \right)_{\beta, \bar{\alpha}}^{b, \bar{a}} \quad \forall b, \beta, y$$

with f the flavour index. I have explicitly contracted propagators and Dirac matrices to reconstruct Wick contractions of previous chapter. This has been made by fixing two pointlike sources $\bar{x} = (\vec{0}, x_4)$ and $\bar{z} = (\vec{0}, z_4)$, by choosing a mixing operator $\Psi_i(y)$ and summing over the fixed colour and Dirac indices. In other words, the *noise average* in formula (4.7) is replaced by the sum over two sets of 12 pointlike sources. In both tests the values of z_4 and x_4 were fixed respectively to the first and last allowed timeslice. This has been done for random sea fields and their gauge transformed fields. The propagators are expected to transform in the following way:

$$\left(S^{(f)}(y, \bar{x})[\Omega U \Omega^\dagger] \right)_{\beta, \bar{\alpha}}^{b, \bar{a}} = \Omega(y)^{b,c} \left(S^{(f)}(y, \bar{x})[U] \right)_{\beta, \bar{\alpha}}^{c,d} \Omega^\dagger(\bar{x})^{d,\bar{a}}$$

⁷ i.e. in absence of sea quarks, neglecting the fermion determinant in (2.1).

thus the traces appearing in the Wick contractions (3.4) are gauge invariant. The check of gauge invariance has been successfully achieved by comparing two set of data of three points correlators obtained using a (random) configuration and its gauge transformed duplicate. The gauge transformations $\Omega(x)$ were randomly generated. Figure 4.2 shows the output of the described test, in which the intermediate operator is $\Psi_3(y)$. Since the three points correlators are real, only the real part is plotted. Such reality property is proven in D.2.

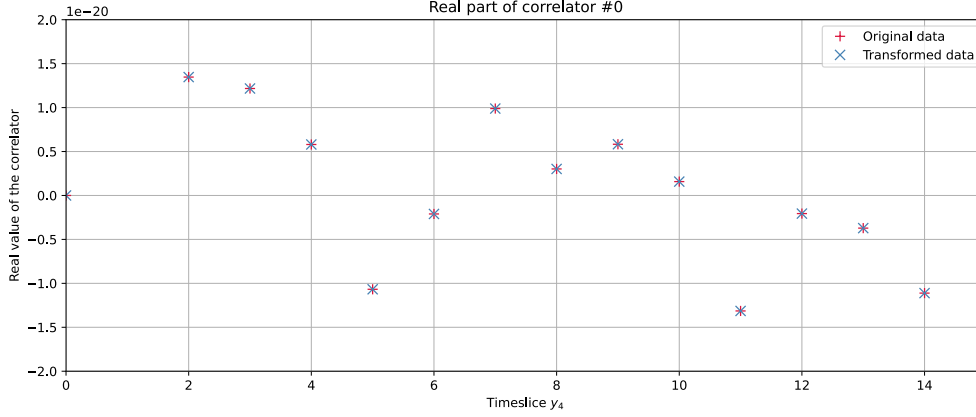


Figure 4.2. Check of Gauge invariance on the 3 points correlators. The plot shows the three point correlator $\sum_{\vec{y}} \langle \bar{K}^0(14a, \vec{0}) \Psi_3(y_4, \vec{y}) \bar{K}^0(a, \vec{0}) \rangle$ versus the timeslice y_4 . The gauge fields are randomly generated, the sources are a γ_5 and an \mathbb{I}_4 to emulate Kaon sources in OS twist. The point in $y_4 = 1$ is out of range, but exhibits the same gauge invariance property. I stress that these data are not physically meaningful.

In both the tests the finite precision of the solver generates discrepancies between the two data sets, but they are visible only at scales much smaller than the correlators scale. It has been verified that these errors decrease requiring more and more precision in the inversion of the propagators. Moreover all the physical parameters were not well tuned, since they were not useful to the scope of the checks.

The second test aims to verify gauge invariance of the three points correlators calculated through the noise spinors method, equation (4.7). It consists in the following steps. First of all, it has been generated a set of random unphysical link variables $U_\mu(x)$ and they were used to compute correlators through formula (4.7). Then data were stored and analyzed. The second part consisted in the generation of random gauge transformations $\Omega(x)$. The previous gauge configuration has been transformed and it followed a re-computation of the correlators. The two data sets must coincide up to errors. This test served to quantify the minimum number of noise spinors N_{noise} to make the stochastic method effective. To better understand it, a set of graphs in Figure 4.3 shows the plots of such test using respectively $N_{\text{noise}} = 5, 20, 50, 100$ noise spinors. In order to quantify the error due to different number of stochastic sources, I introduced the following estimator:

$$\varepsilon(N_{\text{noise}}) = \frac{1}{N_T - 2} \sum_{y_4} \left(\frac{|C(y_4) - \tilde{C}(y_4)|}{C(y_4) + \tilde{C}(y_4)} \right)$$

The values of such estimator for different choices of number of stochastic sources are listed in Table 4.1. The values seems to be rapidly decreasing for $N_{\text{noise}} \lesssim 35$ while stabilizing for $N_{\text{noise}} \gtrsim 35$. To complete the study of the numebr of noise spinors

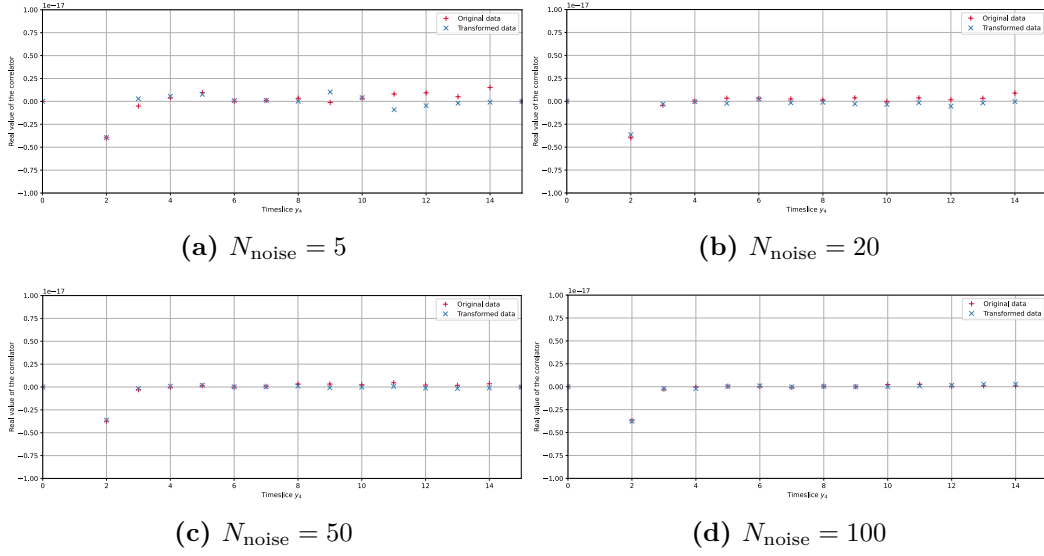


Figure 4.3. Second gauge invariance test executed on random link variables. Such $U_\mu(x)$ are the same for each of the four tests. The plots show the real part of the integrated correlator $\sum_{\vec{y}} \langle \bar{K}^0(14a, \vec{0}) \Psi_3(y_4, \vec{y}) \bar{K}^0(a, \vec{0}) \rangle$ for different values of N_{noise} . The distribution served to extract the random η^i is $U(1)$.

through this estimator, a set of ε s for a large amount of configurations should be tested.

N_{noise}	5	20	35	50	70	100
ε	2.140	2.598	1.350	1.342	1.243	0.533

Table 4.1. Values of the estimator ε for different values of N_{noise} from a single simulation.

Another test has been done on an ensemble of 54 gauge configurations generated using the `OpenQCD-1.2` program. The gauge configurations have been generated with and inverse lattice coupling $\beta = 6/g_0^2 = 6.0$ - corresponding to an inverse lattice spacing $a^{-1} \sim 2.0$ GeV[5] - in the quenched approximation. The value of the coefficient c_0 in equation (2.4) is set to $5/3$, then the simulated action is the *tree level Symanzik improved*. The lattice has dimension $16 \times 16 \times 16 \times 32$, where 32 is the number of points in time direction. First of all the configurations have been tested on the program that calculates two points correlators. The simulation involved $N_{\text{noise}} = 30$ noise spinors and the hopping parameters used were not at their critical value, thus the maximal twist is not achieved. Despite this, the simulation furnishes a test on the two point functions behaviour. The correspondig graph, in logarithmic scale, is presented in Figure 4.4. Here $x_4 < y_4$ with fixed $x_4 = a$. The behaviour of the two point correlators is, as expected, similar to the one in Figure 6 in [33]. Such behaviour is proportional to:

$$\propto C + \log [\sinh (M_i(T - y_4)) \cdot \sinh (M_i x_4)] = C' + M_i (T + x_4 - y_4) + \log [f(x_4, y_4)]$$

that's a line plus a logarithm of a function f of the time coordinates. The two points correlators considered are the scalar and pseudoscalar propagators, i.e. $G_{12}^{\text{FR}}(y_4, x_4)$ and $G_{34}^{\text{FR}}(y_4, x_4)$.

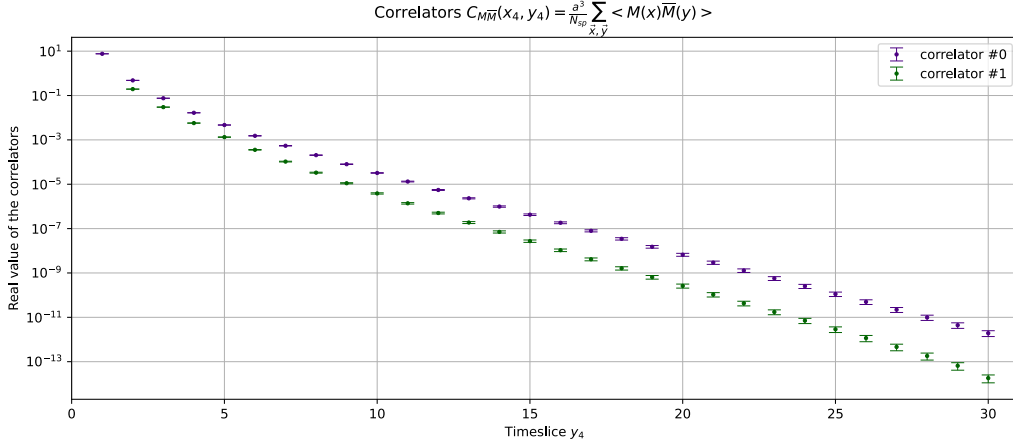


Figure 4.4. Two points correlators $\sum_{\vec{x}, \vec{y}} \langle \bar{K}^0(y) K^0(x) \rangle$ and $\sum_{\vec{x}, \vec{y}} \langle \bar{K}^{0'}(y) K^{0'}(x) \rangle$. Test executed with hopping parameters different from the critical value and twisted mass terms different from zero.

Then the case of three points correlators is inspected. The correlators were calculated through $N_{\text{nosie}} = 20$ noise spinors and the Figure 4.5 shows the results.

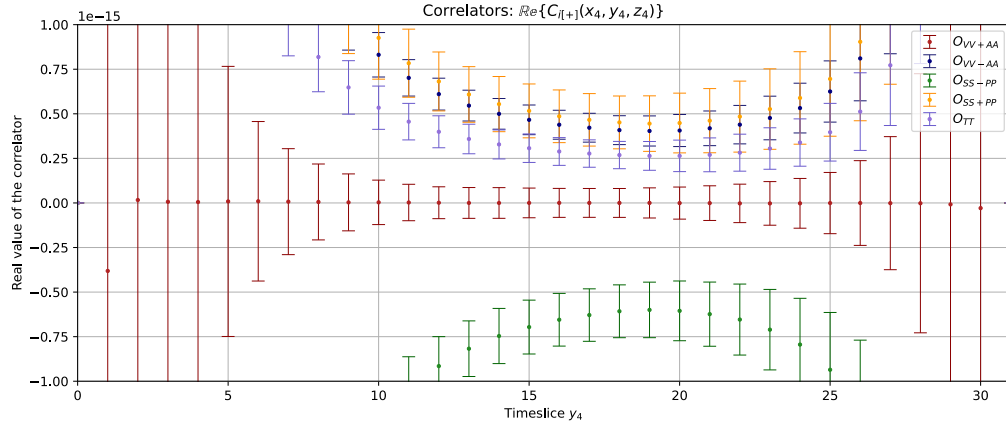


Figure 4.5. Test of the simulation program on 54 quenched configurations on a $16 \times 16 \times 16 \times 32$ lattice, $\beta = 6.0$, tree level improved Symanzik gauge action.

Clearly the plot is not at all satisfactory because there are no plateau regions. On the other hand, the fermion physical parameters had no physical meaning because their determination requires a lot of work, not necessary for a simple test such that. Then the maximal twist is not achieved and such correlators are meaningless. Usually the physical parameters, such as K_{crit} and μ_i s, are given along with the configuration, when available and already been studied. Moreover the first correlator has values extremely small - by one order or more - compared to values from the other operators. The imaginary part of these correlators have been plotted and the plot confirms that these correlators are real. The plot is reported in Appendix D.2.

The last test of the simulation program was made on 37 gauge configurations in quenched approximation. They are generated through `OpenQCD-1.2` program, with

$\beta = 6.0$ and $c_0 = 1.0$ and a $16 \times 16 \times 16 \times 32$ lattice. These parameters are chosen to simulate the plaquette Gauge action. The reason behind this choice relies in the results of paper [5]. In such paper the critical hopping parameter of twisted fermions has been studied for such configurations and the most precise result gives $K_{\text{crit}} = 0.135217$. This results has been used to simulate three points correlators, along with other parameters:

- down quark twisted mass: $a|\mu_d| = 0.0038$.
- strange quark twisted mass used is: $a\mu_s = 0.1482$.
- the coefficient of Sheikholeslami-Wohlert term is set to $c_{SW} = 1.769$, from [35].

Due to the use of K_{crit} , the maximal twist is achieved. The plot of the integrated correlators C_i^{FR} are shown in Figure 4.6 below:

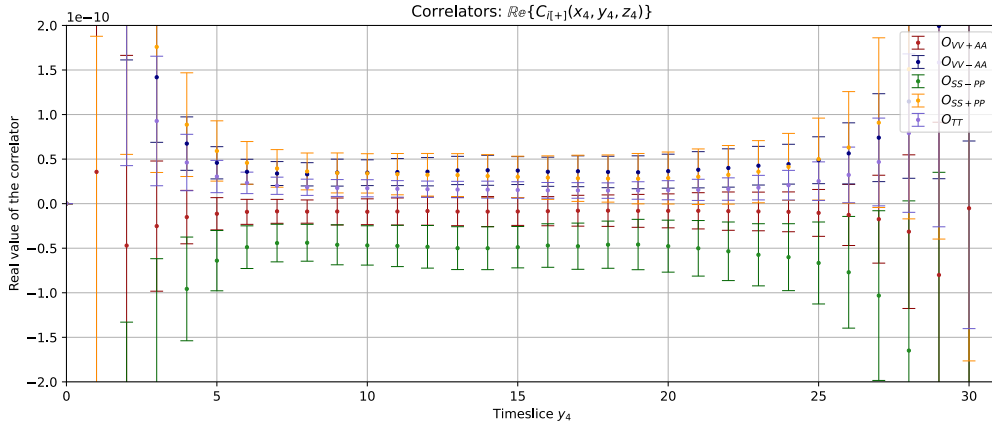


Figure 4.6. Test of the simulation program on 37 quenched configurations on a $16 \times 16 \times 16 \times 32$ lattice, $\beta = 6.0$, plaquette action.

As can be seen, the good choice of fermion parameters associated to the configurations generated more evident plateaux regions. Large error bars are due to the small number of noise sources and the small number of configurations analyzed. Moreover the first operator does not exhibit a null plateaux, unlike what is shown in Figure 4.5.

The results of C_i^{FR} are used to recover the lattice ratios:

$$\mathcal{R}_i(a; y_4) = \sum_{j=2}^5 \Lambda_{ij} \frac{C_j^{\text{FR}}(T - a, y_4, a)}{C_1^{\text{FR}}(T - a, y_4, a)}$$

Because of lack of large number of data, statistics results too low to determine a plateaux region with satisfactory precision.

Future developments

Future developments involve the calculation of three points correlators by using faithful sea configurations and tuning the fermion parameters. The purpose is to do that using the Coordinated Lattice Simulations⁸, generated through the open-QCD⁹

⁸ Coordinated Lattice Simulations: <https://wiki-zeuthen.desy.de/CLS/>

⁹ Open-QCD packages: <https://luscher.web.cern.ch/luscher/openQCD/index.html>

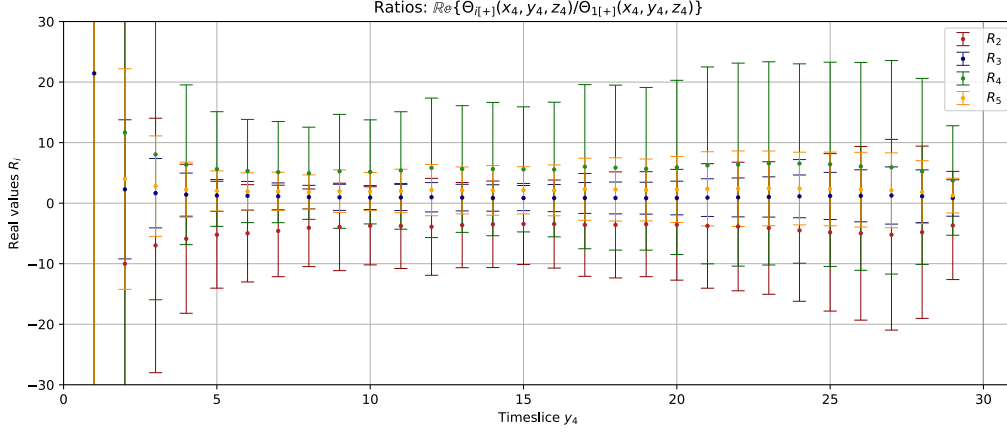


Figure 4.7. Ratios $\mathcal{R}_i(a; y_4)$ with lattice spacing $a \sim (2\text{Gev}^{-1})$ on the last set of gauge configurations.

(CLS) ensembles [10] with $N_f = 2 + 1$ improved sea quarks. These configurations have been studied in a wide literature of works¹⁰ and contains $N_f = 2 + 1$ quarks in the sea. On these ensembles the fermion parameters are well tuned through complex and precise procedures [10] [4]. The two points meson correlators are studied, for example in [28]. To do that, a match between sea quarks masses and valence masses is required, as done in [12]. The results of bare bag parameters B_i on CLS configurations will be a cutting edge result.

¹⁰ For some examples, consult Bibliography at the end of the thesis.

Appendix A

Notations and conventions

The metric employed in this study is the Euclidean metric $g_{\mu\nu} = \delta_{\mu\nu}$. In this context, there is no differentiation between upper and lower Dirac indices. I usually prefer to use lower indices.

The Dirac matrices employed belong to the so-called “chiral representation” [29]. Dirac matrices and Lorentz generators for spinors are as follows:

$$\begin{aligned}\gamma_i &= \sigma_2 \otimes \sigma_i & \gamma_0 &= -\sigma_1 \otimes \mathbb{I}_2 = -\gamma_4 \\ \gamma_5 &= \gamma_0 \gamma_1 \gamma_2 \gamma_3 = \sigma_3 \otimes \mathbb{I}_2 \\ \text{properties } \{\gamma_\mu, \gamma_\nu\} &= 2\delta_{\mu\nu} \mathbf{I}_4 \text{ and } \{\gamma_\mu, \gamma_5\} = 0 \\ \sigma_{\mu\nu} &= \frac{i}{2} [\gamma_\mu, \gamma_\nu] = i(\gamma_\mu \gamma_\nu - \delta_{\mu\nu} \mathbf{I}_4) \\ \tilde{\sigma}_{\mu\nu} &= \frac{1}{2} \epsilon_{\mu\nu\rho\omega} \sigma_{\rho\omega} = \gamma_5 \sigma_{\mu\nu}\end{aligned}$$

The Lagrangian densities in Minkowski and Euclidean spaces are:

$$\begin{aligned}\mathcal{L}_M &= -\bar{\psi} (\gamma_\mu (\partial_\mu + iA_\mu) + m) \psi \\ \mathcal{L}_E &= \bar{\psi} (\gamma_\mu (\partial_\mu + iA_\mu) + m) \psi\end{aligned}$$

This leads to the Dirac equation and its Dirac conjugate (valid in both Minkowski and Euclidean metrics):

$$\begin{aligned}(\gamma_\mu (\partial_\mu + iA_\mu) + m) \psi &= 0 \\ \bar{\psi} (\gamma_\mu (\partial_\mu + iA_\mu) - m) &= 0\end{aligned}$$

Dirac bilinears are typically expressed in the following form: $\bar{\psi}^1 \Gamma^\alpha \psi^2$ with ψ^1 and ψ^2 representing two distinct flavours. The Dirac operators belong to this set:

$$\Gamma^\alpha \in \{\mathbb{I}_4, \gamma_\mu, \gamma_5, \gamma_\mu \gamma_5, \sigma_{\mu\nu}, \tilde{\sigma}_{\mu\nu}\}$$

and a shorthand notation is $X^{12} = \bar{\psi}^1 \Gamma^\alpha \psi^2$ where $X = S, V, P, A, T, \tilde{T}$ indicates which matrix is chosen. For example $V^{12} A^{34} = \bar{\psi}^1 \gamma_\mu \psi^2 \bar{\psi}^3 \gamma_\mu \psi^4$.

A very useful property [29] follows:

$$\begin{aligned}\left(\bar{\psi}^1 \Gamma^\alpha \psi^2\right)^* &= \left(\bar{\psi}^1 \Gamma^\alpha \psi^2\right)^\dagger = -\bar{\psi}^2 \bar{\Gamma}^\alpha \psi^1 \\ \text{with } \bar{\Gamma}^\alpha &= \gamma_0 \Gamma^{\alpha, \dagger} \gamma_0.\end{aligned}\tag{A.1}$$

for example in the case of Kaons $(K^0)^* = \bar{K}^0$.

Appendix B

Twisted basis vs physical basis

B.1 Twisted and physical basis in tmQCD

In the context of twisted mass lattice QCD described in 2.3.4, it is possible to define a physical fermion basis as follows:

$$\chi = \mathbf{T}(\alpha) \psi \quad \bar{\chi} = \bar{\psi} \mathbf{T}(\alpha)$$

Here, $\mathbf{T}(\alpha)$ represents the twist rotation (2.8). In this scenario, the twisted mass action takes the following form:

$$S_{\text{tm}}^{\text{phys}}[\chi, \bar{\chi}, U] = a^4 \sum_{x,y} \bar{\chi}(x) \left(D_{xy}^{\text{tm}} + M_q \mathbb{I}_2 \delta_{xy} \right) \chi(y) \quad (\text{B.1})$$

where the new bilinear operator is given by:

$$D_{xy}^{\text{tm}} = -\frac{1}{2a} \sum_{\mu=\pm 1}^{\pm 4} [(\mathbf{T}(-2\alpha) - \gamma_\mu) U_\mu(x) \delta_{x+\hat{\mu},y}] + \frac{4}{a} \mathbf{T}(-2\alpha)$$

The key steps to establish this are:

1. Recall the properties $(\gamma_5)^2 = \mathbb{I}_4$ and $(\sigma^3)^2 = \mathbb{I}_2$
2. Expand the exponential: $\mathbf{T}(\alpha) = \cos(\alpha/2) \mathbb{I}_4 \otimes \mathbb{I}_2 + i \sin(\alpha/2) \gamma_5 \otimes \sigma^3$
3. Use the Clifford algebra $\{\gamma_\mu, \gamma_\nu\} = 2\delta_{\mu\nu} \mathbb{I}_4$ and Lie algebra of $SU(2)$ $[\sigma^a, \sigma^b] = 2i\epsilon^{abc} \sigma^c$ to modify the Wilson-Dirac operator $D_{xy} \mapsto D_{xy}^{\text{tm}}$

The new set of variables $\{\chi, \bar{\chi}\}$ is referred to as the *physical* basis because it doesn't involve the (unphysical) term μ_q . In other words, the mass is entirely transformed and encapsulated in $M_q = \sqrt{m^2 + \mu_q^2}$. The twist rotation modifies the Wilson term, which undergoes modification. Despite this, it is known [36] that the Wilson term vanishes in the continuum limit. Consequently, the action (B.1) tends towards the physical continuum action. Thus, it represents the “true” discretization of the continuum theory, while the twisted action defined in (2.9) is the modified action. The link between the two actions lies in the twist rotation of fermion fields. I will demonstrate that an expectation value can be computed in both theories. It's important to keep in mind that the framework in which the theory is applied is the

functional integral formalism, so we must pay attention to the integration measure. The variable change:

$$\mathcal{D}\chi \mathcal{D}\bar{\chi} \mapsto \mathcal{D}\psi \mathcal{D}\bar{\psi}$$

it is not anomalous¹. Moreover, the Jacobian is a constant $\mathbf{T}^2(\alpha)$. Since a constant doesn't affect the observables expectation values, I state - with abuse of this term - that the Jacobian is the identity. Next, I present the main result of this section: for a field-dependent observable \mathcal{X} , its expected value in both formulations coincides:

$$\langle \mathcal{X}[\chi, \bar{\chi}, U] \rangle_{(M_q, 0)} = \langle \mathcal{X}'[\psi, \bar{\psi}, U] \rangle_{(m, \mu_q)}$$

with $\mathcal{X}'[\psi, \bar{\psi}, U] = \mathcal{X}[\mathbf{T}(\alpha)\psi, \bar{\psi}\mathbf{T}(\alpha), U]$. The power of tmQCD theory lies in this substitution of variables.

Now, I provide a list of some straightforward operators - currents and densities - along with their transformation rules. First of all I define four quantities:

$$\text{Scalar density:} \quad S^{0, \text{phys}} = \bar{\chi}\chi$$

$$\text{Pseudoscalar densities:} \quad P^{a, \text{phys}} = \bar{\chi}\gamma_5 \frac{\sigma^a}{2} \chi$$

$$\text{Vector currents:} \quad V_\mu^{a, \text{phys}} = \bar{\chi}\gamma_\mu \frac{\sigma^a}{2} \chi$$

$$\text{Axial vector currents:} \quad A_\mu^{a, \text{phys}} = \bar{\chi}\gamma_\mu \gamma_5 \frac{\sigma^a}{2} \chi$$

where the superscript “phys” refers to the physical basis $\{\chi, \bar{\chi}\}$. Analogous definitions hold for the basis $\{\psi, \bar{\psi}\}$. I apply a twist $\mathbf{T}(\alpha)$ to get the twisted operators:

$$\begin{aligned} S^{0, \text{phys}} &= \cos(\alpha) S^{0, \text{tm}} + 2i \sin(\alpha) P^{3, \text{tm}} \\ P^{a, \text{phys}} &= \begin{cases} P^{a, \text{tm}} & \text{if } a = 1, 2 \\ \cos(\alpha) P^{3, \text{tm}} + \frac{i}{2} \sin(\alpha) S^{0, \text{tm}} & \text{if } a = 3 \end{cases} \\ V_\mu^{a, \text{phys}} &= \begin{cases} \cos(\alpha) V_\mu^{a, \text{tm}} + \epsilon^{3ab} \sin(\alpha) A_\mu^{b, \text{tm}} & \text{if } a = 1, 2 \\ V_\mu^{3, \text{tm}} & \text{if } a = 3 \end{cases} \\ A_\mu^{a, \text{phys}} &= \begin{cases} \cos(\alpha) A_\mu^{a, \text{tm}} + \epsilon^{3ab} \sin(\alpha) V_\mu^{b, \text{tm}} & \text{if } a = 1, 2 \\ A_\mu^{3, \text{tm}} & \text{if } a = 3 \end{cases} \end{aligned}$$

The very special case of maximal twist ($\alpha = \pm\pi/2$) reads:

$$\begin{aligned} S^{0, \text{phys}} &= \pm 2i P^{3, \text{tm}} \\ P^{a, \text{phys}} &= \begin{cases} P^{a, \text{tm}} & \text{if } a = 1, 2 \\ \pm \frac{i}{2} S^{0, \text{tm}} & \text{if } a = 3 \end{cases} \\ V_\mu^{a, \text{phys}} &= \begin{cases} \pm \epsilon^{3ab} A_\mu^{b, \text{tm}} & \text{if } a = 1, 2 \\ V_\mu^{3, \text{tm}} & \text{if } a = 3 \end{cases} \\ A_\mu^{a, \text{phys}} &= \begin{cases} \pm \epsilon^{3ab} V_\mu^{b, \text{tm}} & \text{if } a = 1, 2 \\ A_\mu^{3, \text{tm}} & \text{if } a = 3 \end{cases} \end{aligned}$$

¹ i.e. it does not introduce measure anomalies

B.2 Twisted and physical basis in OS regularization

In the case of OS regularization, the physical and twisted basis are related as follows:

$$\begin{cases} f = \mathbf{J}(\alpha, r) q \\ \bar{f} = \bar{q} \mathbf{J}(\alpha, r) \end{cases} \quad \text{and} \quad \begin{cases} q = \mathbf{J}(-\alpha, r) f \\ \bar{q} = \bar{f} \mathbf{J}(-\alpha, r) \end{cases}$$

Expanding the exponential in a series, it can be shown that $\mathbf{J}(\alpha, r) = \mathbb{I}_4 \cos(\alpha r/2) + i\gamma_5 \sin(\alpha r/2)$. The demonstration that the two actions outlined in section 2.3.5 are equivalent is straightforward and relies on the following identities:

$$\begin{aligned} \mathbf{J}(\alpha, r) \gamma_\mu &= \gamma_\mu \mathbf{J}(-\alpha, r) \\ \mathbf{J}(\alpha, r) \gamma_5 &= \gamma_5 \mathbf{J}(\alpha, r) \\ \mathbf{J}(\alpha, r) \mathbf{J}(\beta, r) &= \mathbf{J}(\alpha + \beta, r) \end{aligned}$$

Once again, the change of coordinates introduces no anomalous term in the integration measure. Furthermore, the Jacobian of the transformation is the identity:

$$\mathcal{D}f \mathcal{D}\bar{f} = \mathcal{D}q \mathcal{D}\bar{q}$$

In this scenario as well, masses are rotated, and formula (2.10) is still valid. I can then use (B.2) to express some observables in the twisted basis at maximal twist $\alpha = \pi/2$. I will consider two different cases:

1. Observables of the form $\bar{f}_1 \Gamma f_2$ in which the Wilson parameters are equal and absolute value 1 $r_1 = r_2 = \pm 1$.
2. Observables of the same form, but Wilson parameters are of opposite sign and absolute value 1: $r_1 = -r_2 = \pm 1$.

Let's introduce with some definitions, applicable in both cases:

$$\text{Scalar densities:} \quad S_{12}^{\text{phys}} = \bar{f}_1 f_2$$

$$\text{Pseudoscalar densities:} \quad P_{12}^{\text{phys}} = \bar{f}_1 \gamma_5 f_2$$

$$\text{Vector currents:} \quad V_{\mu,12}^{\text{phys}} = \bar{f}_1 \gamma_\mu f_2$$

$$\text{Axial vector currents:} \quad A_{\mu,12}^{\text{phys}} = \bar{f}_1 \gamma_\mu \gamma_5 f_2$$

$$\text{Tensor currents:} \quad T_{\mu\nu,12}^{\text{phys}} = \bar{f}_1 \sigma_{\mu\nu} f_2$$

$$\text{Pseudotensor currents:} \quad \tilde{T}_{\mu\nu,12}^{\text{phys}} = \bar{f}_1 \gamma_5 \sigma_{\mu\nu} f_2$$

Identical definitions are used in the twisted basis.

Case #1: $r_1 = r_2 = \pm 1$

$$\begin{aligned} S_{12}^{\text{phys}} &= \cos(\alpha) S_{12}^{\text{tw}} \pm i \sin(\alpha) P_{12}^{\text{tw}} \xrightarrow{\alpha=\pi/2} \pm i P_{12}^{\text{tw}} \\ P_{12}^{\text{phys}} &= \cos(\alpha) P_{12}^{\text{tw}} \pm i \sin(\alpha) S_{12}^{\text{tw}} \xrightarrow{\alpha=\pi/2} \pm i S_{12}^{\text{tw}} \\ V_{\mu,12}^{\text{phys}} &= V_{\mu,12}^{\text{tw}} \xrightarrow{\alpha=\pi/2} V_{\mu,12}^{\text{tw}} \\ A_{\mu,12}^{\text{phys}} &= A_{\mu,12}^{\text{tw}} \xrightarrow{\alpha=\pi/2} A_{\mu,12}^{\text{tw}} \\ T_{\mu\nu,12}^{\text{phys}} &= \cos(\alpha) T_{\mu\nu,12}^{\text{tw}} \pm i \sin(\alpha) \tilde{T}_{\mu\nu,12}^{\text{tw}} \xrightarrow{\alpha=\pi/2} \pm i \tilde{T}_{\mu\nu,12}^{\text{tw}} \\ \tilde{T}_{\mu\nu,12}^{\text{phys}} &= \cos(\alpha) \tilde{T}_{\mu\nu,12}^{\text{tw}} \pm i \sin(\alpha) T_{\mu\nu,12}^{\text{tw}} \xrightarrow{\alpha=\pi/2} \pm i T_{\mu\nu,12}^{\text{tw}} \end{aligned} \tag{B.2}$$

Case #2: $r_1 = -r_2 = \pm 1$

$$\begin{aligned}
S_{12}^{\text{phys}} &= S_{12}^{\text{tw}} \xrightarrow{\alpha=\pi/2} S_{12}^{\text{tw}} \\
P_{12}^{\text{phys}} &= P_{12}^{\text{tw}} \xrightarrow{\alpha=\pi/2} P_{12}^{\text{tw}} \\
V_{\mu,12}^{\text{phys}} &= \cos(\alpha) V_{\mu,12}^{\text{tw}} \mp i \sin(\alpha) A_{\mu,12}^{\text{tw}} \xrightarrow{\alpha=\pi/2} \mp i A_{\mu,12}^{\text{tw}} \\
A_{\mu,12}^{\text{phys}} &= \cos(\alpha) A_{\mu,12}^{\text{tw}} \mp i \sin(\alpha) V_{\mu,12}^{\text{tw}} \xrightarrow{\alpha=\pi/2} \mp i V_{\mu,12}^{\text{tw}} \\
T_{\mu\nu,12}^{\text{phys}} &= T_{\mu\nu,12}^{\text{tw}} \xrightarrow{\alpha=\pi/2} T_{\mu\nu,12}^{\text{tw}} \\
\tilde{T}_{\mu\nu,12}^{\text{phys}} &= \tilde{T}_{\mu\nu,12}^{\text{tw}} \xrightarrow{\alpha=\pi/2} \tilde{T}_{\mu\nu,12}^{\text{tw}}
\end{aligned} \tag{B.3}$$

These two cases have a direct application in the change from the physical to twisted basis in operators $O_{i,[+]}^{\text{phys}} \mapsto O_{i,[+]}^{\text{tw}}$ discussed in Chapter 3.

A particular application of the above formulae involve the PCAC and PCVC relations. In the physical basis, in continuum limit, they read: $\partial_\mu A_{\mu,12}^{\text{phys}} = (m_1 + m_2) P_{12}^{\text{phys}}$ and $\partial_\mu A_{\mu,12} = 0$. They must change according to the twist transformations. Again, I consider the two cases:

Case #1: $r_1 = r_2 = \pm 1$

$$\text{PCAC: } \partial_\mu A_{\mu,12}^{\text{tw}} = (m_1 + m_2) \left[\cos(\alpha) P_{12}^{\text{tw}} \pm i \sin(\alpha) S_{12}^{\text{tw}} \right] \xrightarrow{\alpha=\pi/2} \pm i (m_1 + m_2) S_{12}^{\text{tw}}$$

$$\text{PCVC: } \partial_\mu V_{\mu,12}^{\text{tw}} = 0$$

Case #2: $r_1 = -r_2 = \pm 1$

$$\text{PCAC: } \partial_\mu A_{\mu,12}^{\text{tw}} = \cos(\alpha) (m_1 + m_2) P_{12}^{\text{tw}} \xrightarrow{\alpha=\pi/2} 0$$

$$\text{PCVC: } \partial_\mu V_{\mu,12}^{\text{tw}} = \pm i \sin(\alpha) (m_1 + m_2) P_{12}^{\text{tw}} \xrightarrow{\alpha=\pi/2} \pm i (m_1 + m_2) P_{12}^{\text{tw}}$$

Appendix C

Fierz transformations

Suppose to have four flavours of quarks $\{\psi^1, \psi^2, \psi^3, \psi^4\}$ and a product of two Dirac bilinears in the following form:

$$\mathcal{E} = (\bar{\psi}^1 \Gamma^\alpha \psi^2) \cdot (\bar{\psi}^3 \Gamma^\beta \psi^4)$$

where $\Gamma^{\alpha,\beta} \in \{\mathbb{I}_4, \gamma_\mu, \gamma_5, \gamma_\mu \gamma_5, \sigma_{\mu\nu}\}$. I aim to express the same quantity \mathcal{E} by contracting $\bar{\psi}^1$ with ψ^4 and $\bar{\psi}^3$ with ψ^2 . In other words, I want to find M and N such that:

$$\mathcal{E} = (\bar{\psi}^1 M \psi^4) \cdot (\bar{\psi}^3 N \psi^2)$$

To construct M and N , I need the following theorem:

C.1 Fierz decomposition

I know that the set $\mathcal{B} = \{\mathbb{I}_4, \gamma_\mu, \gamma_5, \gamma_\mu \gamma_5, \sigma_{\mu\nu}\}$ is a basis for $\text{Mat}(4 \times 4, \mathbb{C})$. Furthermore, this is a normal basis, i.e. there exists a scalar product such that the matrices of the basis are normal:

$$\begin{aligned} \text{Tr} [\Gamma^\alpha \Gamma^\beta] &= 4\delta^\alpha_\beta \\ \text{with } \Gamma_\alpha &= (\Gamma^\alpha)^{-1} = \pm \Gamma^\alpha \end{aligned}$$

in particular $\Gamma_\alpha \in \{\mathbb{I}_4, \gamma_\mu, \gamma_5, -\gamma_\mu \gamma_5, -\sigma_{\mu\nu}\} := \mathcal{B}^{-1}$. Then any matrix $X \in \text{Mat}(4 \times 4, \mathbb{C})$ can be expressed as follows:

$$X = x_\alpha \Gamma^\alpha = \frac{1}{4} \Gamma^\alpha \text{Tr} [\Gamma_\alpha X] \quad \text{i.e.} \quad x_\alpha = \frac{1}{4} \text{Tr} [\Gamma_\alpha X] \quad (\text{C.1})$$

As usual, repeated indices imply a sum. Making the indices explicit:

$$\frac{1}{4} (\Gamma^\alpha)_{ij} (\Gamma_\alpha)_{kl} = \delta_{il} \delta_{jk}$$

□

Now let's go back to the specific \mathcal{E} case. I rewrite it with explicit indices and I emphasize that $[\psi^2 \bar{\psi}^3]$ is a matrix:

$$\mathcal{E} = \bar{\psi}_i^1 \Gamma_{ij}^\alpha [\psi^2 \bar{\psi}^3]_{jk} \Gamma_{kl}^\beta \psi_l^4$$

now I express the matrix $X = [\psi^2 \bar{\psi}^3]$ using formula (C.1):

$$\begin{aligned} [\psi^2 \bar{\psi}^3]_{jk} &= \frac{1}{4} (\Gamma^\lambda)_{jk} \text{Tr}([\psi^2 \bar{\psi}^3] \Gamma_\lambda) = \frac{1}{4} (\Gamma^\lambda)_{jk} \psi_s^2 \bar{\psi}_r^3 (\Gamma_\lambda)_{rs} = \\ &= -\frac{1}{4} (\Gamma^\lambda)_{jk} \bar{\psi}_r^3 (\Gamma_\lambda)_{rs} \psi_s^2 = -\frac{1}{4} (\Gamma^\lambda)_{jk} (\bar{\psi}^3 \Gamma_\lambda \psi^2) \end{aligned}$$

Pay attention to the minus sign coming from the fermion variables exchange. Consequently, the expression \mathcal{E} becomes:

$$\mathcal{E} = (\bar{\psi}^1 \Gamma^\alpha \psi^2) \cdot (\bar{\psi}^3 \Gamma^\beta \psi^4) = -\frac{1}{4} (\bar{\psi}^1 \Gamma^\alpha \Gamma^\lambda \Gamma^\beta \psi^4) \cdot (\bar{\psi}^3 \Gamma_\lambda \psi^2) \quad (\text{C.2})$$

The last formula is known under the name of *Fierz transformation* of Dirac bilinears and it is commonly used to re-express Fermi interactions [29]. Similar Fierz transformations can be developed in $SU(N)$ Lie groups by following the same procedure.

C.2 Application to Θ_3 and Θ_5

Now I just apply the transformations (C.2) to the operators Θ_3 and Θ_5 defined in (1.7). Consequently, the colour indices a, b are contracted in the same couple of fermions as the Dirac indices and the evaluation of Wick contractions is simplified. I will develop the explicit calculation in the case of Θ_3 and the case of Θ_5 is similar. I report only the essential steps. The main properties used are:

- Fierz transformation (C.2).
- Properties of the left and right Weyl projectors:

$$\begin{aligned} P_{L,R} &= \frac{\mathbb{I}_4 \pm \gamma_5}{2} & P_L P_R &= P_R P_L = 0 \\ P_L \gamma_\mu &= \gamma_\mu P_R & P_R \gamma_\mu &= \gamma_\mu P_L & \{P_{L,R}, \gamma_5\} &= 0 \end{aligned}$$

Then:

$$\begin{aligned} \Theta_3 &= [\bar{s}^a (1 + \gamma_5) d^b] \cdot [\bar{s}^b (1 + \gamma_5) d^a] = -\frac{1}{4} [\bar{s}^a (1 + \gamma_5) \Gamma^\alpha (1 + \gamma_5) d^a] \cdot [\bar{s}^b \Gamma_\alpha d^b] = \\ &= -[\bar{s}^a P_R \Gamma^\alpha P_R d^a] \cdot [\bar{s}^b \Gamma_\alpha d^b] = -[\bar{s}^a P_R d^a] [\bar{s}^b \mathbb{I} d^b] - [\bar{s}^a P_R \gamma_5 d^a] [\bar{s}^b \gamma_5 d^b] + \\ &+ [\bar{s}^a P_R \sigma_{\mu\nu} d^a] [\bar{s}^b \sigma_{\mu\nu} d^b] := \frac{1}{2} (-SS - PS - SP - PP + TT + \tilde{T}T) \end{aligned}$$

The game consists into multiply together the projectors, thus evaluate Γ^ξ such that $P_R \Gamma^\alpha P_R = P_R \Gamma^\xi$. Due to the projectors properties, only a subset of the Dirac matrices will survive. The parity even and parity odd parts are respectively:

$$\begin{aligned} \Theta_3^{[+]} &= \frac{1}{2} (-SS - PP + TT) & \Theta_3^{[-]} &= \frac{1}{2} (-PS - SP + \tilde{T}T) \\ \Theta_5^{[+]} &= \frac{1}{2} (AA - VV) & \Theta_5^{[-]} &= \frac{1}{2} (AV - VA) \end{aligned}$$

Appendix D

Some proofs

In this supplementary chapter, I aim to provide proofs for certain aspects that were not covered in the main thesis chapters.

D.1 Proof that $\langle \Omega | \bar{K}^0(0) | \bar{K}^0 \rangle$ is real

Based on the Goldstone theorem [26] there exist pseudoscalar single particle states $|\phi^a(\vec{p})\rangle$ (Nambu Goldstone bosons) and corresponding local operators $\phi^a(x)$ that interpolate these states in a simple manner, expressed as $\langle \Omega | \phi^a(x) | \phi^b(\vec{p}) \rangle = \delta^{ab} e^{ipx}$. In this case I will use $|\phi^a(\vec{p})\rangle = |K^0(\vec{0})\rangle \equiv |K^0\rangle$. The operators ϕ^a are related, within QCD, to the vector axial currents by:

$$j_\mu^{A,a}(x) = F_\pi^a \partial_\mu \phi^a(x) \quad \Rightarrow \quad \partial_\mu j_\mu^{A,a}(x) = F_\pi^a m_{\pi^a}^2 \phi^a(x)$$

However, the vector axial current is also defined as $j_\mu^a(x) = \bar{\psi}^i(x) T_{ij}^a \gamma_\mu \gamma_5 \psi^j(x)$ where T^a are SU(3) generators and i, j are flavour indices. By applying the four divergence to $j_\mu^a(x)$ and by using the Dirac equation in Euclidean notation (Appendix A), I obtain:

$$\partial_\mu j_\mu^{A,a}(x) = (m_i + m_j) T_{ij}^a \bar{\psi}^i(x) \gamma_5 \psi^j(x) := (m_i + m_j) T_{ij}^a P^{ij}(x)$$

Through a comparison of the four divergences, I obtain the equality:

$$(m_i + m_j) T_{ij}^a P^{ij}(x) = F_\pi^a m_{\pi^a}^2 \phi^a(x)$$

in particular $(m_s + m_d) \bar{K}^0(x) = F_K m_K^2 \phi^{\bar{K}^0}(x)$ according to definition (1.2) of the operator $\bar{K}^0 = P^{ds}$. Now I remember that I use, as sources, the pseudoscalar densities $P^{ij}(x)$ and not the unknown operators $\phi^a(x)$, then our matrix elements are:

$$\langle \Omega | \bar{K}^0(0) | \bar{K}^0 \rangle = \langle \Omega | K^0(0) | K^0 \rangle = \frac{F_K m_K^2}{m_s + m_d} \quad (\text{D.1})$$

As these are real values, they are also equal to their conjugates $\langle K^0 | \bar{K}^0(0) | \Omega \rangle$ and $\langle \bar{K}^0 | K^0(0) | \Omega \rangle$. The masses m_s and m_d used here are the renormalized quark masses. \square

D.2 Reality of three point correlators

I want to prove that the continuum three point correlators in formula (3.3)

$$\langle \bar{K}^0(x) Q_i(y) \bar{K}^0(z) \rangle$$

are real. To make it, I make use of formula (A.1). First of all, let's calculate the complex conjugate of the sources:

$$(\bar{K}^0)^* = (\bar{d}\gamma_5 s)^* = -\bar{s}\gamma_0\gamma_5^\dagger\gamma_0 d = \bar{s}\gamma_5 d = K^0$$

Then I need to calculate the complex conjugate of the operators. I simplify the operation by permuting such calculation on the “components” of Q_i s:

$$\begin{aligned} Q_{VV}^* &= (\bar{s}\gamma_\mu d \cdot \bar{s}\gamma_\mu d)^* = (\bar{s}\gamma_\mu d)^* (\bar{s}\gamma_\mu d)^* = \bar{d}\gamma_\mu s \cdot \bar{d}\gamma_\mu s \equiv \tilde{Q}_{VV} \\ Q_{AA}^* &= (\bar{s}\gamma_\mu\gamma_5 d \cdot \bar{s}\gamma_\mu\gamma_5 d)^* = \bar{d}\gamma_\mu\gamma_5 s \cdot \bar{d}\gamma_\mu\gamma_5 s \equiv \tilde{Q}_{AA} \\ Q_{SS}^* &= (\bar{s}d \cdot \bar{s}d)^* = \bar{d}s \cdot \bar{d}s \equiv \tilde{Q}_{SS} \\ Q_{PP}^* &= (\bar{s}\gamma_5 d \cdot \bar{s}\gamma_5 d)^* = \bar{d}\gamma_5 s \cdot \bar{d}\gamma_5 s \equiv \tilde{Q}_{PP} \\ Q_{TT}^* &= (\bar{s}\sigma_{\mu\nu} d \cdot \bar{s}\sigma_{\mu\nu} d)^* = \bar{d}\sigma_{\mu\nu} s \cdot \bar{d}\sigma_{\mu\nu} s \equiv \tilde{Q}_{TT} \end{aligned}$$

where it is clear that $\tilde{Q}_{\Gamma\Gamma}$ is the operator $Q_{\Gamma\Gamma}$ in which there is an exchange $s \leftrightarrow d$. Then I have proven that:

$$\langle \bar{K}^0(x) Q_i(y) \bar{K}^0(z) \rangle^* = \langle K^0(x) \tilde{Q}_i(y) K^0(z) \rangle$$

Moreover I know that:

$$\langle \bar{K}^0(x) Q_i(y) \bar{K}^0(z) \rangle = \langle K^0(x) \tilde{Q}_i(y) K^0(z) \rangle$$

because B -parameters are real. This is straightforward: I can express the above correlators through the asymptotic expansion (3.12) and substitute $\langle \bar{K}^0 | O_{i,[+]} | K^0 \rangle$ with the definition of bag parameters (1.8). I'm doing the calculation with the Q_i and not the Θ_i , thus I need to insert a *linear combination* of the bag parameters, but the essence is unchanged. Since the B_i are real¹, their complex conjugates coincide with them. □

It follows a computational check of reality of three points correlators. The plot in Figure D.1 shows how the immaginary part of the correlators, in asymptotic regime, tend to zero. For more information about this simulation, see Section 4.4.

D.3 Proof of $\gamma_5 S_{(i,\pm)}(u, v) \gamma_5 = S_{(i,\mp)}^\dagger(v, u)$

The starting point is a well known property of the Dirac-Wilson operator D_W : $\gamma_5 D_W(x, y) \gamma_5 = D_W^\dagger(y, z)$. The bilinear operator of the Osterwalder-Seiler theory is $D_W \pm i\gamma_5 \mu$, and the quark propagator is just its inverse:

$$\sum_z (D_W \pm i\gamma_5 \mu)(x, z) S_{(\pm)}(z, y) = \delta_{xy}^{(4)}$$

¹ this is not proven here.

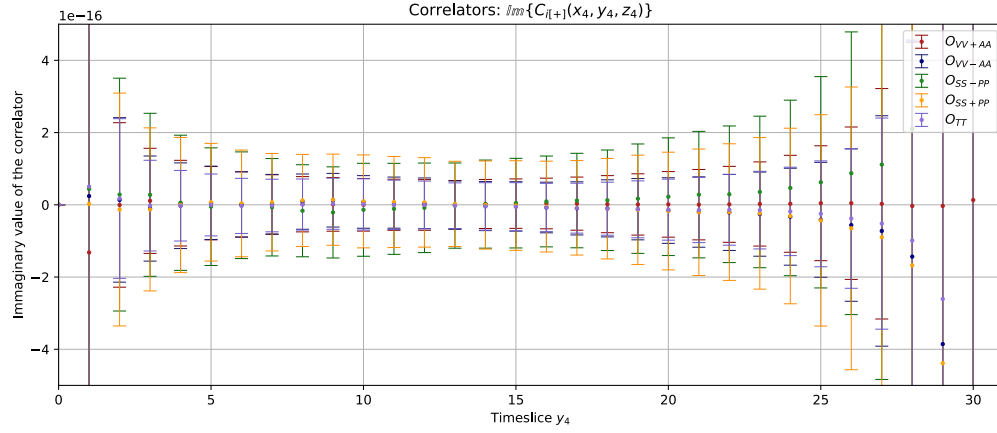


Figure D.1. Test of simulation of three points correlators on a set of 54 quenched configurations, $\beta = 6.0$, tree level improved Symanzik gauge action. It has been used a $16 \times 16 \times 16 \times 32$ lattice.

By multiplying γ_5 to the left, to the right and inserting a $\mathbb{I} = (\gamma_5)^2$ between the operator and the propagator:

$$\sum_z (D_W \mp i\gamma_5 \mu)^\dagger(z, x) \left[\gamma_5 S_{(\pm)}(z, y) \gamma_5 \right] = \delta_{xy}^{(4)}$$

Now I remember that D_W doesn't contain the usual derivatives, but only terms like $\delta_{x;y+\hat{\mu}}^{(4)}$ or $\delta_{x;y-\hat{\mu}}^{(4)}$. In other words, the Dirac-Wilson operator on the lattice is just a matrix. Then it can be exchanged with other matrices M - i.e. $D_W(u, v)M(w, l) = M(w, l)D_W(u, v)$. As a consequence:

$$\sum_z \left[\gamma_5 S_{(\pm)}(z, y) \gamma_5 \right] (D_W \mp i\gamma_5 \mu)^\dagger(z, x) = \delta_{yx}^{(4)}$$

The term $\gamma_5 S_{(\pm)}(z, y) \gamma_5$ it is clearly $S_{(\mp)}^\dagger(y, z)$ for definition.

□

D.4 Proof of connection of Gauge fields space

The proof of the connection of the $SU(3)$ Gauge field space is reported below and taken from [34]. The proof is based on the continuum theory. Because of the mentioned theorem in [31], for $a \rightarrow 0$ the lattice space of Gauge fields tends to have the same topological connection properties of the one described below.

(*) *proof:*

It is well known that Gauge potentials $A_\mu(x)$ can be described as $\text{End}(E)$ -valued 1-forms, where E is the G -bundle over a smooth manifold M [3]. In this case M is the manifold obtained from the following product of spaces: $M = [0, T] \times \mathbb{T}^3$ and \mathbb{T}^3 is the three dimensional torus, topologically equivalent to the space $[0, L] \times [0, L] \times [0, L]$ with periodic boundary conditions.

In the paper by Luscher [34] there is an interesting statement: “since M is contractible to a three dimensional torus, all $SU(3)$ principal bundles over M are trivializable”.

A direct consequence of this *global* trivialization is that Gauge fields are globally defined over all the manifold M .

At this point, the proof is essentially complete. I must check that, given two Gauge fields $A_\mu^{(1)}$ and $A_\mu^{(2)}$, there always exists a smooth path in the fields space which connects them. The proof is divided in three parts:

(i) *Each A_μ can be constinously deformed to another A'_μ in temporal Gauge.*

It is defined a family of Gauge transformations $\Lambda_s(x)$, $s \in [0, 1]$ satisfying the following conditions:

$$(\partial_4 + sA_4(x)) \Lambda_s^{-1}(x) = 0$$

$$\Lambda_0(x)|_{x_4=0} = \mathbb{I}_3$$

I apply the Gauge transformation to a generic $A_\mu(x)$ that satisfies Open Boundary Conditions. I must prove that the transformed field $A_\mu^s(x)$ satisfies the temporal gauge and it still has Open Boundary Conditions .

$$A_\mu^s(x) = \Lambda_s(x)A_\mu(x)\Lambda_s^{-1}(x) + \Lambda_s(x)\partial_\mu\Lambda_s^{-1}(x)$$

- Temporal Gauge in $s = 1$:

$$A_4^0(x) = \Lambda_1(x)A_4(x)\Lambda_1^{-1}(x) - \Lambda_1(x)A_4(x)\Lambda_1^{-1}(x) = 0$$

- Open Boundary Conditions $\forall s \in [0, 1]$: I perfectly know how the strength tensor transforms under Gauge transformations:

$$F_{\mu\nu}(x) \mapsto F_{\mu\nu}^s(x) = \Lambda_s(x)F_{\mu\nu}(x)\Lambda_s^{-1}(x)$$

Then it is trivial to assert that $F_{0i}^s(\vec{x}, 0) = F_{0i}^s(\vec{x}, T) = 0$. The transformed fields satisfy Open Boundary Conditions.

(ii) *Each A_μ in temporal Gauge can be contracted to the null Gauge field $A_\mu = 0$.*

This part of the proof is trivial: I choose te path $A_\mu^s = s \cdot A_\mu$

At this point it is proven that each A_μ satisfying Open Boundary Conditions can be smoothly contracted to the null potential. Then each couple of potentials $A_\mu^{(1)}$ and $A_\mu^{(2)}$ satisfying Open Boundary Conditions are connected in the fields space. \square

D.5 Pseudoscalar propagator with OBC

I want to derive the form of the propagator (4.9) in presence of Open Boundary Conditions on fermion fields. For simplicity, I work the calculation in continuum QCD. First of all, I must derive the boundary conditions on pseudoscalar mesons. I do it by looking at appendix D.1: the generic pseudoscalar meson operator is proportional to the pseudoscalar density $P^{ab}(x) = \bar{\psi}^a(x)\gamma_5\psi^b(x)$ Then I can infere its boundary conditions from the conditions in the fermion fields (2.15).

I can write the identity in the following way $\mathbb{I}_4 = P_+ + P_-$. Then I can insert it in a pseudoscalar density evaluated in $x_4 = 0$:

$$\bar{\psi}^a\gamma_5\psi^b\Big|_0 = \bar{\psi}^a\gamma_5(P_+ + P_-)\psi^b\Big|_0 = \bar{\psi}^a\gamma_5P_-\psi^b\Big|_0 =$$

now I make use of time reflection symmetry:

$$\mathbb{T} : \begin{cases} \psi(\vec{x}, x_4) \mapsto -\gamma_1 \gamma_3 \psi(\vec{x}, T - x_4) \\ \bar{\psi}(\vec{x}, x_4) \mapsto -\bar{\psi}(\vec{x}, T - x_4) \gamma_3 \gamma_1 \end{cases}$$

thus:

$$= (-)^2 \bar{\psi}^a \gamma_3 \gamma_1 \gamma_5 P_- \gamma_1 \gamma_3 \psi^b \Big|_T = \bar{\psi}^a \gamma_5 \gamma_3 \gamma_1 \gamma_1 P_+ \gamma_3 \psi^b \Big|_T = \bar{\psi}^a \gamma_5 \gamma_3 \gamma_3 P_- \psi^b \Big|_T = 0$$

the same holds for the case $x_4 = T$. Then the boundary conditions on the pseudoscalar densities are:

$$P^{ab}(\vec{x}, 0) = P^{ab}(\vec{x}, T) = 0 \quad \forall a, b = 1, 2, 3 \quad (\text{D.2})$$

To simplify the notation, I will use π to refer to the generic P^{ab} .

In first order of Chiral Perturbation Theory, the generic pion satisfies the Klein Gordon equation, that in euclidean notation reads²:

$$\left(-\frac{\partial^2}{\partial t^2} - \nabla_3^2 + m^2 \right) \pi(\vec{x}, t) = 0$$

where ∇_3^2 is the Laplace operator in \mathbb{E}^3 . A generic non homogeneous equation can be solved by using the associated Green function that must satisfy the same boundary conditions of the field [38]. The spatial part of the equation is solved through the Fourier transform method (as done in every course of quantum field theory) and helps to reduce the equation for the Green function in this way:

$$\left(-\frac{\partial^2}{\partial t^2} - \vec{p}^2 + m^2 \right) G_\omega(t, t') = \left(-\frac{\partial^2}{\partial t^2} - \omega^2 \right) G_\omega(t, t') = L_\omega G_\omega(t, t') = 0$$

Notice that, in this case, we do not have $G_\omega(t - t')$ but $G_\omega(t, t')$ because these boundary conditions, unlike the periodic ones, break the time translation invariance. The generic solution is:

$$G_\omega(t, t') = \theta(t - t') \phi^{\text{sup}}(t) \alpha(t') + \theta(t' - t) \phi^{\text{inf}}(t) \beta(t')$$

where:

$$\begin{cases} L_\omega \phi^{\text{sup}}(t) = 0 \\ \phi^{\text{sup}}(T) = 0 \end{cases} \quad \text{and} \quad \begin{cases} L_\omega \phi^{\text{inf}}(t) = 0 \\ \phi^{\text{inf}}(0) = 0 \end{cases}$$

with this choice the boundary conditions are automatically satisfied. The coefficients $\alpha(t')$ and $\beta(t')$ must be chosen in order to make $G_\omega(t, t')$ continuous and its first derivative must be an Heaviside $\theta(t - t')$. By imposing these conditions I found:

$$\begin{aligned} G_\omega(t, t') = & \theta(t - t') \frac{\sinh(\omega(T - t)) \cdot \sinh(\omega t')}{2\omega \sinh(\omega T)} + \\ & + \theta(t' - t) \frac{\sinh(\omega(T - t')) \cdot \sinh(\omega t)}{2\omega \sinh(\omega T)} \end{aligned}$$

Then I remember that $G_\omega(t, t') = \tilde{G}(\vec{p}, t, t')$, the propagator in three-momentum space and euclidean time. The summation over spatial coordinates will set $\vec{p} = 0$ as outlined in section 3.5.

□

² here the variables t, t' are the euclidean times x_4, y_4 .

Bibliography

- [1] C.R. Allton et al. “B-parameters for $\Delta S = 2$ supersymmetric operators”. In: *Physics Letters B* 453.1-2 (Apr. 1999), pp. 30–39. DOI: 10.1016/s0370-2693(99)00283-x.
- [2] Y. Aoki et al. “FLAG Review 2021”. In: *The European Physical Journal C* 82.10 (Oct. 2022). DOI: 10.1140/epjc/s10052-022-10536-1.
- [3] J. Baez and J. P. Muniain. *Gauge fields, knots and gravity*. 1995.
- [4] Gunnar S. Bali et al. *Towards the continuum limit with improved Wilson fermions employing open boundary conditions*. 2017. arXiv: 1702.01035 [hep-lat].
- [5] D. Bećirević et al. “Exploring twisted mass lattice QCD with the Clover term”. In: *Physical Review D* 74.3 (Aug. 2006). ISSN: 1550-2368. DOI: 10.1103/physrevd.74.034501.
- [6] V. Bertone et al. “Kaon mixing beyond the SM from $N_f = 2$ tmQCD and model independent constraints from the UTA”. In: *Journal of High Energy Physics* 2013.3 (Mar. 2013). DOI: 10.1007/jhep03(2013)089.
- [7] Gustavo C. Branco, Luis Lavoura, and Joao P. Silva. *CP Violation*. Vol. 103. 1999.
- [8] Mattia Bruno, Tomasz Korzec, and Stefan Schaefer. “Setting the scale for the CLS 2+1 flavor ensembles”. In: *Physical Review D* 95.7 (Apr. 2017). DOI: 10.1103/physrevd.95.074504. URL: <https://doi.org/10.1103/physrevd.95.074504>.
- [9] Mattia Bruno et al. *On the extraction of spectral quantities with open boundary conditions*. 2014. arXiv: 1411.5207 [hep-lat].
- [10] Mattia Bruno et al. “Simulation of QCD with $N_f = 2 + 1$ flavors of non-perturbatively improved Wilson fermions”. In: *Journal of High Energy Physics* 2015.2 (Feb. 2015). DOI: 10.1007/jhep02(2015)043. URL: [https://doi.org/10.1007/JHEP02\(2015\)043](https://doi.org/10.1007/JHEP02(2015)043).
- [11] John Bulava and Stefan Schaefer. “Improvement of $N_f=3$ lattice QCD with Wilson fermions and tree-level improved gauge action”. In: *Nuclear Physics B* 874.1 (2013), pp. 188–197. ISSN: 0550-3213. DOI: <https://doi.org/10.1016/j.nuclphysb.2013.05.019>.
- [12] Andrea Bussone et al. *Matching of $N_f = 2 + 1$ CLS ensembles to a tmQCD valence sector*. 2019. arXiv: 1903.00286 [hep-lat].
- [13] Andrea Bussone et al. *Matching of $N_f = 2 + 1$ CLS ensembles to a tmQCD valence sector*. 2019. arXiv: 1903.00286 [hep-lat].
- [14] N. Carrasco et al. *$K^0 - \bar{K}^0$ mixing in the Standard Model from $N_f = 2 + 1 + 1$ Twisted Mass Lattice QCD*. 2011. arXiv: 1111.1262 [hep-lat].

- [15] John C. Collins. *Renormalization: An Introduction to Renormalization, The Renormalization Group, and the Operator Product Expansion*. Vol. 26. Cambridge Monographs on Mathematical Physics. Cambridge: Cambridge University Press, 1986. ISBN: 978-0-521-31177-9, 978-0-511-86739-2, 978-1-00-940180-7. DOI: 10.1017/CB09780511622656.
- [16] M. Constantinou et al. “BK-parameter from $N_f=2$ twisted mass lattice QCD”. In: *Physical Review D* 83.1 (Jan. 2011). ISSN: 1550-2368. DOI: 10.1103/PhysRevD.83.014505.
- [17] P. Dimopoulos et al. “Non-perturbative renormalisation and running of BSM four-quark operators in $N_f = 2$ QCD”. In: *The European Physical Journal C* 78.7 (July 2018). ISSN: 1434-6052. DOI: 10.1140/epjc/s10052-018-6002-y.
- [18] A. Donini et al. “Non-perturbative renormalization of lattice four-fermion operators without power subtractions”. In: *The European Physical Journal C* 10.1 (Aug. 1999), pp. 121–142. DOI: 10.1007/s100529900097.
- [19] John F. Donoghue, Eugene Golowich, and Barry R. Holstein. *Dynamics of the Standard Model*. 2nd ed. Cambridge Monographs on Particle Physics, Nuclear Physics and Cosmology. Cambridge University Press, 2014. DOI: 10.1017/CB09780511803512.
- [20] R. Frezzotti and G.C. Rossi. “Chirally improving Wilson fermions I. $O(a)$ improvement”. In: *Journal of High Energy Physics* 2004.08 (Aug. 2004), pp. 007–007. DOI: 10.1088/1126-6708/2004/08/007. URL: <https://doi.org/10.1088/1126-6708/2004/08/007>.
- [21] R. Frezzotti and G.C. Rossi. “Chirally improving Wilson fermions II. Four-quark operators”. In: *Journal of High Energy Physics* 2004.10 (Oct. 2004), pp. 070–070. DOI: 10.1088/1126-6708/2004/10/070. URL: <https://doi.org/10.1088/1126-6708/2004/10/070>.
- [22] Roberto Frezzotti et al. *Lattice QCD with a chirally twisted mass term*. 2001. arXiv: hep-lat/0101001 [hep-lat].
- [23] Kazuo Fujikawa. “Erratum: Path integral for gauge theories with fermions”. In: *Phys. Rev. D* 22 (6 Sept. 1980), pp. 1499–1499. DOI: 10.1103/PhysRevD.22.1499.
- [24] Kazuo Fujikawa. “Path-Integral Measure for Gauge-Invariant Fermion Theories”. In: *Phys. Rev. Lett.* 42 (18 Apr. 1979), pp. 1195–1198. DOI: 10.1103/PhysRevLett.42.1195.
- [25] Christof Gattringer and Christian B. Lang. *Quantum chromodynamics on the lattice*. Vol. 788. Berlin: Springer, 2010. ISBN: 978-3-642-01849-7, 978-3-642-01850-3. DOI: 10.1007/978-3-642-01850-3.
- [26] Jeffrey Goldstone, Abdus Salam, and Steven Weinberg. “Broken Symmetries”. In: *Phys. Rev.* 127 (3 Aug. 1962), pp. 965–970. DOI: 10.1103/PhysRev.127.965.
- [27] Herdoiza, Gregorio et al. “A tmQCD mixed-action approach to flavour physics”. In: *EPJ Web Conf.* 175 (2018), p. 13018. DOI: 10.1051/epjconf/201817513018. URL: <https://doi.org/10.1051/epjconf/201817513018>.
- [28] Gregorio Herdoiza et al. “Light meson physics and scale setting from a mixed action with Wilson twisted mass valence quarks”. In: *Proceedings of The 38th International Symposium on Lattice Field Theory — PoS(LATTICE2021)*. Vol. 396. 2022, p. 258. DOI: 10.22323/1.396.0258.

- [29] C. Itzykson and J. B. Zuber. *Quantum Field Theory*. International Series In Pure and Applied Physics. New York: McGraw-Hill, 1980. ISBN: 978-0-486-44568-7.
- [30] Tomasz Korzec. “Mesons Correlators”. In: *private document* (2013).
- [31] Martin Luscher. *Topology, the Wilson flow and the HMC algorithm*. 2014. arXiv: 1009.5877 [hep-lat].
- [32] Martin Lüscher. “The Schrödinger functional in lattice QCD with exact chiral symmetry”. In: *Journal of High Energy Physics* 2006.05 (May 2006). ISSN: 1029-8479. DOI: 10.1088/1126-6708/2006/05/042.
- [33] Martin Lüscher and Stefan Schaefer. “Lattice QCD with open boundary conditions and twisted-mass reweighting”. In: *Computer Physics Communications* 184.3 (Mar. 2013), pp. 519–528. DOI: 10.1016/j.cpc.2012.10.003. URL: <https://doi.org/10.1016%2Fj.cpc.2012.10.003>.
- [34] Martin Lüscher and Stefan Schaefer. “Lattice QCD without topology barriers”. In: *Journal of High Energy Physics* 2011.7 (July 2011). DOI: 10.1007/jhep07(2011)036. URL: <https://doi.org/10.1007%2Fjhep07%282011%29036>.
- [35] Martin Lüscher et al. “Non-perturbative $O(a)$ improvement of lattice QCD”. In: *Nuclear Physics B* 491.1–2 (Apr. 1997), pp. 323–343. ISSN: 0550-3213. DOI: 10.1016/S0550-3213(97)00080-1.
- [36] I. Montvay and G. Münster. *Quantum Fields on a Lattice*. Cambridge Monographs on Mathematical Physics. Cambridge University Press, 1994. ISBN: 9780521599177.
- [37] A. Morel. “Chiral logarithms in quenched QCD”. In: *Journal de Physique* 48 (7), pp.1111-1119. (1987). DOI: <https://doi.org/10.1051/jphys:019870048070111100>.
- [38] Michela Petrini, Gianfranco Pradisi, and Alberto Zaffaroni. *A Guide to Mathematical Methods for Physicists*. WSP, 2019. DOI: 10.1142/q0162.
- [39] Stefan Schaefer, Rainer Sommer, and Francesco Virota. “Critical slowing down and error analysis in lattice QCD simulations”. In: *Nuclear Physics B* 845.1 (Apr. 2011), pp. 93–119. DOI: 10.1016/j.nuclphysb.2010.11.020.
- [40] Stefan Schaefer, Rainer Sommer, and Francesco Virota. *Investigating the critical slowing down of QCD simulations*. 2009. arXiv: 0910.1465 [hep-lat].
- [41] Matthew D. Schwartz. *Quantum Field Theory and the Standard Model*. Cambridge University Press, Mar. 2014. ISBN: 978-1-107-03473-0, 978-1-107-03473-0.
- [42] Rainer Sommer. “ $O(a)$ improved lattice QCD”. In: *Nuclear Physics B - Proceedings Supplements* 60.1 (1998), pp. 279–293. ISSN: 0920-5632. DOI: [https://doi.org/10.1016/S0920-5632\(97\)00490-8](https://doi.org/10.1016/S0920-5632(97)00490-8).
- [43] Steven Weinberg. *The quantum theory of fields. Vol. 2: Modern applications*. Cambridge, UK: Univ. Pr. (1996) 489 p. 1996.
- [44] Kenneth G. Wilson. “Confinement of Quarks”. In: *Phys. Rev. D* 10 (1974). Ed. by J. C. Taylor, pp. 2445–2459. DOI: 10.1103/PhysRevD.10.2445.
- [45] R. L. Workman et al. “Review of Particle Physics”. In: *PTEP* 2022 (2022), p. 083C01. DOI: 10.1093/ptep/ptac097.